MERCAPTURIC ACID PATHWAY: A NOVEL OPPORTUNITY FOR TARGETING *VHL*-MUTANT RENAL CELL CARCINOMA

DISSERTATION

Presented to the Graduate Council of the

Graduate School of Biomedical Sciences

University of North Texas Health Science Center at Fort Worth

In Partial Fulfillment of the Requirements

For the Degree of

DOCTOR of PHILOSOPHY

By

Lokesh Prasad Gowda Dalasanur Nagaprashantha, M.B.B.S., M.S.

Fort Worth, Texas

May, 2011

ACKNOWLEDGEMENTS

During the course of PhD, I had been really fortunate to be mentored by renowned experts in their respective fields in an atmosphere of intense research. First, I would like to convey my sincere regards and gratitude to my major professor Dr. Sanjay Awasthi for not only providing me a precious opportunity to do my doctoral project in his laboratory but also for serving as an exemplary source of inspiration and invaluable guidance to focus on research aimed at addressing pressing contemporary challenges in oncology. Dr. Awasthi's continuous support, confidence and guidance during the challenging phases helped me to enthusiastically pursue my project. I would like to express my sincere gratitude and respect to my co-major professor Dr. Laszlo Prokai who accepted me to work in his laboratory towards my doctoral project. The expert guidance and kind words of encouragement by Dr. Prokai during various experimental procedures and prolonged phases of brain-storming data analyses provided the much needed support to sustain the intense course of research. Working in two laboratories focused on cancer research and the application of mass spectrometry based proteomics provided a great opportunity to learn the productive application of integrated research strategies which was made possible only due to the patience and excellent guidance provided by my major professors Dr. Awasthi and Dr. Prokai. I would like to sincerely thank my committee members Dr. Albert Yurvati for encouraging and providing time to discuss research findings. I express my gratitude and sincere regards to Dr. Maya Nair for providing helpful suggestions during the PhD. I sincerely thank my university member Dr. Robert Luedtke for the constructive suggestions during important milestones of PhD training.

I would like to immensely thank my mentor Dr. Sharad Singhal who patiently trained me on various aspects of experimental protocols, animal handling, manuscript preparation and for being a great source of support. My sincere regards and gratitude go towards Mrs. Jyotsana Singhal for helping with the cell culture experiments. I sincerely thank Dr. Rit Vatsyayan for providing and helping with experimental protocols. I would like to thank Dr. Josef Borvak and Dr. Sushma Yadav who provided continuous source of support during my research. I would like to thank my lab mates Mukesh, Kathryn and Archana in Dr. Awasthi's laboratory for their friendly support.

I sincerely thank Dr. Katalin Prokai-Tatrai for affectionate advise and inspiration provided to pursue my career goals. My sincere thanks to Dr. Navin Rauniyar for teaching me the methods of proteomic analysis. I thank Dr. Vien Nguyen for kindly helping during technical problems with instrumentation. I would like to thank my lab mates Jia Guo and Tatjana Talamantes in Dr. Prokai's laboratory for their continuous friendly support.

I would like to sincerely thank my graduate advisor, Dr. Alakananda Basu for guidance during the course of my doctoral studies. I also would like to thank Dr. Yogesh Awasthi for providing inspiration and advise during important phases of my project.

On a personal note, when I look at the broader picture which supported the pursuit of my PhD, my first respects and gratitude go towards my parents for the innumerable positive ways they have shaped my life. I am blessed to have a highly industrious and caring elder brother, Sarvesh who has affectionately nourished my career goals and younger sister Sukrutha who has always supported the pursuit of my PhD. Finally, I would like to thank all my teachers, professors, friends and relatives who have extended their good will and provided inspiration for positive accomplishments during the course of my research towards PhD.

TABLE OF CONTENTS

CHAPTER

ABBREVIATIONS

2HF 2'-Hydroxyflavanone

4-HNE 4-Hydroxy-2-nonenal

AKR1C1 Aldoketo reductase family1member C1

CDK1 Cyclin dependent kinase 1

Da Dalton (molecular mass unit)

EGFR Epidermal growth factor receptor

EMT Epithelial mesenchymal transition

GSTπ Glutathione S-transferase pi

LC Liquid chromatography

IGFR Insulin growth factor receptor

LC–MS/MS Liquid chromatography–tandem mass spectrometry

LTQ-FTICR-MS Linear quadrupole ion trap-Fourier transform ion cyclotron resonance-mass spectrometer

m/z Mass-to-charge

MS Mass spectrometry

MS/MS Tandem mass spectrometry

PI3K Phosphoinositide-3 kinase

TGF Transforming growth factor

VEGF Vascular endothelial growth factor

VHL Von-Hippel-Lindau

SELECTED PEER-REVIEWED PUBLICATIONS

Nagaprashantha, L.D., Vatsyayan, R., Singhal, J., Lelsani, P.C., Prokai, L., Awasthi, S. and Singhal, S.S. (2011) 2'-Hydroxyflavanone inhibits proliferation, tumor vascularization and promotes normal differentiation in *VHL*-mutant Renal Cell Carcinoma. *Carcinogenesis;*32:568-575.

Nagaprashantha, L.D., Singhal, J., Guo, J., Vatsyayan, R., Rauniyar, N., Awasthi, S. Singhal, S.S., and Prokai, L. (2011) Proteomic Analysis of Signaling Networks Regulation in Renal Cell Carcinomas with Differential Hypoxia Inducible Factor 2α Expression *J of Proteome Research* (*Submitted*).

LIST OF TABLES

CHAPTER

Table

LIST OF ILLUSTRATIONS

CHAPTER

Figure

CHAPTER I

INTRODUCTION

Renal cell carcinoma

Renal cell carcinoma (RCC) is one of the top ten leading causes of cancer deaths in USA. The National Cancer Institute's statistics reveal doubling of the risk of RCC in past 50 years and recent data indicates that RCC contributes to loss of 195,000 person-years of productivity per calendar year making it an important public health problem [1]. Hence, analysis of the specific signaling pathways and networks in aggressive types of RCC and characterization of the mechanisms of action of novel anti-cancer agents that selectively target the processes of oncogenic transformation and tumor progression in kidney has gained momentum in the translational research in renal oncology.

RCC was first described by Konig in the year 1826. The proximal renal tubular origin of many renal tumors was confirmed by Robin and Waldeyer in 1855 and 1867, respectively [2]. The major histological sub-types of renal epithelial tumors are comprised of clear cell RCC (75%), papillary type 1 RCC (5%), papillary type 2 RCC (10%), chromophobe RCC (5%) and oncocytoma (5%) [3]. RCC occurs in both sporadic and hereditary forms. The deletions and loss of function mutations in the tumor suppressor von Hippel-Lindau (*VHL)* gene which is located on chromosome 3p25.3 leading to "*VHL* syndrome" (Online Mendelian Inheritance in Man, OMIM, catalogue number: 193300) is a major genetic risk factor for the incidence of clear cell RCC, a major sub-type of RCC [4-6]. The *VHL* syndrome was first described more than a

century ago by Treacher Collins and Eugene von Hippel following the observation of familial inheritance pattern of retinal angiomas [7,8]. Later, Arvind Lindau, a neuropathologist, described the incidence of cerebellar hemangioblastomas [9]. The *VHL* syndrome is also characterized by an increased predisposition to tumors of adrenal glands, inner ear, spine, and pancreatic cysts and hemangioblastomas [10-15]. Hereditary loss of *VHL* leads to incidence of multifocal, bilateral and highly vascular tumors in kidneys characterized by an aggressive and metastatic course of progression in younger years of life in contrast to sporadic RCC which generally affects mainly elderly population [16]. The *VHL* mutations have also been detected in many cases of sporadic RCC which in turn reveals the susceptibility of *VHL* locus to acquired mutations during life time [17]. The life-style and environmental risks for the incidence of sporadic RCC include cigarette smoking, obesity and asbestos exposure [17-20].

The significance of *VHL* in tumor formation and progression is due to its designated role in oxygen-sensing machinery of the cell which in turn regulates a plethora of cellular proliferative, metabolic and transcriptional processes. The cellular levels of oxygen in drosophila as well as mammals are sensed by a family of hypoxia inducible factors (HIF), proteins characterized by the presence of basic-helix-loop-helix structure and a PAS (dimerization) domain characteristic of many transcription factors. The human HIFs include HIF1-α, HIF1-β, HIF2-α, HIF2-β, HIF3-α and HIF3-β which participate in oxygen dependent re-programming of cellular transcription [21, 22]. The HIF-α subunits have N-terminal transactivation domain (NTAD) and C-terminal transactivation domain (CTAD) which are specifically regulated in oxygen dependent manner [23]. In hypoxic conditions, the transcriptional co-activators like cAMP-response-element-binding protein (CREB)-binding protein (CBP) and p300 bind to CTAD of HIF-α. This leads to

activation of hypoxia inducible genes like EGFR, VEGF, PDGFβ and TGFα which in turn contribute to enhanced angiogenic and mitogenic potential to survive in hypoxic environment [24-27]. The *VHL* gene product, pVHL, plays a vital role in regulating the function of HIF-α when oxygen levels are normal in cells. In normoxic conditions, the HIF-α proteins are hydroxylated at asparagine residue in NTAD by factor inhibiting HIF-α (FIH) and at proline residues by HIF prolyl-hydroxylases [28,29]. The prolyl hydroxylation of HIF-α at NTAD leads to binding of pVHL-elongin-cullin2 complex to HIF-α followed by polyubiquitination and proteosomal degradation [29-33]. Thus, pVHL contributes to inhibition of HIF-α signaling.

The function of pVHL extends beyond regulation of hypoxic signaling in the cells. The pVHL is required for regulation of integrins and tight junctions in epithelial cells and *VHL* mutant (*VHL*-mut) cells have increased levels of HIF2-α, α5-integrin, cyclin D1 and lower p27 levels along with loss of epithelial morphology [34]. The introduction of pVHL into *VHL*-mut RCC leads to cell cycle arrest, epithelial differentiation and suppression of tumor forming ability [35, 36]. Thus, pVHL plays a vital role in regulating multiple signaling processes of importance in oncogenic transformation, survival of tumors in hypoxic conditions along with a role in maintaining epithelial phenotype.

Role of oxidative stress in proliferation, apoptosis and drug-resistance

Oxidative stress is a significant input into the cellular metabolic framework which impacts the consequent behavior of the cells depending on cellular phenotype and conditioning of the cells. Physiological level of oxidative stress is an integral part of cell metabolism due to the generation of free radicals during mitochondrial respiration and is effectively buffered by the antioxidant system of the cells comprised of enzymes like superoxide dismutase, catalase, glutathione transferases (GSTs) and non–enzymatic components like glutathione (GSH), thioredoxins, periredoxins, glutaredoxins, vitamin C and vitamin E [37,38]. Free radicals are generated due to oxidative stress induce lipid peroxidation in the cells [39**]**. Oxidative stress leads to increased generation of products of lipid peroxidation like 4-hydroxy-2-nonenal (4HNE) and malondialdehyde (MDA) in the cells. 4HNE, an α, β unsaturated aldehyde is the major product of the lipid peroxidation of ω-6 polyunsaturated fatty acids in the cells. 4HNE contains 3 reactive groups: an aldehyde group, a hydroxyl group at position 4 and a C=C double bond at position 2 **[**40]. A fraction of synthesized 4HNE is reduced to acid, 4-hydroxynon-2-enoic acid (4HNA), by aldehyde dehydrogenase and a minor fraction is oxidized to the corresponding alcohol, 1, 4-dihydroxynonanol (DHN) by aldose reductase [41-43]. The majority of 4HNE is metabolized to a Michael-adduct thioether with glutathione, GS-HNE, a reaction catalyzed by glutathione S-transferases (GSTs). GS-HNE can susbsequently be reduced by aldose reductase to GS-DHN (**Fig 1**). The intracellular concentration of glutathione conjugates of 4HNE metabolites is regulated by the transport activity of glutathione-conjugate efflux pumps, of which RLIP76 is dominant. Both GS-HNE and GS-DHN are physiological substrates for ATP-dependent efflux by RLIP76 (a 76 kDa splice variant encoded by the human RALBP1 gene), the

rate-limiting step of the mercapturic acid pathway, a primary enzymatic defense against oxidants and electrophiles generated during oxidative stress.

Oxidative stress has a biphasic response in regulating cellular toxicity [44]. It has been shown that mild treatment with hydrogen peroxide, UV radiation and other oxidative stress stimuli favors proliferation of cells [45, 46]. Moderate levels of oxidative stress, in adapted tumor cells compared to normal cells, initiates proliferative signaling whereas high level of oxidative stress as induced by radiation and chemotherapy drugs triggers a cell death response [47]. 4HNE, at sub lethal concentrations can enhance cell viability through induction of thioredoxin reductase 1(TR1) in PC12 pheochromocytoma cells by activating Nrf-2 (nuclear factor related factor 2, the erythroid derived transcription factor) [48].

Rapidly proliferating tumor cells have elevated levels of oxidative stress due to high rates of proliferation which is not balanced by vascularization. Formation of lipid peroxidation products like 4HNE at concentrations surpassing the cancer cell ability for detoxification leads to extensive damage to the integrity of lipid membranes, DNA and proteins. Cellular variations in the generation and detoxification of 4HNE out of cells has tremendous impact on cell signaling and cell integrity due to the ability of 4HNE to form both reversible and irreversible adducts with many proteins in cells. Reaction of 4HNE with lysines leads to formation of Michael adducts, Schiff bases and 2-pentylpyrrole forms whereas 4HNE can form Michael adducts with cysteine and histidine residues in proteins [49-51]. Modification of specific amino acid residues in the proteins can have a vital impact on protein localization due to changes in the charge of proteins. Changes in the amino acid residues can influence the folding of proteins by affecting masking of

active sites or by exposing cryptic reactive sites for various cellular enzymes and proteins [52]. Enhanced oxidative stress can damage the intracellular calcium channels in mitochondria leading to enhanced cytosolic calcium and initiation of apoptosis [53-55]. The highly reactive hydroxyl radicals (OH) can also directly damage DNA causing DNA strand breaks, oxidized bases (8-oxo-dG), activation of p53 and apoptosis [56-58].

Tumor cells with higher levels of oxidative stress continue to survive due to inherent adaptations in cellular anti-oxidant networks. Exposure of cells to sub lethal concentrations of oxidative stress leads to cellular adaptations which enhance the expression of cellular detoxification enzymes like GSTs [59]. Such pre-conditioning to mild oxidative stress enhances the ability of cells to survive subsequent exposure to higher levels of oxidative stress [60]. The emergence of drug resistance is a major challenge which leads to recurrence of refractory tumors resistant to previously administered chemotherapy drugs and reduction of overall survival. The cancer cells develop drug resistance through multiple mechanisms like mutations in the target proteins, enhanced ability to cope with oxidative stress, increase in DNA repair proteins and inhibition of apoptosis by up regulating anti-apoptotic proteins [61-64]. The cellular adaptations to oxidative stress also regulate the sensitivity of cancer cells to chemotherapy drugs. Some of the anti-cancer drugs for RCC like sorafenib, a multi-specific tyrosine kinase inhibitor, induce apoptosis in tumor cells by elevating cytosolic calcium levels and inducing ROS production [65]. But, the major mechanism for drug resistance in tumor cells is the enhanced ability of tumor cells to actively transport the anti-cancer drugs out of cells thereby reducing the effective intracellular concentration of administered chemotherapy drugs [66, 67]. Hence, tumor anti-

oxidant and drug-metabolizing pathways represent attractive targets for effective anti-cancer interventions.

Mercapturic acid pathway: Central axis of oxidative stress regulation and drug metabolism

The mercapturic acid pathway represents the central axis of cellular anti-oxidant and drug-metabolizing networks (**Fig 2**). In the first step of this pathway, xenobiotics are activated by the cytochrome P-450 monooxygenase system to yield electrophilic metabolites. Endogenous substrates of P450 include ω-6 polyunsaturated fatty-acids (arachidonic acid, linoleic acid, γ-linolenic acid), the oxidative cleavage of which gives rise to the endogenous electrophile, 4HNE [68]. For xenobiotics that already possess electrophilic sites (i.e. alkylating agents), the need for P450 is bypassed. GSTs represent a diverse family of cytosolic and microsomal enzymes that catalyze the next step, phase II biotransformation, the attack of glutathione (GSH) on electrophilic sites of activated xenobiotics, as well as lipid-peroxidation-derived alkylating agents [68]. The most abundant of these lipid derived electrophilic toxin is 4HNE. It is metabolized primarily to its glutathione conjutate (GS-HNE) through a GST-catalyzed mechanism. Alkylating agent chemotherapy drugs (melphalan, chlorambucil, thiotepa) are effectively glutathionylated by GSTs, and the resulting glutathione-electrophile conjugates (collectively, GS-E) are substrates for ATP-dependent transmembrane transport by the glutathione-conjugate transporter, RLIP76. RLIP76 catalyzes the ATP-dependent transport of GS-E derived from lipid peroxidation products and chemotherapy drugs out of cells [69-71]. The effluxed GS-E are carried in extracellular fluid and plasma to the kidney where renal tubular cell rich in γ -glutamyl- transferase, located in the extracellular surface of renal epithelial cells, catalyzes the cleavage of the isopeptide bond (between the γ- carboxyl group of glutamate and

the amino group of cysteine) to yield a cysteinylglycine-electrophile conjugate [72]. The cysteinylglycine-electrophile conjugate is further cleaved to a cysteine-conjugate by the extracellular cysteinylglycine dipeptidase [73, 74]. The cysteine conjugates are taken up by renal tubular cells and converted into mercapturic acids (N-acetyl-S-cysteine conjugates) through N-acetylation by N-acetyltransferase [75]. The mercapturic acid end products formed are water soluble and excreted through organic ion transporters in renal tubular epithelium [76].

RLIP76 is also ubiquitously over-expressed in cancers, including RCC. Because ATP-dependent efflux of GS-E by RLIP76 is directly coupled with, and is the rate determining step of clathrin-dependent endocytosis (CDE), biological therapies based on extracellular ligand-cellular receptor interactions, including peptides, antibodies, nanoparticle and lipid particles that are subject to signal activation or inactivation through CDE, are also directly affected by RLIP76 [88]. Thus, the mercapturic acid pathway represents a natural and mechanistically significant metabolic axis for therapeutic intervention in kidney cancer for single-agent and combinatorial bio-chemotherapy in RCC.

Role of RLIP76 in regulating proliferation and drug resistance

The multifunctional role of mercapturic acid pathway transporter RLIP76 in regulating fundamental signaling processes of importance in cancer incidence, survival and drug-resistance has revealed an existential requirement of RLIP76 for the incidence and progression of many cancers [77-79]. RLIP76 contains two ATP binding sites-one each at the amino terminus (^{69}GKKKGK^{74}) and carboxyl terminus (^{418}GGIKDLSK^{425}) which regulate the ATP dependent efflux of GS-E and chemotherapy drugs [80, 81]. The transport function of RLIP76 is enhanced

by phosphorylation of T^{297} by PKCα [82-83]. RLIP76 binds to AP2 in the amino terminus [84]. The first central domain has Rac/cdc42 GAP activity leading to adhesion dependent Rac activation and cell spreading whereas the second central domain binds to Ral [85]. The carboxyl terminus of RLIP76 binds to Hsf1, POB1and CDK1 (**Fig 3**) [86, 87]. The binding of Hsf1 and AP2/POB1 inhibits the transport function or RLIP76 which also regulates the clathrin-mediated endocytosis of EGFR, IGFR and TGFβ [87, 88].

Hsf1 is a transcription factor which regulates the cellular transcriptional reprogramming to enable survival in the presence of enhanced oxidative stress [89]. During normal oxidative stress levels, Hsf1 and AP2/POB1 bind to RLIP76 and thus the transport function of RLIP76 and heat shock response due to Hsf1 are inhibited. Increase in oxidative stress leads to increased generation of GS-E of products of lipid peroxidation, activation of PKCα which together stimulate the activation of RLIP76 transport function along with favoring parallel translocation of Hsf1 to nucleus to stimulate the transcription of heat shock response genes [90]. Thus, the activation of RLIP76 not only enhances the detoxification of toxic metabolites and chemotherapy drugs but also stimulates the long-term cellular adaptive response to oxidative stress through Hsf1 mediated transcription of heat-shock proteins that help survival of cells in enhanced oxidative stress conditions.

Dietary compounds in cancer research

The research on the association between diet and the diseases spans a period of thousands of years. Hippocrates, the father of medicine had long before suggested that “Let food be thy medicine and medicine be thy food” [91]. The term nutraceutical (derived from “nutrition” and

"pharmaceutical") was coined by Stephen DeFelice in 1989 and refers to any substance that is a component of human diet with medicinal properties [92]. The human race has long been dependent on well characterized dietary regimens to prevent ill health and specialized herbal dietary preparations had been the mainstay to treat the incident diseases in many parts of the world including traditional Indian medicine and traditional Chinese medicine. The rapid advances in science and technology have elaborated the mechanistic framework of disease and have contributed to precise characterization of the active constituents of human diet leading to focused and well directed development of therapeutic interventions for respective diseases.

Natural phytochemicals have served as the lead compounds for many of the current anti-cancer drugs in clinical practice and other drugs in various stages of development. Curcumin, an active anti-cancer compound from the Indian spice turmeric, inhibits many key tumor signaling nodes including Bcl2, survivin, cyclin D1 and VEGF which has made it an attractive drug candidate for malignancies of many organs like breast, colon, lung and prostate [93, 94]. Silibinin, a natural compound in phase II clinical trials, has the potential to decrease prostate specific antigen (PSA) levels along with inhibiting metastases in both androgen-dependent and aggressive androgen-independent prostate cancer [95, 96]. Apigenin is another flavanone which effectively targets $HER2^{+}$ breast cancers along with inhibiting constitutive and TNF-α stimulated NF-κB activity in prostate cancers [97, 98]. Because of the proven record of prolonged and safe human consumption, the nutraceuticals have been attractive candidates for targeted therapeutic interventions for various malignancies.

Proteomics in cancer research

The incidence and progression of tumors from the normal cells in respective organs is accompanied by extensive and complex reprogramming of cellular transcriptional machinery which in turn causes significant changes in the global proteomic profile of cancer cells. The initial phase of cancer research focused on characterizing the master regulators of tumor transformation was focused on “tumor suppressors”, the loss of which promotes oncogenic transformation in normal cells and “oncogenes”, the over-expression or constitutive activation of which leads to incidence and invasive progression of cancers [99-101]. The later advances in cancer research expanded various proteins and molecules that regulate survival, invasion and malignant progression like matrix metalloproteinases, integrins and VEGF in transformed cells [102-104]. Further molecular and genetic studies elucidated the enhanced dependence of some of the cancers on specific signaling nodes compared to other tumors which lead to evolution of the conceptual framework of cancer into differentially regulated and highly interactive signaling networks in respective tumors.

Proteomics refers to the field of science focused on the study of global profile of cellular proteins in order to characterize the impact on associated protein networks, pathways and disease processes [105]. Thus, characterization of the proteomic profile of tumor cells with particular genetic aberrations would elucidate the alternations in the levels of major molecular effectors that mediate the tumor incidence, progression and drug action in respective tumors [105-107].

Mass spectrometry (MS) represents an advanced and sophisticated platform for the analysis and quantification of molecules. Mass spectrometry is based on the concept of detection

of mass-to-charge ratio (*m/z)* of ionized analyte molecules [108]. Proteins represent the principal molecular effectors in cells. Mass spectrometry based proteomic methods have contributed significantly to understanding the proteomic profile of various cancer genotypes [109]. In most proteomic studies, the protein samples are enzymatically digested using trypsin to generate peptides which are subjected to online chromatographic separation using reversed-phase liquid-chromatography (RP-LC) followed by detection of analyte peptides in the mass spectrometer [110]. The principal components of mass spectrometer include: a source of ionization where the analyte molecules in the solvent are converted to gas phase-ions, mass analyzers that function in separating the analyte molecules based on *m/z* of ionized analytes and an ion detector which detects the number of ions corresponding to particular *m/z* (**Fig 4**). The development of soft ionization techniques like electrospray ionization (ESI) have advanced the analytical procedures focused on polar and thermally unstable proteins and peptides [108,111]. The advanced mass spectrometers employ two stages of analysis of ions generated during MS analysis which is commonly referred to as MS/MS or tandem mass spectrometry [112]. In tandem mass spectrometry, during initial MS analysis or MS^1, the ionized ions from sample are separated according to *m/z.* The selected precursor ions are further fragmented by collision induced dissociation [113]. The fragmented ions are analyzed at the second stage which is also called MS/MS or MS^2. The quantification of ions corresponding to particular *m/z* leads to quantitative information about a particular peptide in the sample.

The data obtained from MS and MS/MS are further processed using bioinformatic softwares like Mascot (Matrix Science, Boston, MA) to identify peptides and corresponding proteins from protein databases followed by data analysis using additional softwares like

Scaffold (Proteome Software Inc., Portland, OR) to validate protein identifications and if required by the study to detect the differential levels of proteins in analyzed samples based on the sequence and abundance of fragmented peptides of respective proteins. The impact of differences in protein levels can be further analyzed by bioinformatic softwares like Ingenuity Pathway Analysis (Ingenuity Systems, Redwood City, CA) to characterize the differentially regulated biological networks, pathways and disease processes [114, 115]. Thus, in effect, proteomics has both expanded and deepened the understanding of the critical players and their complex interactions in the signaling networks of respective malignancies. The development of proteomics has not only lead to better understanding of cancer disease processes but has also significantly contributed to the elucidation of mechanisms of action of candidate drugs at different differentially regulated signaling networks in respective cancers.

DEVELOPMENT OF RESEARCH GOALS AND OBJECTIVES

The *VHL*-mutant (*VHL*-mut) RCC is mainly characterized by an up-regulation of HIF2-α relative to *VHL*-wild type (*VHL*-wt) RCC whereas HIF1-α mediates the effect of loss/inactivation of *VHL* in other organ tumors [116, 117]. In this regard, proteomic analysis of *VHL*-mut, HIF2-α over-expressing RCC relative to *VHL*-wt, HIF2-α lacking RCC was performed to characterize differential regulation of cellular metabolic and drug detoxification pathways by signaling networks analyses. The proteomic analyses between *VHL*-mut and *VHL*-wt RCC revealed lack of aldoketoreductase family1 member C1 (AKR1C1) and over-expression of mercapturic acid pathway enzyme GSTπ in *VHL*-mut RCC. Increased content and activity of the GSTπ, which catalyzes initial step in mercapturic acid pathway enzyme, was one of the earliest methods for identifying the transition between pre-neoplastic and neoplastic nodules in hepatic carcinogenesis [118]. The enzyme mediating the next step in mercapturic acid pathway, RLIP76 is known to transport current drugs of choice in RCC like sorafenib and sunitinib [67]. Previous studies in our laboratory had characterized that the inhibition of the mercapturic acid pathway transporter RLIP76 causes effective regression of RCC in mice xenografts without any overt toxicity [77-80]. Hence, further proteomic analyses were performed to elucidate the differentially regulated proteins by RLIP76 in *VHL*-mut RCC. While investigating the differential expression of AKR1C1 and GSTπ in *VHL*-mut and *VHL*-wt RCC, 2'-hydroxyflavanone (2HF, **Fig 5**) which is a known AKR1C inhibitor turned out to be significantly effective in inhibiting *VHL*-mut RCC. Hence, the anti-cancer effects of 2HF were further investigated to elucidate the mechanisms of action of 2HF in *VHL*-mut RCC.

This dissertation describes the differential regulation of signaling networks between *VHL*-mut, HIF2-α over-expressing RCC and *VHL*-wt, HIF2-α lacking RCC followed by the analyses of RLIP76 induced differential regulation of proteins in *VHL*-mut RCC which in turn expands the mechanistic basis for the potent anti-cancer effects of RLIP76 along with characterizing the role of 2HF for novel and safe chemopreventive interventions in *VHL*-mut RCC.

REFERENCES

1. Atkins, M.B., Ernstoff, M.S., Figlin, R.A., et al. (2007) Innovations and challenges in renal cell carcinoma: summary statement from the Second Cambridge Conference. *Clin Cancer Res*;**13**:667s-670s.

2. Linehan, W.M., Rini, B.I.and Yang J.C. Cancer of the Kidney DeVita, Hellman, and Rosenberg's Cancer: Principles & Practice of Oncology. *Lippincott-Williams*;8th Ed:1331-1332.

3. Linehan, W.M., Zbar B, and Klausner RD. Renal carcinoma.IN:Vogelstein B, Kinzler KW, eds. The genetic basis of human cancer McGraw-Hill;2nd Ed:2002:455.

4. Latif, F., Tory, K., Gnarra, J., et al. (1993) Identification of the von Hippel-Lindau disease tumor suppressor gene. *Science*;**260**:1317-20.

5. McKusick, V.A. Mendelian inheritance in man. *Johns Hopkins University Press*;12th Ed:http://www.omim.org/.

6. Kim, W.Y., and Kaelin, W.G. Role of VHL gene mutation in human cancer. (2004) *J Clin Oncol*;**22**:4991-5004.

7. Collins, E. T. (1894) Intra-ocular growths (two cases, brother and sister, with peculiar vascular new growth, probably retinal, affecting both eyes). *Trans Ophthalmol Soc* UK;**14**:141–149.

8. von Hippel, E. (1904) Ueber eine sehr seltene Erkrankung der Nethaut. *Graefe Arch Ophthalmol*;**59**:83–106.

9. Lindau, A. (1927) Zur Frage der Angiomatosis Retinae und Ihrer Hirncomplikation. *Acta Ophthalmol*;**4**:193–226.

10. Richard, S., Campello, C., Taillandier, L., Parker, F. and Resche, F. (1998) Haemangioblastoma of the central nervous system in von Hippel–Lindau disease. *J Int Med*; **243**:547–553.

11. Lamiell, J., Salazar, F., and Hsia, Y. (1989) von Hippel-Lindau disease affecting 43 members of a single kindred. *Medicine (Baltimore)*;**68**:1-29.

12. Maher, E., Webster, A.R., and Moore, A. (1995) Clinical features and molecular genetics of von Hippel-Lindau disease. *Ophthalmic Genet*;**16**:79-84.

13. Binkovitz, L., Johnson, C., and Stephens, D. (1990) Islet cell tumors in von Hippel-Lindau disease: Increased prevalence and relationship to the multiple endocrine neoplasias. *AJR Am J Roentgenol*;**155**:501-5.

14. Manski, T., Heffner, D., Glenn, G., et al. (1997) Endolymphatic sac tumors-A source of morbid hearing loss in von Hippel-Lindau disease. *JAMA*;**277**:1461-66.

15. Maher, E. and Kaelin, W. G. (1997) von Hippel–Lindau disease. *Medicine*;**76**:381–391.

16. Rini, B.I., Campbell, S.C. and Escudier, B. (2009) Renal cell carcinoma. *Lancet*;**373**:1119-1132.

17. Gnarra, J.R., Tory, K., Weng, Y., et al. (1994) Mutations of the *VHL* tumour suppressor gene in renal carcinoma. *Nat Genet*;**7**:85-90.

18. Hunt, J.D., van der Hel, O.L., McMillan, G.P., Boffetta, P. and Brennan, P. (2005) Renal cell carcinoma in relation to cigarette smoking: meta-analysis of 24 studies. *Int J Cancer*;**114**:101-108.

19. Shapiro, J.A., Williams, M.A. and Weiss, N.S. (1999) Body mass index and risk of renal cell carcinoma. *Epidemiology*;**10**:188-191.

20. Ross, R.K., Paganini-Hill, A., Landolph, J., Gerkins, V. and Henderson, B.E. (1989) Analgesics, cigarette smoking, and other risk factors for cancer of the renal pelvis and ureter. *Cancer Res*;**49**:1045-1048.

21. Semenza, G. L. and Wang, G. L. (1992) A nuclear factor induced by hypoxia via de novo protein synthesis binds to the human erythropoietin gene enhancer at a site required for transcriptional activation. *Mol Cell Biol*;**12**:5447–5454.

22. Wang, G. L., Jiang, B. -H., Rue, E. A. and Semenza, G. L. (1995) Hypoxia-inducible factor 1 is a basic-helix-loop-helix-PAS heterodimer regulated by cellular O2 tension. *Proc Natl Acad Sci USA*;**92**:5510–5514.

23. Bruick, R. and McKnight, S. (2002) Oxygen sensing gets a second wind. *Science*;**295**:807–808.

24. Kaelin, W.G.,Jr. (2002) Molecular basis of the VHL hereditary cancer syndrome. *Nat Rev Cancer*;**2**:673-682

25. Dames, S., Martinez-Yamout, M., De Guzman, R., Dyson, H. and Wright, P. (2002) From the cover: structural basis for Hif-1α/CBP recognition in the cellular hypoxic response. *Proc Natl Acad Sci USA*;**99**:5271–5276.

26. de Paulsen, N., Brychzy, A., Fournier, M.C., et al. (2001) Role of transforming growth factor-alpha in von Hippel--Lindau (VHL)(-/-) clear cell renal carcinoma cell proliferation: a

possible mechanism coupling VHL tumor suppressor inactivation and tumorigenesis. *Proc Natl Acad Sci U S A*;**98**:1387-1392.

27. Lager, D., Slagel, D. and Palechek, P. (1994) The expression of epidermal growth factor receptor and transforming growth factor-α in renal cell carcinoma. *Modern Pathol*;**7**:544–548.

28. Hewitson, K.S., McNeill, L.A., Riordan, M.V., et al. (2002) Hypoxia-inducible factor (HIF) asparagine hydroxylase is identical to factor inhibiting HIF (FIH) and is related to the cupin structural family. *J Biol Chem*;**277**:26351-26355.

29. Lando, D., Peet, D.J., Whelan, D.A., Gorman, J.J. and Whitelaw, M.L. (2002) Asparagine hydroxylation of the HIF transactivation domain a hypoxic switch. *Science*;**295**:858-861.

30**.** Ivan, M., Kondo, K., Yang, H., et al. (2001) HIFalpha targeted for VHL-mediated destruction by proline hydroxylation: implications for O2 sensing. *Science*;**292**:464-468.

31**.** Hon, W.C., Wilson, M.I., Harlos, K., et al. (2002) Structural basis for the recognition of hydroxyproline in HIF-1 alpha by pVHL. *Nature*;**417**:975-978.

32. Stebbins, C. E., Kaelin, W. G. and Pavletich, N. P. (1999) Structure of the VHL–elongin-C–elongin-B complex: implications for VHL tumor suppressor function. *Science*;**284**:455–461.

33. Bangiyeva, V., Rosenbloom, A., Alexander, A.E., Isanova, B., Popko, T. and Schoenfeld, A.R. (2009) Differences in regulation of tight junctions and cell morphology between VHL mutations from disease subtypes. *BMC Cancer*;**9**:229.

34. Iliopoulos, O., Kibel, A., Gray, S. and Kaelin, W. G. (1995) Tumor suppression by the human von Hippel–Lindau gene product. *Nature Med*;**1**:822–826.

35. Siemeister, G., Weindel, K., Mohrs, K., Barleon, B., Martiny-Baron, G. and Marme, D. (1996) Reversion of deregulated expression of vascular endothelial growth factor in human renal carcinoma cells by von Hippel-Lindau tumor suppressor protein. *Cancer Res*;**56**:2299-2301.

36. Davidowitz, E., Schoenfeld, A. and Burk, R. (2001) VHL induces renal cell differentiation and growth arrest through integration of cell–cell and cell–extracellular-matrix signaling. *Mol Cell Biol*;**21**:865–874.

37. Dieber-Rotheneder, M., Puhl, H., Waeg, G., Striegl, G., and Esterbauer, H. (1991) Effect of oral supplementation with D-alpha-tocopherol on the vitamin E content of human low density lipoproteins and resistance to oxidation. *J Lipid Res*;**32**:1325-1332.

38. Rahman, I., Biswas, S.K, Jimenez, L.A., Torres, M., and Forman, H.J. (2005) Glutathione, stress responses, and redox signaling in lung inflammation. *Antioxid Redox Signal*;**7**:42-59.

39. Bartsch, H., and Nair, J. (2006) Chronic inflammation and oxidative stress in the genesis and perpetuation of cancer: Role of lipid peroxidation, DNA damage, and repair. *Langenbecks Arch Surg*;**391**:499-510.

40. Esterbauer, H., Schaur, R.J., Zollner, H. (1991) Chemistry and biochemistry of 4-hydroxynonenal, malonaldehyde and related aldehydes. *Free Radic Biol Med*;**11**:81-128.

41. Sayre, L.M., Arora, P.K., Iyer, R.S. and Salomon, R.G. (1993) Pyrrole formation from 4-hydroxynonenal and primary amines. *Chem Res Toxicol*;**6**:19-22.

42. Petersen, D.R., and Doorn, J.A. (2004) Reactions of 4-hydroxynonenal with proteins and cellular targets. *Free Radic Biol Med*;**37**:937-945.

43. Mitchell, D.Y., and Petersen, D.R. (1987) The oxidation of alpha-beta unsaturated aldehydic products of lipid peroxidation by rat liver aldehyde dehydrogenases. *Toxicol Appl Pharmacol*; **87**:403-410.

44. Hancock, J.T., Desikan, R. and Neill, S.J. (2001) Role of reactive oxygen species in cell signalling pathways. *Biochemical Society Transactions*;**29**:345-350.

45. Dwivedi, S., Sharma, A., Patrick, B., et al. (2007) Role of 4-hydroxynonenal and its metabolites in signaling. *Redox Reports*;**12**:4-10.

46. Yadav, S., Zajac, E., Singhal, S.S. et al. (2007). Linking stress-signaling, glutathione metabolism, signaling pathways and xenobiotic transporters. *Cancer and Metastasis Reviews*;**26**: 59-69.

47. Yang, Y., Sharma, R., Sharma, A., et al. (2003). Lipid peroxidation and cell cycle signaling: 4-hydroxynonenal, a key molecule in stress mediated signaling. *Acta Biochimica Polonica*;**50**: 319-336.

48. Chen, Z.H., Saito, Y., Yoshida, Y., Sekine, A., Noguchi, N., and Niki, E. (2005) 4-hydroxynonenal induces adaptive response and enhances PC12 cell tolerance primarily through induction of thioredoxin reductase 1 via activation of Nrf2. *J Biol Chem*;**280**:41921-41927.

49. Isom, A.L., Barnes, S., Wilson, L., Kirk, M., Coward, L., and Darley-Usmar, V. (2004) Modification of cytochrome c by 4-hydroxy- 2-nonenal: Evidence for histidine, lysine, and arginine-aldehyde adducts. *J Am Soc Mass Spectrom*;**15**:1136-1147.

50. Fenaille, F., Guy, P.A., and Tabet, J.C. (2003) Study of protein modification by 4-hydroxy-2-nonenal and other short chain aldehydes analyzed by electrospray ionization tandem mass spectrometry. *J Am Soc Mass Spectrom*;**14**:215-226.

51. Liu, Z., Minkler, P.E., and Sayre, L.M. (2003) Mass spectroscopic characterization of protein modification by 4-hydroxy-2-(E)-nonenal and 4-oxo-2-(E)-nonenal. *Chem Res Toxicol*;**16**:901-911.

52. Sampey, B.P., Carbone, D.L., Doorn, J.A., Drechsel, D.A., and Petersen, D.R. (2007) 4-hydroxy-2-nonenal adduction of extracellular signal-regulated kinase (erk) and the inhibition of

hepatocyte erk-est-like protein-1-activating protein-1 signal transduction. *Mol Pharmacol*; **71**:871-883.

53. Pelicano, H., Feng, L., Zhou, Y., et al (2003). Inhibition of mitochondrial respiration: a novel strategy to enhance drug-induced apoptosis in human leukemia cells by a reactive oxygen species-mediated mechanism. *J Biol Chem*;**278**:37832–37839.

54. Carmody, R.J., and Cotter, T.G., (2001) Signalling apoptosis: a radical approach. *Redox Rep*;**6**:77–90.

55. Randerath, K., Randerath, E., Smith, C.V. and Chang, J. (1996) Structural origins of bulky oxidative DNA adducts (type II I-compounds) as deduced by oxidation of oligonucleotides of known sequence. *Chem Res Toxicol*;**9:**247-254.

56. Lloyd, D.R., Phillips, D.H. and Carmichael, P.L. (1997) Generation of putative intrastrand cross-links and strand breaks in DNA by transition metal ion-mediated oxygen radical attack. *Chem Res Toxicol*;**10**:393-400.

57. Dipple, A. 1995. DNA adducts of chemical carcinogens. Carcinogenesis;**16**:437–441.

58. Jiang, M., Wei, Q., Pabla, N., et al. (2007) Effects of hydroxyl radical scavenging on cisplatin-induced p53 activation, tubular cell apoptosis and nephrotoxicity. *Biochem Pharmacol*;**73**:1499-1510.

59. Singhal, S.S., Godley, B.F., Chandra, A., et al. (1999) Induction of glutathione S-transferase hGST 5.8 is an early response to oxidative stress in RPE cells. *Invest Ophthalmol Vis Sci*;**40**:2652-2659.

60. Yang, Y., Sharma, A., Sharma, R., et al. (2003) Cells preconditioned with mild, transient UVA irradiation acquire resistance to oxidative stress and UVA-induced apoptosis: role of 4-hydroxynonenal in UVA-mediated signaling for apoptosis. *J Biol Chem*;**278**:41380-41388.

61. Sos, M.L., Koker, M., Weir, B.A., et al. (2009) PTEN loss contributes to erlotinib resistance in EGFR-mutant lung cancer by activation of Akt and EGFR. *Cancer Res*;**69**:3256-3261.

62. Takeda, M., Okamoto, I., Fujita, Y., et al. (2010) De novo resistance to epidermal growth factor receptor-tyrosine kinase inhibitors in EGFR mutation-positive patients with non-small cell lung cancer. *J Thorac Oncol*;**5**:399-400.

63. Xu, Z., Chen, Z.P., Malapetsa, A., et al. (2002) DNA repair protein levels vis-a-vis anticancer drug resistance in the human tumor cell lines of the National Cancer Institute drug screening program. *Anticancer Drugs*;**13**:511-519.

64. Teixeira, C., Reed, J.C. and Pratt, M.A. (1995) Estrogen promotes chemotherapeutic drug resistance by a mechanism involving Bcl-2 proto-oncogene expression in human breast cancer cells. *Cancer Res*;**55**:3902-3907.

65. Rahmani, M., Davis, E.M., Crabtree, T.R., et al. (2007) The kinase inhibitor sorafenib induces cell death through a process involving induction of endoplasmic reticulum stress. *Mol Cell Biol*;**27**:5499-5513.

66. Awasthi, S., Sharma, R., Singhal, S.S., Zimniak, P., and Awasthi, Y.C. (2002) RLIP76, a novel transporter catalyzing ATP-dependent efflux of xenobiotics. *Drug Metab Dispos* ;**30**:1300–10.

67. Singhal, S.S., Sehrawat, A., Sahu, M., et al. (2010) RLIP76 transports sunitinib and sorafenib and mediates drug resistance in kidney cancer. *Int J Cancer*;**126**:1327–38.

68. Marchand, D.H. and Abdel-Monem, M.M. (1985). Glutathione S-transferases catalyzed conjugation of 1,4-disubstituted butanes with glutathione in vitro. *Biochem Biophys Res Commun*;**128**:360-367.

69. Singhal, S.S., Yadav, S., Singhal, J., Sahu, M., Sehrawat, A., and Awasthi, S. (2008). Diminished drug transport and augmented radiation sensitivity caused by loss of RLIP76. *FEBS Lett*;**582**:3408-14.

70. Awasthi, S., Cheng, J., Singhal, S.S., et al (2000). Novel function of human RLIP76: ATP-dependent transport of glutathione-conjugates and doxorubicin. *Biochemistry*;**39**:9327-34.

71. Awasthi, S., Singhal, S.S., Sharma, R., Zimniak, P., and Awasthi, Y.C. (2003). Transport of glutathione-conjugates and chemotherapeutic drugs by RLIP76: a novel link between G-protein and tyrosine-kinase signaling and drug-resistance. *Int J Cancer*;**106**:635-46.

72. Tate, S.S. and Meister, A. (1985). Gamma-Glutamyl transpeptidase from kidney. *Methods Enzymol*;**113**:400-419.

73. Tsao, B. and Curthoys, N.P. (1980). The absolute asymmetry of orientation of gamma-glutamyltranspeptidase and aminopeptidase on the external surface of the rat renal brush border membrane. *J Biol Chem*;**255**:7708-7711.

74. Okajima, K., Inoue, M. and Morino, Y. (1981). Topology and some properties of the renal brush border membrane-bound peptidase(s) participating in the metabolism of S-carbamidomethyl glutathione. *Biochim Biophys Acta*;**675**:379-385.

75. Larsen, G.L. and Bakke, J.E. (1981). Enterohepatic circulation in formation of propachlor (2-chloro-N-isopropylacetanilide) metabolites in the rat. *Xenobiotica*;**11**:473-480.

76. Inoue, M., Okajima, K. and Morino, Y. (1981). Renal transtubular transport of mercapturic acid in vivo. *Biochim Biophys Acta*;**674**:122-128.

77. Singhal, S.S., Awasthi, Y.C. and Awasthi, S. (2006). Regression of melanoma in a murine model by RLIP76 depletion. *Cancer Res*;**66**:2354-2360.

78. Singhal, S.S., Singhal, J., Yadav, S., et al. (2007).Regression of lung and colon cancer xenografts by depleting or inhibiting RLIP76 (RALBP1) *Cancer Res*;**67**:4382-4389.

79. Singhal, S.S., Roth, C., Leake, K., Singhal, J., Yadav, S. and Awasthi, S. (2009) Regression of prostate cancer xenografts by RLIP76 depletion. *Biochem Pharmacol*;**77**:1074-1083.

80. Awasthi, S., Cheng, J., Singhal, S.S., et al. (2000) Novel function of human RLIP76: ATP-dependent transport of glutathione conjugates and doxorubicin. *Biochemistry*;**39**:9327-34.

81. Awasthi, S., Cheng, J.Z., Singhal, S.S., et al. (2001) Functional reassembly of ATP-dependent xenobiotic transport by the N- and C-terminal domains of RLIP76: identification of ATP binding sequences. *Biochemistry*;**40**:4159-68.

82. Singhal, S.S.,Yadav, S., Singhal, J., Drake, K., Awasthi, Y.C., and Awasthi, S. (2000) The Role of PKCα and RLIP76 inTransportmediated Doxorubicin-resistance in Lung Cancer. *FEBS Lett*;**579**:4635-41.

83. Singhal, S.S.,Yadav, S., Singhal, J., Awasthi,Y.C., and Awasthi, S. (2006) Mitogenic and drug-resistance mediating effects of PKC α require RLIP76. *Biochem Biophys Res* Commun;**348**:722-7.

84. Jullien-Flores, V., Mahe, Y., Mirey, G., Leprince, C., Meunier-Bisceuil, B., Sorkin, A. and Camonis, J.H. (2000) RLIP76, an effector of the GTPase Ral, interacts with the AP2 complex: involvement of the Ral pathway in receptor endocytosis. *J Cell Sci*;**113(Pt 16):**2837-2844.

85. Goldfinger, L.E., Ptak, C., Jeffery, E.D., Shabanowitz, J., Hunt, D.F., and Ginsberg, M.H. (2006) RLIP76 (RalBP1) is an R-Ras effector that mediates adhesion-dependent Rac-activation and cell migration. *J Cell Biol*;**174**:877–88.

86. Rosse, C., L'Hoste, S., Offner, N., Picard, A. and Camonis, J. (2003) RLIP, an effector of the Ral GTPases, is a platform for Cdk1 to phosphorylate epsin during the switch off of endocytosis in mitosis. *J Biol Chem*;**278:**30597-30604.

87. Singhal, S.S., Yadav, S., Drake, K., Singhal, J., and Awasthi, S. (2008) Hsf-1 and POB1 induce drugsensitivity and apoptosis by inhibiting Ralbp1. *J Biol Chem*;**283**:19714–29.

88. Singhal, S.S., Wickramarachchi, D., Yadav, S., Singhal, J., Leake, K., Vatsyayan, R., Chaudhary, P., Lelsani, P., Suzuki, S., Yang, S., Awasthi, Y.C. and Awasthi, S. (2011) Glutathione-conjugate transport by RLIP76 is required for clathrin-dependent endocytosis and chemical carcinogenesis. *Mol Cancer Ther;***10:**16-28.

89. Dai, C., Whitesell, L., Rogers, A.B., and Lindquist, S. (2007) Heat shock factor 1 is a powerful multifaceted modifier of carcinogenesis. *Cell*;**130**:1005–1018.

90. Awasthi, S., Singhal, S.S., Awasthi, Y.C., et al. (2008) RLIP76 and Cancer. *Clin Cancer Res*;**14:**4372-4377.

91. Gupta, S.C., Kim, J.H., Prasad, S. and Aggarwal, B.B. (2010) Regulation of survival, proliferation, invasion, angiogenesis, and metastasis of tumor cells through modulation of inflammatory pathways by nutraceuticals. *Cancer Metastasis Rev*;**29**:405-434.

92. Brower, V. (1998) Nutraceuticals: poised for a healthy slice of the healthcare market? *Nat Biotechnol*;**16**:728-731.

93. Cai, X. Z., Wang, J., Li, X. D., et al. (2009). Curcumin suppresses proliferation and invasion in human gastric cancer cells by downregulation of PAK1 activity and cyclin D1 expression. *Cancer Biology & Therapy*;**8**:1360–1368.

94. Kunnumakkara, A. B., Diagaradjane, P., Anand, P., Harikumar, K. B., Deorukhkar, A., and Gelovani, J., et al. (2009). Curcumin sensitizes human colorectal cancer to capecitabine by

modulation of cyclin D1, COX-2, MMP-9, VEGF and CXCR4 expression in an orthotopic mouse model. *Int J of Cancer*;**125**:2187–2197.

95. Zi, X. and Agarwal, R. (1999). Silibinin decreases prostate-specific antigen with cell growth inhibition via G1 arrest, leading to differentiation of prostate carcinoma cells: implications for prostate cancer intervention. *Proc Natl Acad Sci U S A*;**96**:7490-7495.

96. Singh, R.P., Raina, K., Sharma, G. et al. (2008). Silibinin inhibits established prostate tumor growth, progression, invasion, and metastasis and suppresses tumor angiogenesis and epithelial-mesenchymal transition in transgenic adenocarcinoma of the mouse prostate model mice. *Clin Cancer Res*;**14**:7773-7780.

97. Way, T.D., Kao, M.C. and Lin, J.K. (2004) Apigenin induces apoptosis through proteasomal degradation of HER2/neu in HER2/neu-overexpressing breast cancer cells via the phosphatidylinositol 3-kinase/Akt-dependent pathway. *J Biol Chem*;**279**:4479-4489.

98. Shukla, S. and Gupta, S. (2004). Suppression of constitutive and tumor necrosis factor alpha-induced nuclear factor (NF)-kappaB activation and induction of apoptosis by apigenin in human prostate carcinoma PC-3 cells: correlation with down-regulation of NF-kappaB-responsive genes. *Clin Cancer Res*;**10**:3169-3178.

99. Levine, A.J. (1993) The tumor suppressor genes. *Annu. Rev. Biochem.***;62:**623-651

100. Varmus, H.E. (1984) The molecular genetics of cellular oncogenes. *Annu Rev Genet*;**1:**, 553-612.

101. Egeblad, M. and Werb, Z. (2002) New functions for the matrix metalloproteinases in cancer progression. *Nat Rev Cancer*;**2:**161-174.

102. Plate, K.H., Breier, G., Millauer, B., Ullrich, A. and Risau, W. (1993) Up-regulation of vascular endothelial growth factor and its cognate receptors in a rat glioma model of tumor angiogenesis. *Cancer Res*;**5:**5822-5827.

103. Nagaprashantha, L.D., Vatsyayan, R., Lelsani, P.C., Awasthi, S. and Singhal, S.S. (2011) The sensors and regulators of cell-matrix surveillance in anoikis resistance of tumors. *Int J Cancer***;128:**743-752.

104. Celis, J.E. and Gromov, P. (2003) Proteomics in translational cancer research: toward an integrated approach. *Cancer Cell***;3:**9-15.

105. Blackstock, W.P.,and Weir, M.P. (1999). "Proteomics: quantitative and physical mapping of cellular proteins". *Trends Biotechnol*;**17**:121–127.

106. Brichory, F., Beer, D., Le Naour, F., Giordano, T. and Hanash, S. (2001) Proteomics-based identification of protein gene product 9.5 as a tumor antigen that induces a humoral immune response in lung cancer. *Cancer Res;***61:**7908-7912.

107. Stevens, S.M.,Jr, Duncan, R.S., Koulen, P. and Prokai, L. (2008) Proteomic analysis of mouse brain microsomes: identification and bioinformatic characterization of endoplasmic reticulum proteins in the mammalian central nervous system. *J. Proteome Res*;**7:**1046-1054.

108. Fenn, J. B., Mann, M., Meng, C. K., Wong, S. F., and Whitehouse, C. M. (1989) Electrospray ionization for mass spectrometry of large biomolecules. *Science*;**246**:64-71.

109. Aebersold, R. and Mann, M. (2003) Mass spectrometry-based proteomics. *Nature*;**422**:198-207.

110. Mann, M., Hendrickson, R. C., and Pandey, A. (2001) Analysis of proteins and proteomes by mass spectrometry. *Annu Rev Biochem*;**70**:437-473.

111. Rauniyar, N. (2010) "Mass Spectrometry-Based Characterization of Posttranslational Modifications by 4-Hydroxy-2-Nonenal" UNTHSC *Theses and Dissertations.* Paper 65.

112. McLafferty, F.W. (1981) Tandem mass spectrometry. *Science*;**214**:280-287.

113. Papayannopoulos I.A. (1995) The interpretation of collision-induced dissociation tandem mass spectra of peptides. *Mass Spectrometry Reviews*;**14**:49-73.

114. Sivachenko, A.Y. and Yuryev, A. (2007) Pathway analysis software as a tool for drug target selection, prioritization and validation of drug mechanism. *Expert Opin The. Targets*;**11:**411-421.

115. Fenyo, D. (2000) Identifying the proteome: software tools. *Curr Opin Biotechnol;***11:**391-395.

116. Shinojima, T., Oya, M., Takayanagi, A., Mizuno, R., Shimizu, N., and Murai, M. (2007) Renal cancer cells lacking hypoxia inducible factor (HIF)-1alpha expression maintain vascular endothelial growth factor expression through HIF-2 alpha. *Carcinogenesis*;**28**:529–536.

117. Kondo, K., Kim, W. Y., Lechpammer, M., and Kaelin, W. G.,Jr. (2003) Inhibition of HIF2alpha is sufficient to suppress pVHL-defective tumor growth. *PLoS Biol*.;1:E83.

118. Moore MA, Nakagawa K, Satoh K, et al. (1987) Single GST-P positive liver cells-putative initiated hepatocytes. *Carcinogenesis*;**8**:483-486.

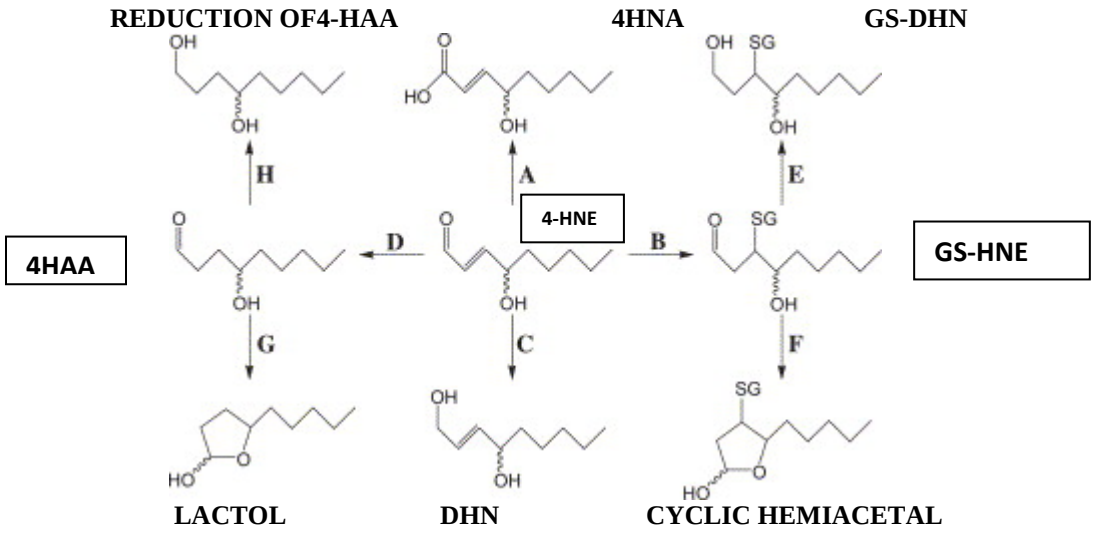

Figure 1. Major pathways of biotransformation of 4HNE (A) Aldehyde dehydrogenase 2 (ALDH2)-catalyzed oxidation to 4HNA. (B) Spontaneous or GST-mediated GSH conjugation yielding GS–4HNE. (C) Enzyme-catalyzed reduction to DHN. (D) Aldehyde oxidase (AO)-mediated reduction of C═C yielding 4HAA. (E) Aldose reductase (AR)-catalyzed reduction to GS-DHN. (F) Spontaneous rearrangement to a cyclic hemiacetal adduct. (G) Spontaneous rearrangement to a lactol. (H) Reduction of 4HAA [42, 43].

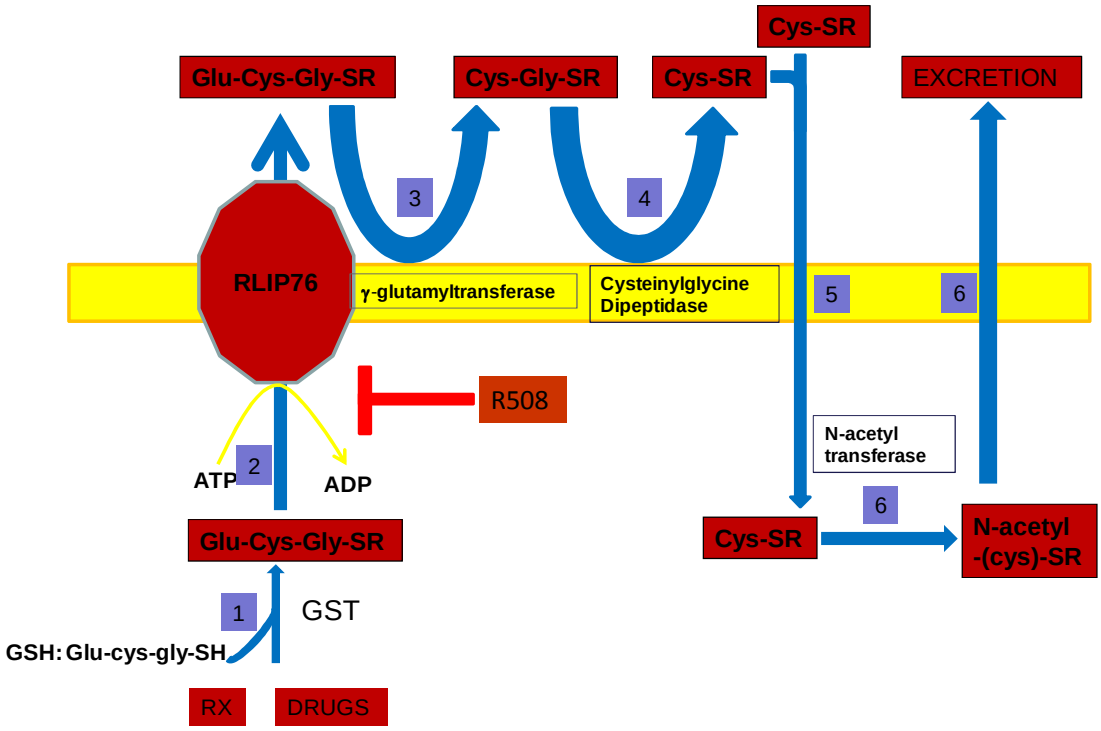

Figure 2. Mercapturic acid pathway-Central axis of oxidative stress regulation and drug metabolism Glutathione S transferases (GSTs) catalyze the first rate limiting step of the attack of glutathione (GSH) on the electrophilic center of products of lipid peroxidation like 4HNE and chemotherapy drugs leading to formation of thioether conjugate of GSH (GS-E). RLIP76 catalyzes the ATP-dependent transport of GS-E of lipid peroxidation products (RX) and chemotherapy drugs out of cells. The γ -glutamyltransferase located in the extracellular surface of the plasma membrane catalyzes the cleavage of isopeptide bond to yield cysteinylglycine conjugates. The cysteinyl glycine conjugate is further cleaved into cysteine conjugate by the extracellular cysteinylglycine dipeptidase. The cysteine conjugates are taken up again by the cells which are converted into mercapturic acid derivatives (N-acetyl-S-cysteine conjugates) by the addition of N-acetyl moiety by the action of N-acetyltransferase. The mercapturic acid end products formed are water soluble and excreted by the renal tubules.

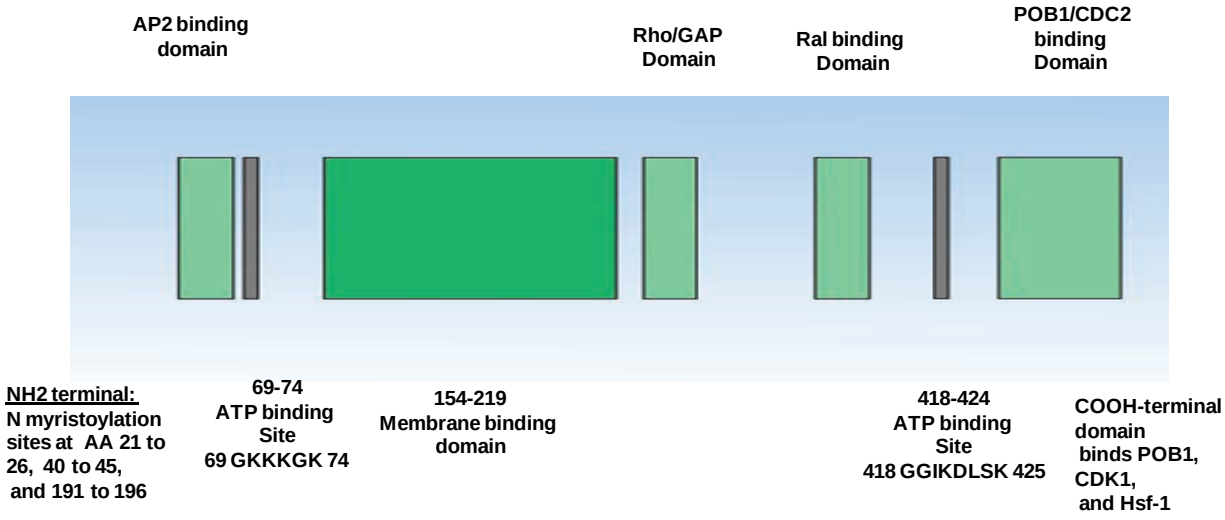

Figure 3. Schematic diagram of the structural domains of RLIP76 RLIP76 contains two ATP binding sites-one each at the amino terminus (^{69}GKKKGK^{74}) and carboxyl terminus (^{418}GGIKDLSK^{425}) which regulate the ATP dependent efflux of GS-E and chemotherapy drugs. RLIP76 binds to AP2 in the amino terminal. The first central Rho/GAP domain mediates adhesion dependent Rac activation whereas the second central domain binds to Ral. The carboxyl terminus of RLIP76 binds to Hsf1, CDC2, POB1, and CDK1 [90].

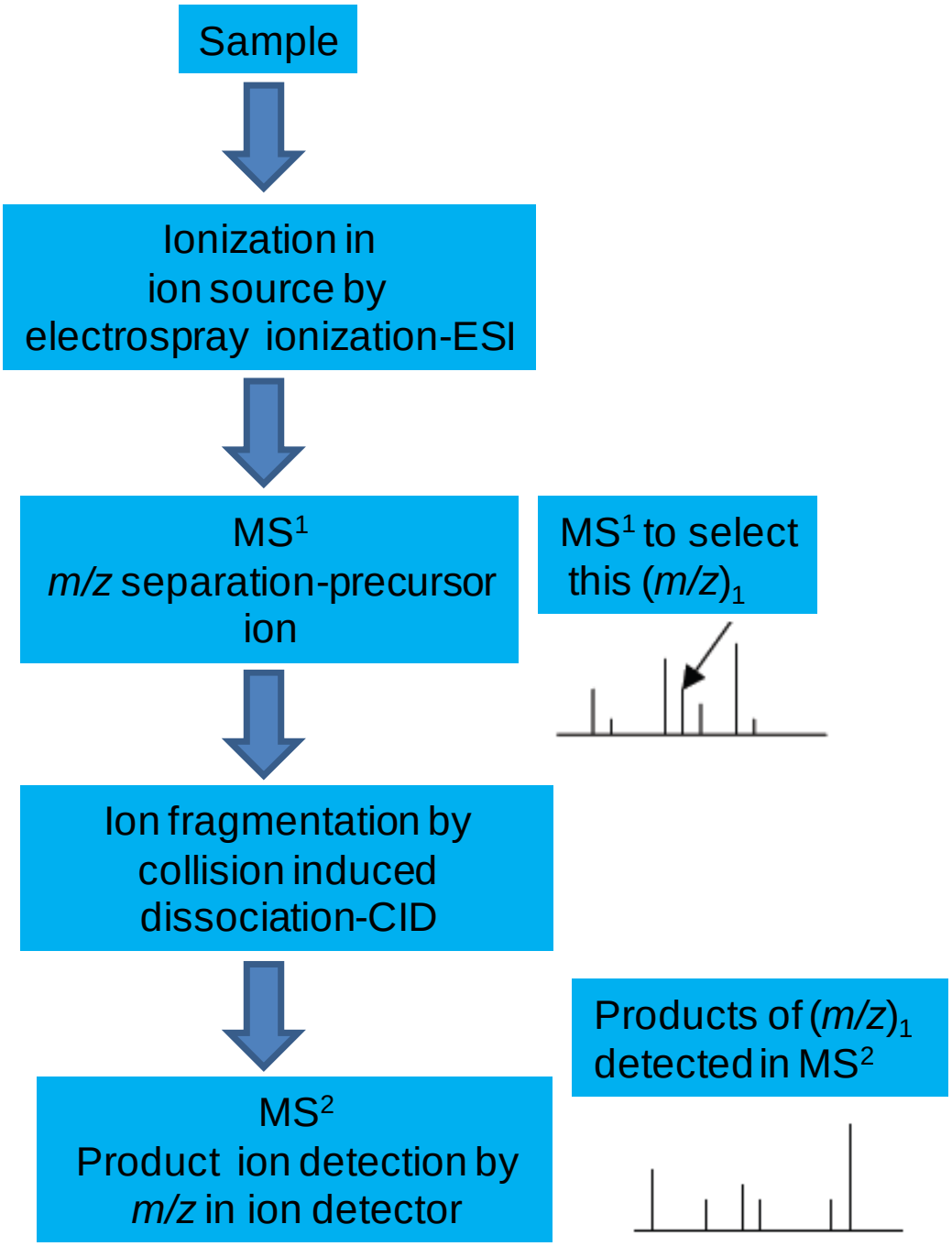

Figure 4. Schematic diagram representing components and the sequence of analysis within the mass spectrometer.

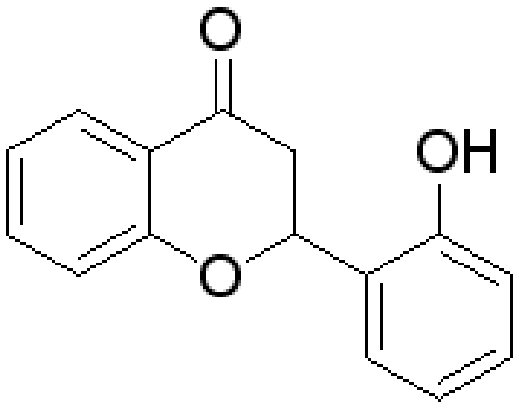

Figure 5. The structure of 2'-Hydroxyflavanone Empirical formula - $C_{15}H_{12}O_{3,}$ Molecular weight-240.25.

CHAPTER II

PROTEOMIC ANALYSIS OF SIGNALING NETWORKS REGULATION IN RENAL CELL CARCINOMAS WITH DIFFERENTIAL *VHL* AND HYPOXIA-INDUCIBLE FACTOR-2α EXPRESSION

INTRODUCTION

Renal cell carcinoma (RCC) is one of the top ten cancers incident in the USA [1]. Loss of the tumor suppressor von Hippel–Lindau (*VHL*) gene is an established genetic risk factor for RCC [2]. *VHL* mutations have been implicated in 75% of clear cell RCC, the most common form of RCC [3]. RCC has been associated with an upward trend over time due to increasing prevalence of common risk factors in the general population like cigarette smoking and obesity [4,5].

Loss-of-function mutations in the *VHL* gene up-regulate hypoxia-inducible factor 1-α (HIF1-α) and hypoxia-inducible factor 2-α (HIF2-α) signaling but advanced stages of RCC have predominantly increased expression of HIF2-α [6,7]. Over-expression of HIF2-α in RCC leads to enhanced angiogenesis and tumor progression even in the absence of HIF1-α [8]. Along with some common molecular targets, the HIF1-α and HIF2-α have distinctly regulated differential molecular targets of importance in transformation and metastatic progression [9]. According to

our knowledge, until today, there are no proteomic studies reporting the transitions in the nature of tumor signaling networks that accompany the *VHL*-mut, HIF2-α over-expressing RCC, particularly in relation to *VHL*-wt, HIF2-α lacking RCC. Such a mechanistic study into the transition of vital tumor signaling networks would be of potential biological and clinical significance. Hence, in the context of dependence of RCC on HIF2-α, we studied the differential regulation of cellular proteome in 786-O (*VHL*-mut, over-expressing HIF2-α) and CAKI-2 (*VHL*-wt, lacking HIF2-α) RCC cell lines. The 786-O cells express HIF2-α according to previous studies and thus represent a molecular environment of *VHL*-mut genotype that corresponds to advanced stages of RCC [6,10].

The drug sensitivity assays in our previously published reports have indicated the enhanced sensitivity of *VHL*-wt CAKI-2 RCC cells to sorafenib compared to *VHL*-mut cells [11]. In this regard, our preliminary proteomic analysis revealed enhanced-expression of aldo keto reductase family 1, member C1 and lack of expression of glutathione S-transferase π in *VHL*-wt RCC [12]. The tumor energetics and proliferation are regulated by hundreds of proteins in tumor cells. Identification of principal up-regulated and down-regulated proteins in the context of specific *VHL* genotypes of RCC would not only enhance the understanding of the major regulators among such hundreds of proteins but also potentially helps to streamline the therapeutic strategies in order to prioritize the drug targets towards a single or set of proteins of unique relevance to particular genotype of RCC.

Correlation between spectral counts and protein quantities has also been convincingly shown by Liu *et al* [13]. Therefore, we performed quantitative proteomic analysis of *VHL*-wt

and *VHL*-mut RCC cells lines using a previously validated and published label-free spectral counting-based LC-MS/MS method [14].

EXPERIMENTAL METHODS

Materials All chemicals and reagents were purchased from Sigma Aldrich (St. Louis, MO).

Cell Lines and Cultures The *VHL*-wt (CAKI-2) human RCC cell line was purchased from ATCC, Manassas, VA. The *VHL*-mut (786-O) cells were kindly authenticated and provided by Dr. William G. Kaelin, Dana-Farber Cancer Institute and Harvard Medical School, Boston, MA. All cells were cultured at 37 °C in a humidified atmosphere of 5 % CO_2 in RPMI-1640 medium supplemented with 10 % FBS and 1% P/S solution. Also, before proteomic analysis, we confirmed the differential expression of HIF2-α between the RCC cell lines (**Fig S1**).

Cell viability assay Cell density measurements were performed using a hemocytometer to count reproductive cells resistant to staining with trypan blue. Approximately 20,000 cells were plated into each well of 96-well flat-bottomed micro-titer plates. After 12 h incubation at 37 ^{o}C, RPMI-1640 medium containing different concentrations of aminooxyacetate (AOA, ranging from 0.1 - 5 mM) were added to the cells. After 24, 48 and 72 h incubation, respectively, 20 μL of 5 mg/mL 3-(4,5-dimethylthiazol-2-yl)-2,5-diphenyltetrazolium bromide (MTT) were introduced to each well and incubated for 2 h of exposure. The plates were centrifuged and medium was decanted. Cells were subsequently dissolved in 100 μL DMSO with gentle shaking for 2 h at room temperature, followed by measurement of optical density at 570 nm [11]. For assessment

of cell viability in medium without glutamine supplementation, the cells were plated and after 12 h incubation at 37 ^{o}C in RPMI-1640 with glutamine the medium was changed to RPMI-1640 medium without glutamine. The MTT assay was performed at 24, 48 and 72 h, as indicated above. Four replicate wells were used at each point in each of three separate measurements (n = 12).

Sample preparation RCC cells were resuspended in buffer containing 20 mM Tris-HCl, 50 mM NaCl, 6 M urea, 10 mM sodium pyrophosphate, 1 mM sodium fluoride and 1 mM sodium orthovanadate and incubated in ice for 30 min followed by six freeze thaw cycles to ensure adequate lysis of the cells. The sample was centrifuged at 13,300 rpm for 30 min at 4 ^{o}C. The clear supernatant was collected carefully and protein concentration was measured using BCA assay (Bio-Rad, CA). 200 µg of protein from each sample was reduced using 2.5 mM dithiothreitol (DTT) at 65 ^{o}C for 30 min followed by carbamidomethylation of thiol groups using 7 mM idoacetamide for 30 min at room temperature in the dark. The unreacted idoacetamide was quenched by addition of DTT to 2.5 mM with additional 15 min incubation. The sample was then diluted in 50 mM ammonium bicarbonate to lower the urea concentration to less than 2 mM followed by digestion with sequencing grade trypsin (Promega, Madison, WI) for 15 h at enzyme: substrate ratio of 1:25. Following digestion, proteolytic activity was terminated by acidifying the reaction mixture with acetic acid to pH <3.0. The samples were desalted using C_{18} cartridges (Supelco, Bellfonet, PA) and the cartridge eluate was evaporated to dryness by lyophilizing at 4 ^{o}C. The residues were reconstituted in 25 µL of loading solvent containing 0.1% (v/v) acetic acid and 5% (v/v) acetonitrile in 94.9% (v/v) water. Five µL aliquots were used for LC–MS/MS analyses.

Liquid chromatography–tandem mass spectrometry LC–ESI-MS/MS analysis of the samples was performed using a hybrid linear quadrupole ion trap–Fourier transform ion cyclotron resonance (7-T) mass spectrometer (LTQ-FT, Thermo Finnigan, San Jose, CA) equipped with a nano-electrospray ionization source and operated with Xcalibur (version 2.2) and Tune Plus (version 2.2) data acquisition software. Online reversed-phase high performance liquid chromatography (RP-HPLC) was performed with an Eksigent nano-LC-2D (Eksigent, Dublin, CA) system. An amount of 5 µL of the sample was automatically loaded onto the IntegraFrit™ sample trap (2.5 cm x 75 µm) (New Objective, Woburn, MA), for sample concentration and desalting, at a flow rate of 1.5 µL/min in a loading solvent containing 0.1% (v/v) acetic acid and 5% (v/v) acetonitrile in 94.9% (v/v) water prior to injection onto a reverse-phase column (NAN75-15-03-C18-PM; 75 µm i.d. x 15 cm, LC Packings, Sunnyvale, CA) packed with C_{18} beads (3 µm, 100 Å pore size, PepMap). Mobile-phase buffer A consisted of 0.1% (v/v) acetic acid and 99.9% (v/v) water, and mobile-phase buffer B consisted of 0.1% (v/v) acetic acid and 99.9% (v/v) acetonitrile. Following desalting and injection onto the analytical column, peptides were separated using the following gradient conditions: (1) 5 min in 95.2% solvent A for equilibration; (2) linear gradient to 40% solvent B over 90 min and holding at 40% solvent B for isocratic elution for 5 min; (3) increasing the gradient to 90% solvent B and maintaining for 5 min; and finally (4) 95.2% solvent A in the next 20 min. The flow rate through the column was 250 nL/min. Peptides eluted through a Picotip emitter (internal diameter 10 ± 1 µm; New Objective) were directly supplied into the nano-electrospray source of the mass spectrometer. Spray voltage and capillary temperature during the gradient run were maintained at 2.0 kV and 250 ºC. Conventional data-dependent mode of acquisition was utilized in which

an accurate *m/z* survey scan was performed in the FTICR cell followed by parallel MS/MS linear ion trap analysis of the top five most intense precursor ions. FTICR full-scan mass spectra were acquired at 50000 mass resolving power (*m/z* 400) from *m/z* 350 to 1500 using the automatic gain control mode of ion trapping. Peptide fragmentation was performed by collision-induced dissociation (CID) in the linear ion trap using a 3.0-Th isolation width and 35% normalized collision energy with helium as the target gas. The precursor ion that had been selected for CID was dynamically excluded from further MS/MS analysis for 60 s.

Database search MS/MS data generated by data dependent acquisition via the LTQ-FT were extracted by BioWorks version 3.3 and searched against a composite IPI human protein sequence database (IPI _human_v 3.73.par) containing both forward and randomized sequences using the Mascot version 2.2 (Matrix Science, Boston, MA) search algorithm. Mascot was searched with a fragment ion mass tolerance of 0.80 Da and a parent ion tolerance of 15.0 ppm assuming the digestion enzyme trypsin with the possibility of one missed cleavage. Carbamidomethylation of cysteine was specified as a fixed modification while oxidation of methionine, N-terminal protein acetylation, N-terminal peptide and lysine carbamoylation, and phosphorylation of serine and threonine were specified as variable modifications.

Data compilation, relative quantification and analysis of signaling networks The software program Scaffold (version Scaffold 3.0, Proteome Software Inc., Portland, OR) was employed to validate MS/MS-based peptide and protein identifications. Initial peptide identifications were accepted if they could be established at greater than 95% probability as specified by the Peptide Prophet algorithm [15]. Protein identifications were accepted if they could be established at

greater than 99% probability and contained at least 2 identified unique peptides. Protein probabilities were assigned by the Protein Prophet algorithm [16]. These identification criteria typically established a <0.01% false discovery rate based on a decoy database search strategy. Scaffold allows for simultaneous comparison of multiple proteomic data sets in which the list of identified proteins can be sorted by various parameters. The spectral counting technique for relative protein quantitation utilizes the total number of MS/MS spectra identified for a particular protein as a measure of protein abundance and, consequently, this parameter was used to classify the RCC protein identifications within Scaffold. The method for relative quantitation followed published protocols in which the change in abundance was inferred from the ratio as follows [17,18]:

$$\text{Ratio} = [(n_{VHL\text{-mut}}/n_{VHL\text{-wt}})]$$

where $n_{VHL\text{-mut}}$ and $n_{VHL\text{-wt}}$ were the total number of identified MS/MS spectra (normalized spectral counts from Scaffold) for a particular protein in the *VHL*-mut and *VHL*-wt RCC cells, respectively. A 50% peptide probability was used for the initial list of high-confidence identifications (99% protein confidence, 95% peptide confidence and containing 2 unique peptides) in order to include peptides with lower Mascot scores that represent true positive identifications and would improve the overall spectral counting sensitivity.

Statistical analyses We analyzed three biological samples of *VHL*-wt and *VHL*-mut RCC cell cultures with two analytical replications for each, making a total of six proteomic analyses for each of the *VHL*-genotype of RCC. A G-statistic test (likelihood ratio test for independence) was then utilized to determine statistical significance for differential expression of each protein having normalized spectral count of at least three in either the *VHL*-wt or *VHL*-mut sample:

$$G=2[C_{VHL\text{-wt}} \ln(C_{VHL\text{-wt}}/t_{ct}) + C_{VHL\text{-mut}} \ln(C_{VHL\text{-mut}}/t_{ct})]$$

where $C_{VHL\text{-wt}}$ is $(n_{VHL\text{-wt}} + 1)$; $C_{VHL\text{-mut}}$ is $[(n_{VHL\text{-mut}} + 1)]$; and t_{ct} is $[(C_{VHL\text{-wt}} + C_{VHL\text{-mut}})/2]$ [14,17,19]. The *G*-value is approximately characterized by a χ^2 distribution with one degree of freedom, allowing *P*-value calculations. $P < 0.05$ was considered statistically significant. Proteins showing zero spectral counts in either *VHL*-mut or *VHL*-wt RCC cells were tabulated as $U^{786\text{-}O}$ (uniquely expressed in *VHL*-mut RCC cells) and $U^{CAKI\text{-}2}$ (uniquely expressed in *VHL*-wt RCC cells), respectively.

The differentially expressed proteins with more than 2-fold change in normalized spectral counts and $P < 0.05$ were further explored by Ingenuity Pathway Analysis (IPA; Ingenuity Systems, Redwood City, CA) to reveal differentially regulated signaling networks and biological processes.

RESULTS AND DISCUSSION

Proteomic analysis of *VHL*-mut and *VHL*-wt RCC cells is summarized schematically in Fig 1. We identified 2666 unique peptides and 315 proteins out of 4633 total spectra. The biological and analytical replication were >95% across all the samples analyzed in both *VHL*-wt and *VHL*-mut cells. Based on reaching normalized spectral counts of at least three in either the *VHL*-mut or *VHL*-wt samples, a minimum of 2-fold change and a *P*-value of <0.05, proteins showing differential expression are listed in Table 1.

Differential regulation of cellular energy pathways in *VHL*-mut and *VHL*-wt RCC cells

Differentially expressed proteins were further examined by Ingenuity Pathway Analysis (IPA) to characterize the predominant signaling pathways and networks that are differentially regulated between respective *VHL* genotypes of RCC cells. IPA revealed signaling pathways that regulate tumor energetics such as the pentose phosphate pathway, and glucose and pyruvate metabolism as the predominantly differentially regulated metabolic pathways in *VHL*-mut relative to *VHL*-wt RCC cells (**Table 2**).

Differentially expressed proteins (**Table 1**), along with the impact on the cellular energy pathways as elucidated by IPA analysis (**Table 2**), revealed significant differences on metabolic preferences of *VHL*-mut and *VHL*-wt RCC. Metabolism in cancer cells is mainly driven by the flux of metabolites through three pathways: glycolysis, pentose phosphate pathway and glutaminolysis [20]. Rapidly proliferating cancer cells have enhanced aerobic glycolysis compared to non-malignant cells which is commonly known as Warburg effect [21] . The Warburg effect has been implicated in the rapid generation of glycolysis driven ATP in tumor cells relative to regular mitochondrial oxidation [20]. Previously published proteomic studies have strongly indicated the up-regulation of glycolysis in RCC cells, but the pathways that maintain cellular energy status specifically in HIF2-α over-expressing *VHL*-mut background that corresponds to advanced stages of RCC have not been reported [22,23]. The rate limiting enzymes of glycolysis include glucose-6-phosphate isomerase that converts glucose-6-phosphate to fructose-6-phosphate during glycolysis. The tumor cells with impaired glycolytic pathway maintain the downstream metabolite flux by deriving the intermediate metabolites, fructose 6-phosphate and dihydroxy acetone phosphate, from the pentose phosphate pathway. To our

surprise, glucose-6-phosphate isomerase (GPI) of glycolytic pathway, as well as UDP glucose-6-dehydrogenase (UGDH) of pentose phosphate pathway were not detectable; however, a significant over-expression of mitochondrial malate dehydrogenase (MDH) was observed in *VHL*-mut RCC cells (**Table 1**). This novel finding regarding the down-regulation of key enzymes of glycolysis and pentose phosphate pathway strongly indicated a possible metabolic shift towards glutaminolysis in advanced stages of RCC that over-express HIF2-α. Glutamine is converted to glutamate and shunted into the tricarboxylic acid (TCA) cycle as α-ketoglutarate that ultimately gets converted to malate. MDH converts malate to oxaloacetate to yield NADH that is further shuttled into mitochondrial respiratory chain to yield ATP [24]. The voltage-dependent anion selective channel (VDAC) in the outer membrane of mitochondria functions as an ADP importer by exchanging ATP into cytoplasm thereby maintaining a favorable mitochondrial ADP gradient to drive ATP synthesis [25]. In addition to over-expression of mitochondrial MDH, there was an over-expression of VDAC and ATP synthase beta in *VHL*-mut RCC cells (**Table 1**). Thus, the up-regulation of MDH and VDAC in *VHL*-mut cells, in conjunction with down-regulation of glucose-6-phosphate isomerase (GPI), strongly indicated a shift towards alternate metabolic pathways in *VHL*-mut RCC.

Normally, HIF1-α, but not HIF2-α, mainly up-regulates glycolysis and pentose phosphate pathway by increasing the expression of glycolytic enzymes like GPI, aldolase and lactate dehydrogenase along with key enzymes involved in pentose phosphate pathway such as glucose-6-phosphate dehydrogenase [9]. As mentioned earlier, the survival and progression of RCC are associated with over-expression of HIF2-α relative to HIF1-α [7,26]. Even though the contribution of glycolysis in the generation of cellular ATP is enhanced due to the Warburg

effect, some of the recent evidence points that cancer cell lines can up-regulate TCA cycle and oxidative phosphorylation that serve as their major source of ATP production [27]. The relative importance of glutaminolysis and glycolysis in RCC has been poorly understood. In the context of down-regulation of key glycolytic and pentose phosphate pathway enzymes, especially GPI and UGDH as evident from proteomic analysis in *VHL*-mut RCC cells, we further investigated the importance of glutaminolysis.

We first analyzed the degree of cell survival using MTT assay after incubation with aminooxyacetate (AOA), an inhibitor of glutaminolysis, at 24, 48 and 72 h (**Figures 2a, 2b and 2c, respectively**). The *VHL*-mut RCC cells were more susceptible to inhibition of glutaminolysis relative to *VHL*-wt RCC cells at all concentrations of AOA and at all time-points tested. In addition to using glutaminolytic inhibitor, we also studied the extent of cell survival upon culturing in medium lacking glutamine. Again, *VHL*-mut RCC cells were more susceptible to glutamine depletion relative to *VHL*-wt RCC cell lines (**Figure 2d**).

By comparing the results of cell survival assays after glutaminolytic pathway inhibition by using AOA and glutamine depletion by using medium lacking in glutamine, we observed that *VHL*-mut cells cultured in glutamine depleted medium had moderately higher survival when compared to survival upon treatment with the glutaminolytic inhibitor. This could be due to the presence of glutamate in the cell culture medium which could compensate for glutamine deprivation when cultured without glutamine. By acting downstream of glutamate, the increased inhibitory effect of AOA could be due to its ability to prevent conversion of glutamine to α-ketoglutarate, which would explain the low survival of *VHL*-mut cells in the presence of AOA

when compared to lack of glutamine substitution in the medium alone. Collectively, the cell survival assay both in the presence of AOA and upon cell cultures in glutamine depleted medium confirmed the predominant dependence of *VHL*-mut RCC on active glutaminolytic pathway for survival relative to *VHL*-wt RCC.

Regulation of complex cellular energetic, proliferative and metastatic signaling networks in *VHL*-mut RCC Ingenuity Pathway Analysis of signaling networks indicated that two major networks were significantly regulated due to differential expression of proteins: one corresponding to free radical scavenging, molecular transport and another implicating DNA replication, nucleic acid metabolism, DNA recombination and repair (**Figures 3 and 4**). Both networks overlapped with energy production.

The regulation of free-radical scavenging, DNA replication and repair networks is of importance for cancers in general and for *VHL*-mut cancers in particular, both with respect to tumor progression and therapeutic responsiveness. The increased proliferation rate of tumor cells coupled with relative decline in oxygen supply elevates the oxidative stress in tumors, which generate increased reactive oxygen species (ROS). Moderate levels of oxidative stress stimulate cancer cell proliferation, whereas high levels of ROS are toxic even to cancer cells [28]. The *VHL*-mut tumors adapt to hypoxic state by activating free-radical scavenging machinery through HIF signaling. The current drugs of choice in the management of advanced renal cancers include sorafenib, a known multi-specific tyrosine kinase inhibitor, and temsirolimus, an inhibitor of the mammalian target of rapamycin (mTOR). In addition to inhibiting tyrosine kinases, sorafenib induces cell death through induction of mitochondrial

oxidative stress [29]. *VHL*-mut RCC cells are relatively more resistant to sorafenib than *VHL*-wt RCC [11]. Thus, the differential regulation of free-radical scavenging networks assumes significance in further directing the investigations into molecular mechanisms that regulate differential drug sensitivity.

The heat shock family of proteins is one of the major regulators of the cellular response to oxidative stress and, hence, regulates the response to chemotherapeutic interventions [30]. The expression of mitochondrial heat shock protein 60 (HSP60 or HSPD1) was significantly elevated while HSP70, aldo-keto reductase (family1, member 10), thioredoxin 1, transaldolase, NAD(P)H dehydrogenase (quinone1) and destrin were decreased in *VHL*-mut RCC cells. HSP60 is a predominant mitochondrial protein involved in maintaining the integrity of mitochondrial proteins and its expression is increased in response to ROS generation induced due to hypoxia, high temperatures and upon exposure to toxic chemicals [31]. The expression of HSP60 has not been widely studied in renal cancers. In addition, HSP60 decreases cytochrome c release and protects the cells from apoptosis. Proteomic studies in ovarian cancers have demonstrated an up-regulation of HSP60 in multi-drug resistant ovarian cancers [32]. Hence, given the fundamental role of HSP60 in oxidative stress, proliferation and drug resistance, further studies on the distinct role of HSP60 in *VHL*-mut RCC would delineate its precise function in regulating the tumor progression and therapeutic responsiveness.

Cofilin and destrin are closely related members of actin de-polymerizing proteins that regulate cytoskeletal reorganization during cellular proliferation and metastatic progression [33]. We observed a delicate regulation of these closely related proteins with enhanced cofilin

expression and lack of destrin expression in *VHL*-mut RCC cells. We also observed a striking up-regulation of 629-kDa neuroblast differentiation associated protein (AHNAK in Hebrew means giant) for the first time in *VHL*-mut RCC cells. AHNAK has been studied in colon cancer cells and has been characterized as a cooperative protein in a tumor suppressor mechanism in adenomatous polyposis coli-induced oncogenic transformation [34]. The mechanistic significance of the up-regulation of AHNAK derives from its binding with DNA ligase IV complex and its ability to stimulate the ligase activity in non-homologous end joining during repair of double stranded DNA breaks [35]. Enhanced DNA damage repair is an enabling feature for cancerous cells in not only that it allows the transformed cells to thrive in spite of damaged DNA but also that it could allow carryover of genetic alternations, which might promote tumorigenesis and metastatic progression.

Regulation of overall molecular functions, physiological processes and diseases due to significant differential protein expression between *VHL* genotypes in RCC IPA molecular function analysis of significant protein differences as detailed in Table 1 revealed 67 cellular processes that were differentially regulated above the threshold ($P<0.05$) between *VHL* genotypes in RCC. Selected molecular functions are represented in Figure 5a. The top five systems among physiological systems and development were nervous system development and function, skeletal and muscular system development and function, renal and urological system development and function, embryonic development and cardiovascular development and function (**Figure 5b**). Complete loss of *VHL* has been proven to be embryonic lethal [36]. In this context, the role of differentially expressed proteins in regulating embryonic development between *VHL* genotypes of RCC further authenticates the conformity of our proteomic results

with established signaling mechanisms of relevance to *VHL* signaling networks. The analysis of the impact on diseases and disorders revealed the highest effect of differential protein expression on cancer (27%) followed by genetic disorders, reproductive system and disease, respiratory disease and the hematological disease (**Figure 5c**).

CONCLUSION

Proteomic studies focused on the tumorigenic and metastatic causative factors of particular importance in RCC specifically over-expressing HIF2-α have potential impact on translational research to steer the course of novel therapeutic interventions. In this regard, we detected significant differential expression of proteins that regulate cancer cell energetics and DNA repair. Specifically, we report a novel finding of down-regulation of glycolytic pathway and dependency of *VHL*-mut RCC on glutaminolysis, when compared to *VHL*-wt RCC. Also, the identification of up-regulated neuroblast differentiation associated protein (AHNAK) with an established role in DNA repair in *VHL*-mut RCC is another finding with potential impact on enabling the cancerous cells to proliferate and metastasize in spite of aberrant genetic alterations. The observation of protein expression differences between *VHL*-mut and *VHL*-wt RCC implicated various signaling networks of importance in cell proliferation, oxidative stress and metastasis. Taken together, our proteomic studies highlighted differentially regulated protein networks that direct and regulate the specificity of cellular energetics, DNA repair and oxidative stress which, in turn, collectively regulate therapeutic responsiveness of aggressive, *VHL*-mut and HIF2-α over-expressing RCCs. Further studies by using knock-in and knock-out models would enhance the understanding of the role of individual proteins in regulating specific cancer

cell processes as elucidated by current findings. In summary, the results from this study have opened potential novel possibilities for translational research in renal oncology by characterizing the differentially regulated proteins and respective signaling networks between *VHL* genotypes of RCC differing specifically in HIF2-α expression.

ACKNOWLEDGEMENTS

This work was supported in part by a USPHS grant CA 77495 from the National Institute of Health (to SA), by the Cancer Research Foundation of North Texas, the Institute for Cancer Research, the Joe & Jessie Crump Fund for Medical Education (to SS), and by the Robert A. Welch Foundation endowment BK-0031 (to LP).

REFERENCES

1. American Cancer Society (2010**)** Cancer Facts and Figures of 2010. Atlanta, GA: *American Cancer Society*,. http://www.cancer.gov/cancertopics/types/commoncancers.

2. Pfaffenroth, E. C.; Linehan, W. M. (2008**)** Genetic basis for kidney cancer: opportunity for disease-specific approaches to therapy. *Expert Opin Biol Ther*;**8**:779–790.

3. Kaelin, W.G.,Jr. (2008) The von Hippel-Lindau tumour suppressor protein: O_2 sensing and cancer. *Nat Rev Cancer*;**8**:865–873.

4. Hunt, J.D., van der Hel, O.L., McMillan, G.P. Boffetta, P., and Brennan, P. (2005) Renal cell carcinoma in relation to cigarette smoking: meta-analysis of 24 studies. *Int J Cancer*; **114**:101– 108.

5. van Dijk, B. A., Schouten, L. J., Oosterwijk, E., et al (2006) Cigarette smoking, von Hippel-Lindau gene mutations and sporadic renal cell carcinoma. *Br J Cancer*;**45**: 374–377.

6. Maxwell, P. H., Wiesener, M. S., Chang, G. W., et al (1999) The tumour suppressor protein VHL targets hypoxia-inducible factors for oxygen-dependent proteolysis. *Nature*;**399**: 271–275.

7. Kondo, K., Kim, W. Y., Lechpammer, M., and Kaelin, W. G.,Jr (2003) Inhibition of HIF2alpha is sufficient to suppress pVHL-defective tumor growth. *PLoS Biol*;**1**:E83.

8. Shinojima, T., Oya, M., Takayanagi, A., Mizuno, R., Shimizu, N., and Murai, M. Renal cancer cells lacking hypoxia inducible factor (HIF)-1alpha expression maintain vascular endothelial growth factor expression through HIF-2alpha. *Carcinogenesis*;**28**:529–536.

9. Hu, C. J., Wang, L. Y., Chodosh, L. A., Keith, B., and Simon, M. C. (2003) Differential roles of hypoxia-inducible factor 1alpha (HIF-1alpha) and HIF-2alpha in hypoxic gene regulation. *Mol Cell Biol*;**23**:9361–9374.

10. Choi, J. W., Park, S. C., Kang, G. H., Liu, J. O. and Youn, H. D. (2004) Nur77 activated by hypoxia- inducible factor-1alpha overproduces proopiomelanocortin in von Hippel-Lindau-mutated renal cell carcinoma. *Cancer Res*;**64**:35–39.

11. Singhal, S. S., Sehrawat, A., Sahu, M., et al. (2010) Rlip76 transports sunitinib and sorafenib and mediates drug resistance in kidney cancer. *Int J Cancer*;**126**:1327–1338.

12. Nagaprashantha, D. L., Singhal, J., Vatsyayan, R., Lelsani, P., Singhal, S. S., and Prokai, L.; and Awasthi, S. (2010) Proteomic analysis of drug metabolizing networks in renal cell carcinomas with differential drug sensitivity and VHL expression. *J Clin Oncol*;e13137

13. Liu, H., Sadygov, R. G., and Yates, J. R. 3rd. (2004) A model for random sampling and estimation of relative protein abundance in shotgun proteomics. *Anal Chem*;**76**:4193–4201.

14. Prokai, L., Stevens, S. M.,Jr, Rauniyar, N., and Nguyen, V. *J.* (2009) Rapid label-free identification of estrogen-induced differential protein expression in vivo from mouse brain and uterine tissue *J. Proteome Res*;**8**:3862–3871.

15. Keller, A., Nesvizhskii, A. I., Kolker, E., and Aebersold, R. (2002) Empirical statistical model to estimate the accuracy of peptide identifications made by MS/MS and database search. *Anal Chem*;**74**:5383–5392.

16. Nesvizhskii, A. I., Keller, A., Kolker, E., and Aebersold, R. (2003) A statistical model for identifying proteins by tandem mass spectrometry. *Anal Chem*;**75**:4646–4658.

17. Old, W. M., Meyer-Arendt, K., Aveline-Wolf, L., et al. (2005) Comparison of label-free methods for quantifying human proteins by shotgun proteomics. *Mol Cell Proteomics***;4**:1487–1502.

18. Higgs, R. E., Knierman, M. D., Gelfanova, V., Butler, J. P., and Hale, J. E. (2005) Comprehensive label-free method for the relative quantification of proteins from biological samples. *J Proteome Res*;**4**:1442–1450.

19. Sokal, R. R., Rohlf, F. J. (1995) Biometry: The Principles and Practice of Statistics in Biological Research; *W. H. Freeman and Company*: New York; pp 729−731.

20. Kroemer, G., and Pouyssegur, J. (2008) Tumor cell metabolism: cancer's Achilles' heel. *Cancer Cell*;**13**:472–482.

21. Warburg, O. (1956) On the origin of cancer cells. *Science*;**123**:309–314.

22. Perroud, B., Lee, J., Valkova, N., et al. (2006) Pathway analysis of kidney cancer using proteomics and metabolic profiling. *Mol Cancer*;**5:**64.

23. Unwin, R. D., Craven, R. A., Harnden, P., et al (2003) Proteomic changes in renal cancer and co-ordinate demonstration of both the glycolytic and mitochondrial aspects of the Warburg effect. *Proteomics*;**3**:1620–1632.

24. DeBerardinis, R. J., Lum, J. J., Hatzivassiliou, G., and Thompson, C. B. (2008) The biology of cancer: metabolic reprogramming fuels cell growth and proliferation. *Cell Metab*;**7**:11–20.

25. Rostovtseva, T., and Colombini, M. (1997) VDAC channels mediate and gate the flow of ATP: implications for the regulation of mitochondrial function. *Biophys J*;**72**:1954–1962.

26. Franovic, A., Holterman, C. E., Payette, J., and Lee, S. (2009) Human cancers converge at the HIF-alpha oncogenic axis. *Proc Natl Acad Sci USA*;**106:**21306–21311.

27. Smolkova, K., Bellance, N., Scandurra, F., et al. (2010) Mitochondrial bioenergetic adaptations of breast cancer cells to aglycemia and hypoxia. *J Bioenerg Biomembr*;**42**:55–67.

28. Schumacker, P. T. (2006) Reactive oxygen species in cancer cells: live by the sword, die by the sword. *Cancer Cell*;**10**:175–176.

29. Chiou, J. F., Tai, C. J., Wang, Y. H., Liu, T. Z., Jen, Y. M., and Shiau, C. Y. (2009) Sorafenib induces preferential apoptotic killing of a drug- and radio-resistant Hep G2 cells

through a mitochondria-dependent oxidative stress mechanism. *Cancer Biol Ther*;**8**:1904–1913.

30. Ciocca, D. R., and Calderwood, S. K. (2005) Heat shock proteins in cancer: diagnostic, prognostic, predictive, and treatment implications. *Cell Stress Chaperones*;**10:**86–103.
31. Singh, M. P., Reddy, M. M., Mathur, N., Saxena, D. K., and Chowdhuri, D. K. (2009) Induction of hsp70, hsp60, hsp83 and hsp26 and oxidative stress markers in benzene, toluene and xylene exposed Drosophila melanogaster: role of ROS generation. *Toxicol Appl Pharmacol*;**235**:226–243.
32. Li, S. L., Ye, F., Cai, W. J., et al. (2010) Quantitative proteome analysis of multidrug resistance in human ovarian cancer cell line. *J Cell Biochem*;**109**:625-633.
33. Didry, D., Carlier, M. F., and Pantaloni, D. (1998) Synergy between actin depolymerizing factor/cofilin and profilin in increasing actin filament turnover. *J Biol Chem*;**273**:25602–25611.
34. Tanaka, M., Jin, G., Yamazaki, Y., Takahara, T., Takuwa, M., and Nakamura, T. (2008) Identification of candidate cooperative genes of the Apc mutation in transformation of the colon epithelial cell by retroviral insertional mutagenesis. *Cancer Sci*;**99**:979–985.
35. Stiff, T., Shtivelman, E., Jeggo, P., and Kysela, B. (2004) AHNAK interacts with the DNA ligase IV-XRCC4 complex and stimulates DNA ligase IV-mediated double-stranded ligation. *DNA Repair*;**3**:245–256.
36. Gnarra, J. R., Ward, J. M., Porter, F. D., et al. (1997) Defective placental vasculogenesis causes embryonic lethality in VHL-deficient mice. *Proc Natl Acad Sci US A*;**94:**9102–9107.

Table 1. List of proteins with statistically significant differential expression between *VHL*-wt (CAKI-2) and *VHL*-mut (786-O) RCCs: Proteins reaching at least 3 as average spectral count in either the CAKI-2 or 786-O sample with ≥2-fold change and $P < 0.05$ by summation-based G-test were considered.

protein name	IPI accession number	Molecular weight (kDa)	Number of unique peptides	Sequence coverage (%)	Average spectral counts in 786-O ± SD[a]	Average spectral counts in CAKI-2 ± SD[a]	Average fold change
60 kDa heat shock protein, mitochondrial	IPI00784154	61	8	19	32±11	2±2	9[b]
70 kDa heat shock protein 1A/1B	IPI00304925	70	4	8	0*	8±3	U[CAKI-2, b]
Aldo-keto reductase family 1 member B10	IPI00105407	36	7	26	1±1	26±4	15
Aldo-keto reductase family 1 member C2	IPI00005668	37	3	11	0*	23±5	U[CAKI-2]
Alpha-enolase	IPI00465248	47	22	63	134±12	47±8	3
ATP synthase subunit beta, mitochondrial	IPI00303476	57	10	30	14±3	0*	U[786-O]
cDNA FLJ54957, highly similar to transketolase	IPI00643920	69	7	15	3±2	15±3	4
Cofilin-1	IPI00012011	19	5	41	25±10	5±1	4
Collapsin response mediator protein 4 long variant	IPI00029111	74	5	10	0*	5±1	U[CAKI-2]
Destrin	IPI00473014	19	4	22	0*	5±2	U[CAKI-2]
Fructose-bisphosphate aldolase A	IPI00465439	39	13	37	8+3	30±6	4
Glucose-6-phosphate isomerase	IPI00027497	63	5	11	0*	7±2	U[CAKI-2]
Glycogen phosphorylase, brain form	IPI00004358	97	3	5	0*	3±1	U[CAKI-2]
Isoform 5 of Thioredoxin reductase 1, cytoplasmic	IPI00554786	55	4	13	0*	5±1	U[CAKI-2]
Malate dehydrogenase, mitochondrial	IPI00291006	36	3	19	6±1	0*	U[786-O]
NAD(P)H dehydrogenase [quinone] 1	IPI00012069	31	5	17	0*	5±2	U[CAKI-2]
Neuroblast differentiation-associated protein AHNAK	IPI00021812	629	11	6	24±10	2±1	10
Poly(rC)-binding protein 1	IPI00016610	37	3	11	1±1	5±1	2
Profilin-1	IPI00216691	15	5	43	23±7	5±2	3
Prostaglandin E synthase 3	IPI00015029	19	3	14	1±0	3±1	3
Retinal dehydrogenase 1	IPI00218914	55	3	9	1±1	7±2	5
Stress-70 protein, mitochondrial	IPI00007765	74	3	6	4±2	0*	U[786-O]
Transaldolase	IPI00744692	38	5	16	1±1	11±1	6
Ubiquitin carboxyl-terminal hydrolase isozyme L1	IPI00018352	25	3	17	1±0	6±2	4

UDP-glucose 6-dehydrogenase	IPI00031420	55	13	39	0*	14±1	U^{CAKI-2}
Voltage-dependent anion-selective channel protein 1	IPI00216308	31	3	14	3±1	0*	U^{786-O}

[a] *N* = 3 biological replicates of RCC with respective *VHL* genotypes; analyses were ran in duplicate. [b] Validated by Western-blot analysis (Fig S2). * No peptides were detected in all the analyses of respective cell lines. U^{CAKI-2}: Proteins uniquely detected in *VHL*-wt (CAKI-2) RCC. U^{786-O}: Proteins uniquely detected in *VHL*-mut (786-O) RCC.

Table 2. Differential regulation of cellular energy pathways between *VHL*-wt and *VHL*-mut RCC.

Name	*P*
Pentose phosphate pathway	$<4.4 \cdot 10^{-7}$
Starch and sucrose metabolism	$<1.9 \cdot 10^{-5}$
Glycolysis/gluconeogenesis	$<2.0 \cdot 10^{-5}$
Pentose and glucuronate interconversion	$<9.3 \cdot 10^{-5}$
Pyruvate metabolism	$<3.2 \cdot 10^{-4}$

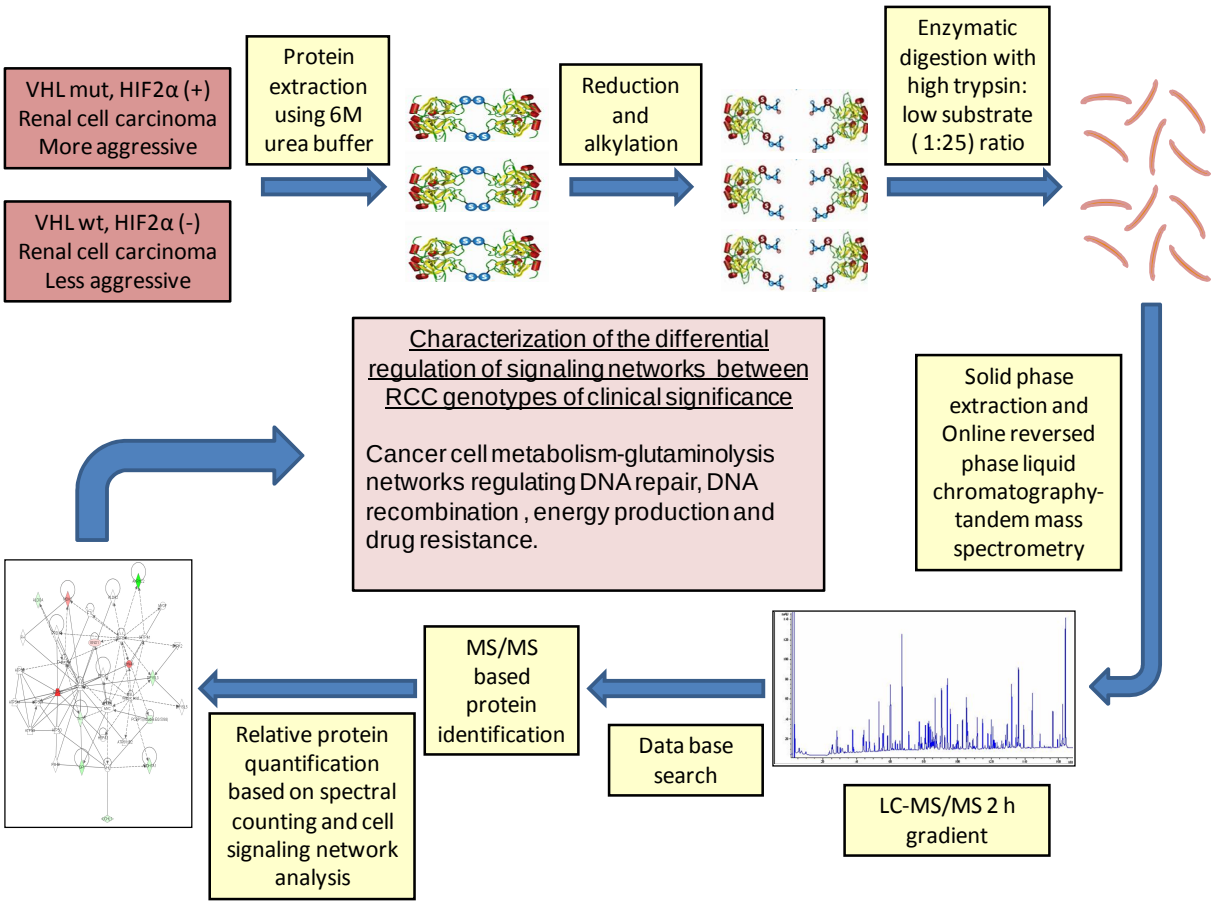

Figure 1. Schematic representation of the experimental design, analysis of differential expression of proteins and consequent regulation of signaling networks of importance in RCC cells: The *VHL*-wt and *VHL*-mut RCC cell lines were analyzed in buffer containing 6 M Urea. The lysate (200 µg of protein) was subjected to reduction and alkylation followed by overnight digestion with sequencing grade trypsin. The samples were desalted by solid phase extraction (SPE) before online reversed phase LC-MS/MS analysis. The MS/MS data generated was first searched against human protein sequence database followed by MS/MS based peptide and protein identifications using Scaffold (version 3.0). The proteins with significant quantitative differences as determined by G-test were submitted to Ingenuity Pathway Analysis (IPA) to reveal differential regulation of signaling networks.

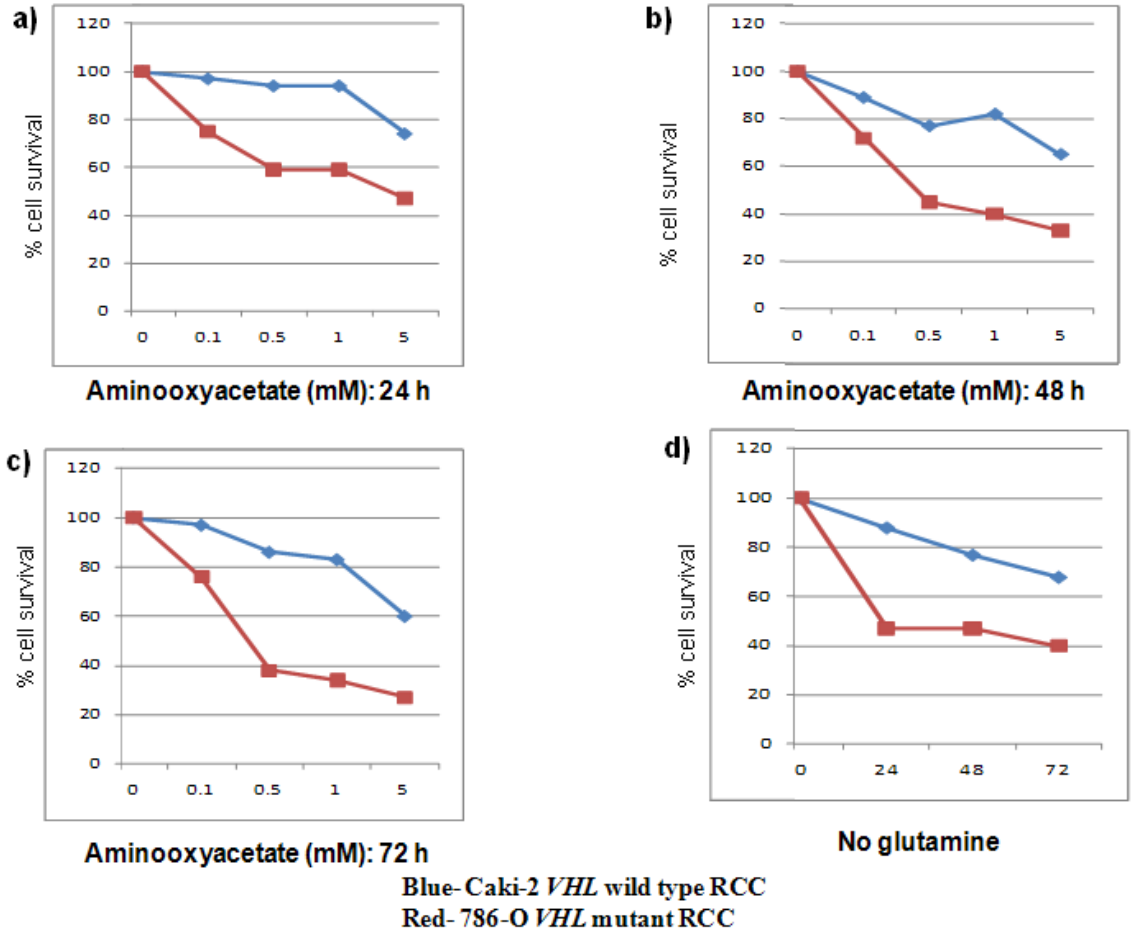

Figure 2. The assessment of RCC cell-survival by MTT assay: The survival of CAKI-2 (*VHL*-wt) and 786-O (*VHL*-mut) RCC cell lines was assessed after treatment with increasing concentrations of the glutaminolytic inhibitor, aminooxyacetate (AOA) at 24 h (a), 48 h (b) and 72 h (c) and in glutamine depleted medium (d). *VHL*-mut 786-O RCC cells were more susceptible to inhibition of glutaminolysis or glutamine depletion at all time-points.

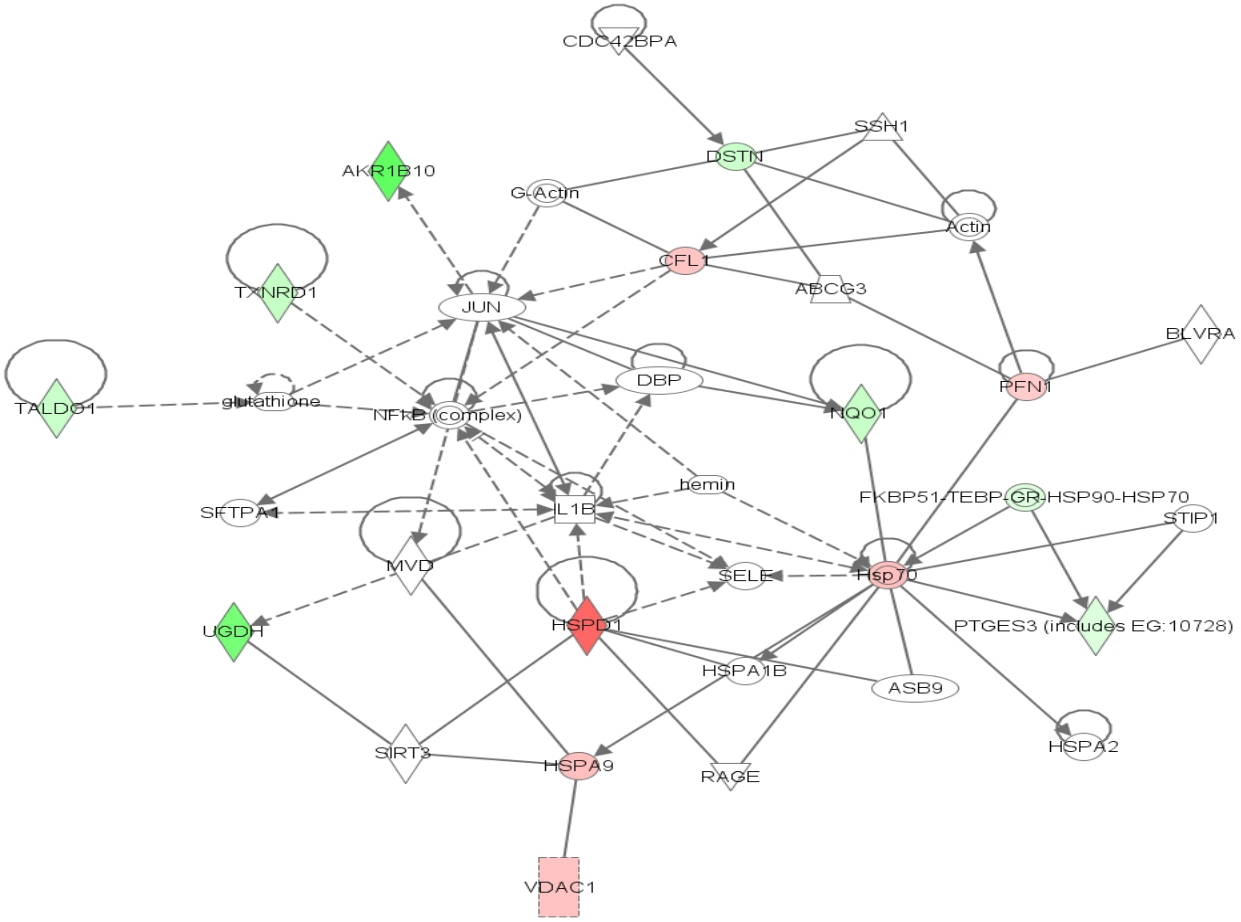

Figure 3. Differential regulation of the network of "Free radical scavenging, molecular transport and energy production" in *VHL*-mut and *VHL*-wt RCC. **Red**, up-regulated in *VHL*-mut RCC, **Green**, down-regulated in *VHL*-mut RCC.

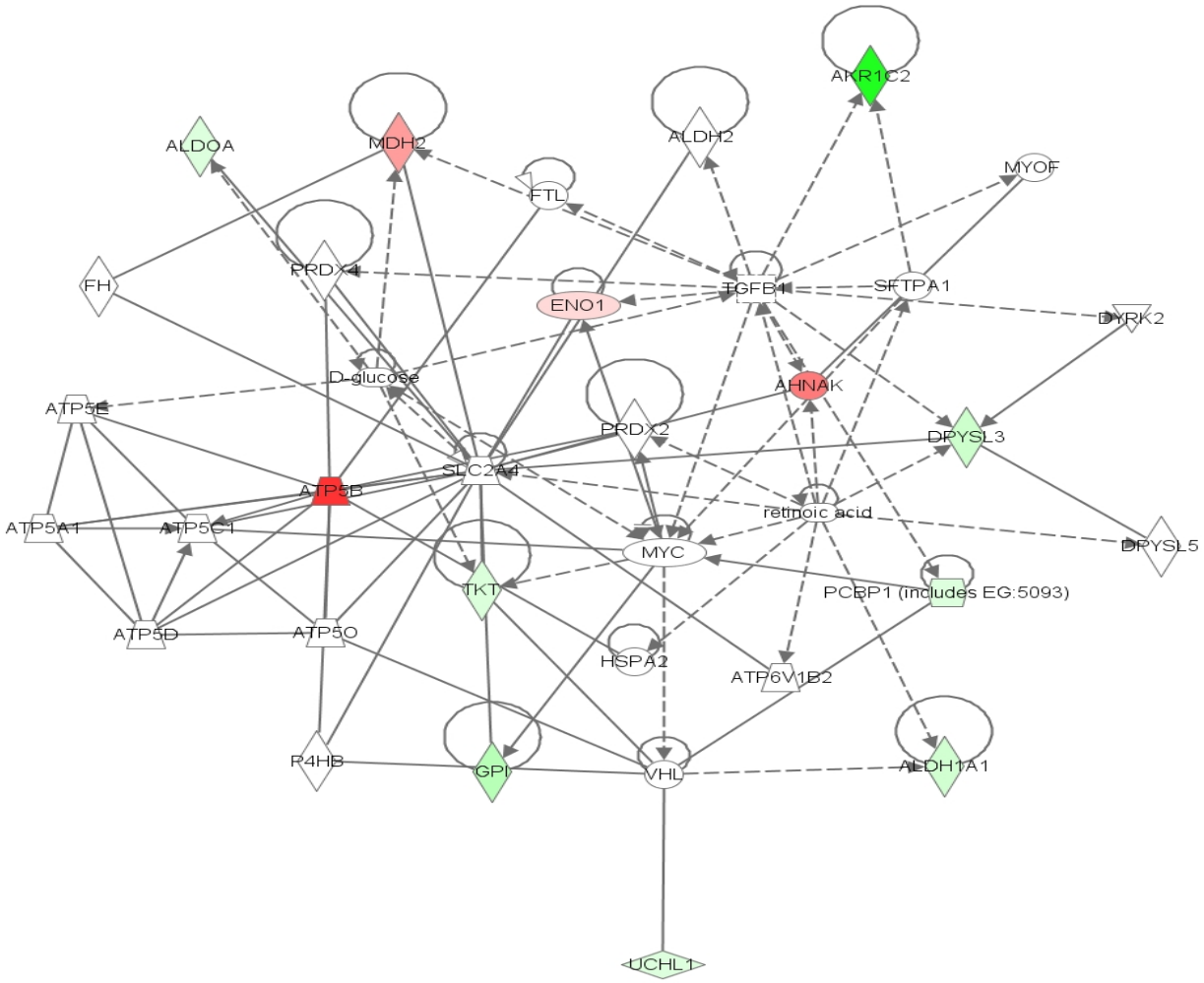

Figure 4. Differential regulation of the network of "DNA replication, recombination and repair, energy production and nucleic acid metabolism" in *VHL*-mut and *VHL*-wt RCC. **Red**, up-regulated in *VHL*-mut RCC, **Green**, down-regulated in *VHL*-mut RCC.

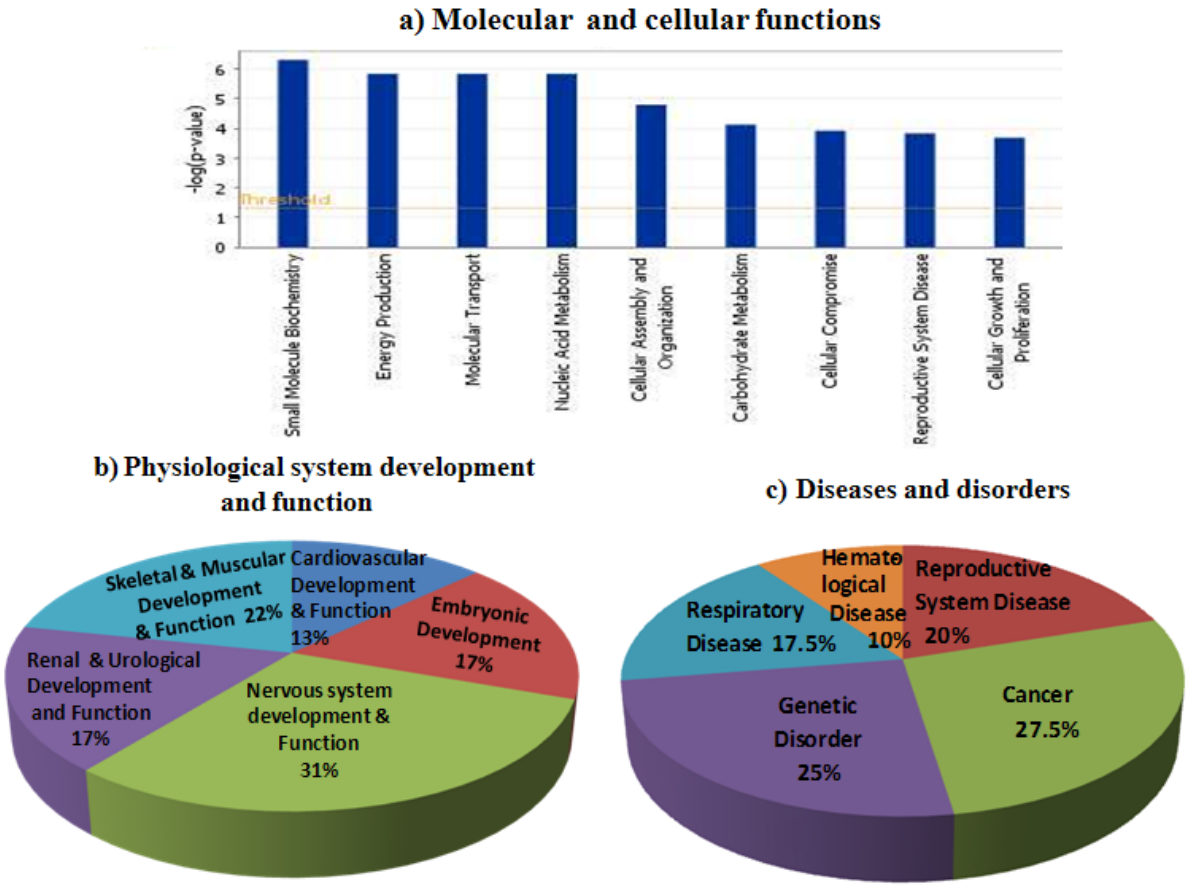

Figure 5. IPA analysis for the impact of differential expression of proteins on (a) molecular and cellular functions, (b) physiological systems and development and (c) diseases and disorders: The molecular and cellular functions differing between the *VHL* genotypes of RCC were revealed by Ingenuity Pathways Analysis (IPA). IPA confirmed the statistical significance of differential regulation of signaling pathways regulating energy production, nucleic acid metabolism, carbohydrate metabolism and cellular growth and differentiation among top molecular functions that are differentially regulated. Incidentally, these differentially regulated molecular functions determine the cancer cell survival, proliferation and metastases (**a**). The impact of differentially expressed proteins on physiological system development and function (**b**), and diseases & disorders (**c**).

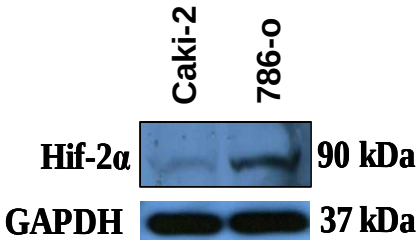

Figure S1. Western blot analysis for the expression of HIF2-α and *VHL* in the RCC cell lines before proteomic analysis: The differential expression of HIF2-α in 786-O (*VHL*-mut) RCC was confirmed.

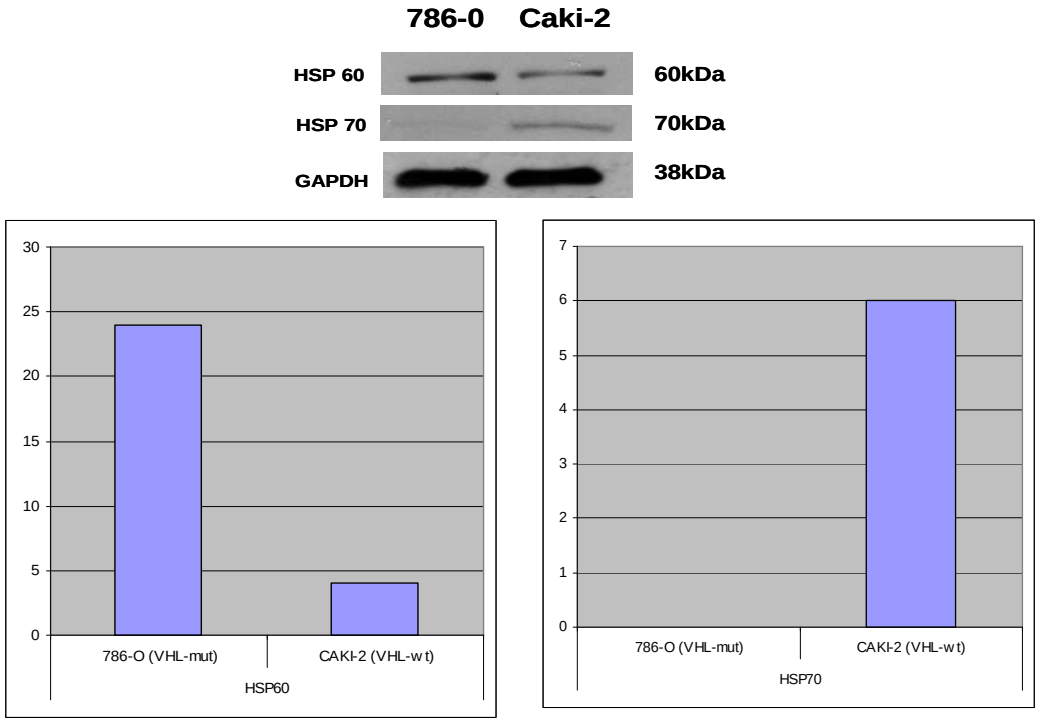

Figure S2. Western blot analysis for the differential expression of HSP60 and HSP70 in the RCC cell lines: The bottom panels show the scanning densitometry for respective protein expression between *VHL* genotypes of RCC.

CHAPTER III

PROTEOMIC ANALYSIS OF SIGNALING NETWORK REGULATION BY RLIP76 IN *VHL*-MUTANT RENAL CELL CARCINOMA

INTRODUCTION

RLIP76, also known as Ral binding protein 1 or RalBP1 is a 76kDa multi-specific, multi-functional mercapturic acid pathway transport protein that is over expressed in multiple organ malignancies [1-6]. RLIP76 was originally characterized to possess dinitrophenyl-S-glutathione conjugate-dependent ATPase (DNP SG ATPase) activity [7-8]. RLIP76 has displayed substrate stimulated, temperature dependent, saturable ATPase driven transport activity for a range of metabolites and anti-cancer drugs like GS-E of products of lipid peroxidation like 4HNE, vinblastine, vincristine, vinorelbine along with drugs like doxorubicin and colchicine which do not form GSH-conjugates [9-12].

RLIP76 is over expressed in renal cell carcinoma (RCC) and recent studies from our laboratory have revealed the ability of RLIP76 to transport current drugs of choice in RCC management like sunitinib and sorafenib [13]. Inhibition or depletion of RLIP76 causes regression of RCC in mice xenograft studies [14]. RLIP76$^{-/-}$ mice are active and viable which infers that complete knock-down of RLIP76 does not cause any normal tissue toxicity [15, 16]. Thus, the multi-specific and multifunctional tumor promoting spectrum of RLIP76 along with absence of toxicity in RLIP76 targeted animal models which taken together in the context of the

activation of mercapturic acid pathway in *VHL*-mut RCC makes RLIP76 an attractive and effective target for anti-cancer interventions in RCC. In this regard, characterization of the specific signaling mediators and differential regulation of key networks due to RLIP76 targeted therapy would further enhance the understanding of mechanisms of action of RLIP76 in *VHL*-mut RCC.

EXPERIMENTAL METHODS

Cell lines and cultures Human kidney cancer 786-O cell lines were kindly authenticated and provided by Dr. William G. Kaelin, Dana-Farber Cancer Institute, Harvard Medical School, Boston, MA. The cells were cultured at 37 °C in a humidified atmosphere of 5 % CO_2 in RPMI medium supplemented with 10 % FBS and 1% P/S solution.

Knock-down of RLIP76 in 786-O RCC cells RLIP76-antisense was purchased from Biosynthesis, Inc., (Lewisville, TX). Approximately 2 x 10^5 cells were plated in six well plates for 24 h. The cells were incubated with either RLIP76 anti-sense or scrambled antisense (10 µg/mL final concentrations for each) in Maxfect transfection reagent (MoleculA), according to the manufacturer provided protocol [5]. After 48 h, the cells were washed with sterile PBS, scraped with sterile cell scrapers, collected in PBS and centrifuged at 5000 rpm for 10 minutes. The cell pellet was stored at -80 ^oC till further analyses.

Over-expression of RLIP76 in 786-O RCC cells Approximately 2 x 10^5 786-O cells were plated in six well plates for 24h. 786-O cells were transfected with 4µg of either empty vector

pcDNA-3.1 or vector+RLIP76 using Lipofectamine 2000 according to the manufacturer's protocol [5]. The over-expression of RLIP76 was confirmed by western blot at 48h. After 48 h, the cells were washed with sterile PBS, scraped with sterile cell scrapers, collected in PBS and centrifuged at 5000 rpm for 10 minutes. The cell pellet was stored at -80 ^{o}C till further analyses.

RT-PCR analysis RNA from control and experimental groups was isolated 48 h after treatment using an Rneasy kit (Qiagen, CA). The RNA (5 µg) was subjected to RT-PCR using random primers and M-MuLV reverse transcriptase (Stratagene, La Jolla, CA) in a 50 µL reaction volume. The RT reaction product (1 µl) was then subjected to 35 cycles of multiplex PCR. The RLIP76 primers [forward primer:334-353 nt and reverse primer :812-831 nt] and STAT1 primers [forward primer:907-928 nt and reverse primer :1003-1024 nt] (Biosynthesis Inc, TX, USA) were used to amplify a 497 bp fragment spanning from 334 to 831 bp of RLIP76 and 117 bp fragment spanning from 907-1024 bp of STAT1 [5, 17]. The PCR products were run on 1.5% agarose gel and visualized by ethidium bromide staining.

Proteomic analysis, database searching and comparison of protein expression levels
Proteomic analyses of RLIP76 antisense transfected and RLIP76 over-expressing 786-O cells was performed according to the method described in chapter 2 [18].

Statistical considerations and Analyses Only protein changes specific to RLIP76 knock-down [(RLIP76-antisense/Scrambled antisense) and RLIP76 over-expression (RLIP76 transfection / empty vector pc DNA3.1 transfection] experiments were considered for analyses in order to minimize non-specific protein changes. Scrambled antisense was considered control for RLIP76-antisense during RLIP76 knock-down and pc DNA3.1 was considered control for

RLIP76 transfection during RLIP76 over-expression in 786-O RCC cells. All data were evaluated with a summation based G-Test [18-20]. A *P*-value of < 0.05 was regarded as statistically significant.

RESULTS AND DISCUSSION

The 786-O cells were treated with RLIP76-antisense to knock-down RLIP76 and transfected with RLIP76 to over-express RLIP76 for 48 h. The knock-down and over-expression of RLIP76 in 786-O cells was confirmed by western blot (**Fig 1**). The LC-MS/MS proteomic analyses of RLIP76 knock-down and RLIP76 over-expressing 786-O *VHL*-mut RCC cells was performed using previously validated label-free quantification method [18]. The results revealed down-regulation of isoform alpha of signal transducer and activator of transcription 1-alpha/beta due to RLIP76 down-regulation relative to RLIP76 over-expression in *VHL*-mut RCC (**Table 1**). The characterization of the enhanced levels of stress responsive proteins like up-regulation of isoform C1 of heterogeneous nuclear ribonucleoprotein C1/C2 (hnRNP C1/C2), 10 kDa heat shock protein (mitochondrial) (HSPE1), stress-70 protein (mitochondrial) (HSPA9), and tubulin beta-3 (TUBB3) chain due to RLIP76 knock-down was in accordance with the established role of RLIP76 in the regulation of oxidative stress [21-26].

The signal transducer and activator of transcription 1(STAT1) is a major transcription factor that plays a vital role in transducing the signals due to activation of janus kinase (JAK) in JAK-STAT pathway [27]. The activating signals lead to autophosphorylation of STAT 1 followed by its dimerization and translocation to the nucleus leading to transcription of STAT1

target genes [28, 29]. RCC is a highly radio-resistant tumor which requires high dose of radiation [30,31]. Our previous studies have shown the over-expression of RLIP76, which mediates chemo and radio-resistance, in RCC [13, 15]. Recent studies have also characterized the over-expression of STAT1 in *VHL*-mut 786-O RCC cell lines and resected tissues of clear cell RCC patients who were resistant to radiotherapy [32]. Hence, we performed RT-PCR analysis to further investigate the role of RLIP76 on STAT1 expression in *VHL*-mut RCC. RT-PCR analysis revealed reduction in the STAT1 mRNA levels due to RLIP76 knock-down and increase in the STAT1 mRNA levels consequent to further over-expression of RLIP76 in *VHL*-mut RCC (**Fig 2**). Thus, the regulation of STAT1 by RLIP76 represents a novel signaling mechanism mediating the effect of RLIP76 in *VHL*-mut RCC.

The IPA analysis for differential regulation of signaling networks revealed that RLIP76 regulates the network of "Cell-to-cell signaling and interaction, cellular assembly and organization, cellular function and maintenance" in *VHL*-mut RCC (**Fig 3**). The IPA pathway analyses revealed significant regulation of metabolic, immune and growth factor signaling pathways by RLIP76 in *VHL*-mut RCC which provide invaluable directions for future research (**Fig 4A**). The IPA analysis also revealed the differential regulation of various disease processes and cellular metabolic pathways by RLIP76 in *VHL*-mut RCC (**Fig 4B and C**, respectively). The regulation of anti-microbial response and infection mechanisms is also reflected by some of our recent studies where RLIP76 is required for the maturation and function of antigen presenting human dendritic cells [33, 34]. The regulation of processes of cancer and cell cycle is in accordance with the fundamental role of RLIP76 in regulating the proliferative potential of multiple organ malignancies [3-6, 35-37].

CONCLUSION

The proteomic analyses of *VHL*-mut RCC cells after RLIP76 knock-down and over-expression lead to characterization of regulation of STAT1 expression by RLIP76 which is a significant finding given the over-expression of both proteins and their established roles in mediating proliferation and radio-resistance in *VHL*-mut RCC [15, 32]. The regulation of STAT1 by RLIP76 denotes an important node of signaling that mediates the therapeutic resistance by complementing the RLIP76 mediated detoxification of products of lipid peroxidation and chemotherapy drugs in *VHL*-mut RCC. The IPA assisted network and pathway analyses elucidated the global regulation of signaling processes of importance in various phases of tumor progression providing corroborative rationale for RLIP76 targeted therapeutic strategies in *VHL*-mut RCC.

REFERENCES

1. Awasthi, S., Sharma, R., Singhal, S.S., Zimniak, P., and Awasthi, Y.C. (2002) RLIP76, a novel transporter catalyzing ATP-dependent efflux of xenobiotics. *Drug Metab Dispos* ;**30**:1300–1310.

2. Awasthi, S., Cheng, J., Singhal, S.S., Saini, M.K., Pandya, U., Pikula, S., et al. (2000) Novel function of human RLIP76: ATP-dependent transport of glutathione-conjugates and doxorubicin. *Biochemistry*;**39**:9327–9334.

3. Singhal, S.S., Singhal, J., Yadav, S., Dwivedi, S., Boor, P., Awasthi, Y.C., et al. (2007) Regression of lung and colon cancer xenografts by depleting or inhibiting RLIP76. *Cancer Res*

;**67**:4382–4389.

4. Singhal, S.S., Roth, C., Leake, K., Singhal. J., Yadav. S., and Awasthi. S. (2009) Regression of prostate cancer xenografts by RLIP76 depletion. *Biochem Pharmacol*;**77**:1074–1083.

5. Singhal, S.S., Yadav, S., Singhal, J., Zajac, E., Awasthi, Y.C., and Awasthi, S. (2005) Depletion of RLIP76 sensitizes lung cancer cells to doxorubicin. *Biochem Pharmacol*;**70**:481–488.

6. Singhal, S.S., Awasthi, Y.C., and Awasthi, S. (2006) Regression of melanoma in a murine model by RLIP76-depletion. *Cancer Res*;**66**:2354–2360.

7. LaBelle, E.F., Singh, S.V., Srivastava, S.K., and Awasthi, Y.C. (1986) Dinitrophenyl glutathione efflux from human erythrocytes is primary active ATP-dependent transport. *Biochem J* ;**238**:443–449.

8. Awasthi, S., Singhal, S.S., Srivastava, S.K., Torman, R.T., Zimniak, P., Pikula, J., et al. (1998) ATP dependent human erythrocyte glutathione-conjugate-transporter. I. Purification, photo-affinity -labeling, and kinetic characteristics of ATPase-activity. *Biochemistry*;**37**:5231–5238.

9. Awasthi, S., Singhal, S.S., Srivastava, S.K., Zimniak, P., Bajpai, K.K., Saxena, M., et al. (1994) Adenosine-triphosphate-dependent transport of doxorubicin, daunomyicn, and vinblastine in human tissues by a mechanism distinct from the Pglycoprotein. *J Clin Invest*;**93**:958–965.

10. Singhal, S.S., Singhal, J., Sharma, R., Singh, S.V., Zimniak, P., Awasthi, Y.C., et al. (2003) Role of RLIP76 in lung cancer doxorubicin-resistance. I. The ATPase activity of RLIP76 correlates with doxorubicin and 4HNE-resistance in lung cancer cells. *Int J Oncol*;**22**:365–375.

11. Stuckler, D., Singhal, J., Singhal, S.S., Yadav, S., Awasthi, Y.C., and Awasthi, S. (2005) RLIP76 transports vinorelbine and mediates drug-resistance in non-small cell lung cancer. *Cancer Res*;**65**:991–998.

12. Awasthi, S., Singhal, S.S., Pandya, U., Gopal, S., Zimniak, P., Singh, S.V., et al. (1999) ATPdependent colchicines transport by human erythrocyte glutathione-conjugate-transporter. *Toxicol Appl Pharmacol*;**155**:215–226.

13. Singhal, S.S., Sehrawat, A., Sahu, M., Singhal, P., Vatsyayan, R., Lelsani, P.C., et al. (2010) RLIP76 transports sunitinib and sorafenib and mediates drug resistance in kidney cancer. *Int J Cancer*;**126**:1327–1338.

14. Singhal, S.S., Singhal, J., Yadav, S., Sahu, M., Awasthi, Y.C., and Awasthi, S. (2009) RLIP76: a target for kidney cancer therapy. *Cancer Res*;**69**:4244–4251.

15. Awasthi, S., Singhal, S.S., Yadav, S., Singhal, J., Drake, K., Nadkar, A., et al. (2005) RLIP76 is a major determinant of radiation-sensitivity. *Cancer Res*;**65**:6022–6028.

16. Singhal, J., Singhal, S.S., Yadav, S., Warnke, M., Yacoub, A., Dent, P., et al. (2008) RLIP76 in defense of radiation and chemical-poisoning. *Int J Rad Oncol Biol Phys*;**72**:553–561.

17. Jiang, L.J., Zhang, N.N., Ding, F., Li, X.Y., Chen, L., Zhang, H.X., et al. (2011) RA-inducible gene-I induction augments STAT1 activation to inhibit leukemia cell proliferation. *Proc Natl Acad Sci U S A*;**108**:1897-1902.

18. Prokai, L., Stevens, S. M.,Jr, Rauniyar, N., and Nguyen, V. J. (2009) Rapid label-free identification of estrogen-induced differential protein expression in vivo from mouse brain and uterine tissue. *J Proteome Res*;**8**:3862–3871.

19. Old, W. M., Meyer-Arendt, K., Aveline-Wolf, L., Pierce, K. G., Mendoza, A., Sevinsky, J. R., et al. (2005) Comparison of label-free methods for quantifying human proteins by shotgun proteomics. *Mol. Cell. Proteomics*;**4:**1487–1502.

20. Sokal, R. R., and Rohlf, F. J. (1995) Biometry: The Principles and Practice of Statistics in Biological Research. *W. H. Freeman and Company*:New York; pp 729−731.

21. Hossain, M.N., Fuji, M., Miki, K., Endoh, M. and Ayusawa, D. (2007) Downregulation of hnRNP C1/C2 by siRNA sensitizes HeLa cells to various stresses. *Mol Cell Biochem*;**296**:151-157.

22. Cicchillitti, L., Penci, R., Di Michele, M., Filippetti, F., Rotilio, D., Donati, M.B., et al. (2008) Proteomic characterization of cytoskeletal and mitochondrial class III beta-tubulin. *Mol Cancer Ther*;**7**:2070-2079.

23. Cappello, F., Di Stefano, A., David, S., Rappa, F., Anzalone, R., La Rocca, G., et al. (2006) Hsp60 and Hsp10 down-regulation predicts bronchial epithelial carcinogenesis in smokers with chronic obstructive pulmonary disease. *Cancer*;**107**:2417-2424.

24. Xie, H., Hu, Z., Chyna, B., Horrigan, S.K. and Westbrook, C.A. (2000) Human mortalin (HSPA9): a candidate for the myeloid leukemia tumor suppressor gene on 5q31. *Leukemia;***14:** 2128-2134.

25. Meloni, B.P., Van Dyk, D., Cole, R. and Knuckey, N.W. (2005) Proteome analysis of cortical neuronal cultures following cycloheximide, heat stress and MK801 preconditioning. *Proteomics;***5:**4743-4753.

26. Yadav, S., Zajac, E., Singhal, S.S., and Awasthi, S.(2007) Linking stress-signaling, glutathione metabolism, signaling pathways and xenobiotic transporters. *Cancer Metastasis Rev*;**26**:59-69.

27. Khodarev, N.N., Roach, P., Pitroda, S.P., Golden, D.W., Bhayani, M., Shao, M.Y., et al (2009) STAT1 pathway mediates amplification of metastatic potential and resistance to therapy. *PLoS One*;**4**:e5821.

28. Gupta, S., Yan, H., Wong, L.H., Ralph, S., Krolewski, J. and Schindler, C. (1996) The SH2 domains of Stat1 and Stat2 mediate multiple interactions in the transduction of IFN-alpha signals. *EMBO J*;**15**:1075-1084.

29. Shuai, K., Horvath, C.M., Huang, L.H., Qureshi, S.A., Cowburn, D. and Darnell, J.E.,Jr. (1994) Interferon activation of the transcription factor Stat91 involves dimerization through SH2-phosphotyrosyl peptide interactions. *Cell*;**76**:821-828.

30. Deschavanne, P.J. and Fertil, B. (1996) A review of human cell radiosensitivity in vitro. Int. J. Radiat. *Oncol Biol Phys*;**34**:251-266.

31. Kjaer, M., Iversen, P., Hvidt, V., Bruun, E., Skaarup, P., Bech Hansen, J. et al. (1987) A randomized trial of postoperative radiotherapy versus observation in stage II and III renal adenocarcinoma. A study by the Copenhagen Renal Cancer Study Group. *Scand J Urol Nephrol*;**21**:285-289.

32. Hui, Z., Tretiakova, M., Zhang, Z., Li, Y., Wang, X., Zhu, J.X., et al. (2009) Radiosensitization by inhibiting STAT1 in renal cell carcinoma. *Int J Radiat Oncol Biol Phys*;**73**:288-295.

33. Borvak,J., Sahu, M., Joy,V., Singhal,J., Yadav, S., Oakford, L.X., et al. (2010) Ral-binding protein is required for the maturation and function of dendritic cells. *American J Immunology*;**6**: 29-42.

34. Margutti, P., Matarrese, P., Conti, F., Colasanti, T., Delunardo, F., Capozzi, A., et al. (2008)Autoantibodies to the C-terminal subunit of RLIP76 induce oxidative-stress and endothelial cell apoptosis in immune-mediated vascular diseases and atherosclerosis. *Blood*;**111**:4559–4570.

35. Awasthi, S., Singhal, S.S., Sharma, R., Zimniak, P., and Awasthi, Y.C. (2003) Transport of glutathione-conjugates and chemotherapeutic drugs by RLIP76: a novel link between G-protein and tyrosine-kinase signaling and drug-resistance. *Int J Cancer*;**106**:635–646.

36. Goldfinger, L.E., Ptak, C., Jeffery, E.D., Shabanowitz, J., Hunt, D.F., and Ginsberg, M.H. (2006) RLIP76 (RalBP1) is an R-Ras effector that mediates adhesion-dependent Rac-activation and cell migration. *J Cell Biol*;**174**:877–888.

37. Rosse, C., L'Hoste, S., Offner, N., Picard, A., and Camonis, J.H. (2003) RLIP, an effector of the Ral-GTPases, is a platform for Cdk1 to phosphorylate epsin during the switch off of endocytosis in mitosis. *J Biol Chem*;**278**:30597–30604.

Protein Name	IPI Index	MW (kDa)	Ratio- RLIP76 knock-down vs. RLIP76 over-expression	Known Function
10 kDa heat shock protein, mitochondrial (HSPE1)	IPI00220362	11	2	Stress responsive protein, loss of HSPE1 predicts bronchial epithelial carcinogenesis in smokers
Isoform Alpha of Signal transducer and activator of transcription 1-alpha/beta	IPI00030781	87	0.5	Mediates radiation resistance in RCC
Isoform C1 of Heterogeneous nuclear ribonucleoproteins C1/C2	IPI00216592	32	2	Stress responsive protein which protects Hela cervical cancer cells from oxidative stress
Stress-70 protein, mitochondrial (HSPA9)	IPI00007765	74	3	Stress responsive protein
Tubulin beta-3 chain	IPI00013683	50	6	Cytoskeletal stress responsive protein

Table 1. Changes in the protein expression as detected by LC-MS/MS proteomic analyses following knock-down and over expression of RLIP76 in 786-O *VHL*-mut RCC.

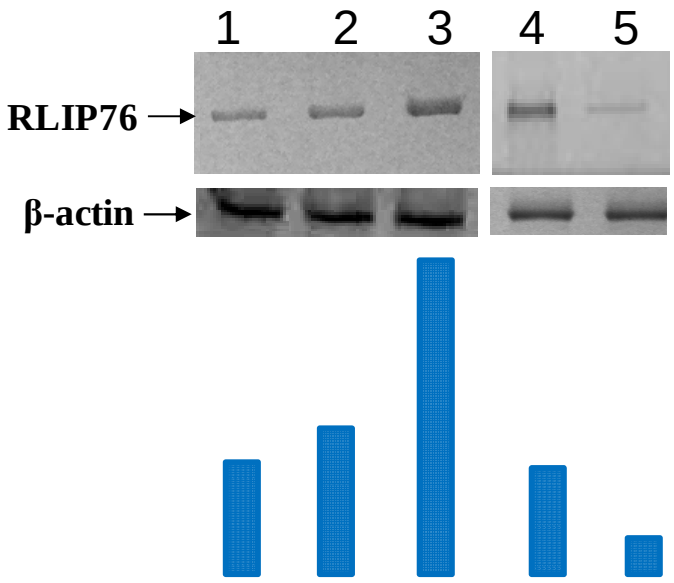

Figure 1. Expression of RLIP76 following knock-down and over-expression of RLIP76: The 786-O *VHL*-mut RCC cells were treated with RLIP76-antisense to knock-down RLIP76 and were transfected with pc-DNA3.1-RLIP76 to over express RLIP76. The RLIP76 protein levels were analyzed by western blot against anti-RLIP76 IgG. Lane 1: control Lane 2: pcDNA 3.1 vector transfection; Lane 3: vector + RLIP76 transfection; Lane 4: scrambled antisense transfection; Lane 5: RLIP76-antisense transfection. A Bar represents densitometry analyses.

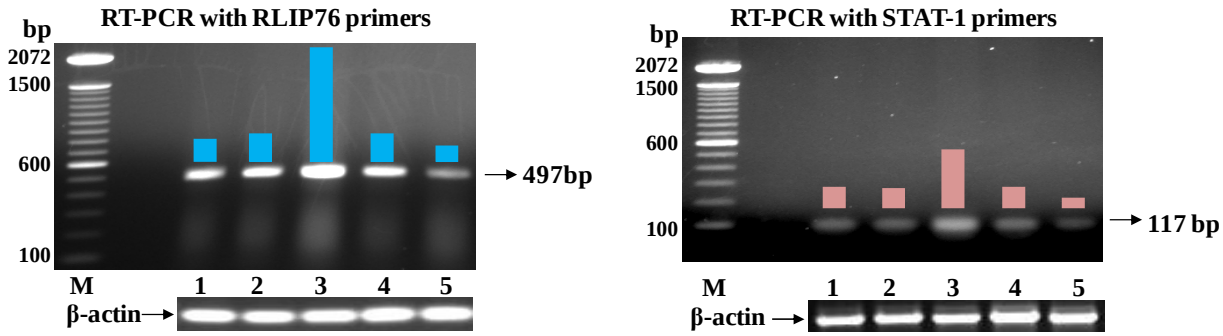

Figure 2. Regulation of the expression of STAT1 following knock-down and over-expression of RLIP76: The 786-O *VHL*-mut RCC cells were treated with RLIP76-antisense to knock-down RLIP76 and were transfected with pc-DNA3.1-RLIP76 to over express RLIP76. The RLIP76 and STAT1 mRNA levels were analyzed by RT-PCR. Lane 1: control Lane 2: pcDNA 3.1 vector transfection; Lane 3: vector + RLIP76 transfection; Lane 4: scrambled antisense transfection; Lane 5: RLIP76-antisense transfection. A Bar represents densitometry analyses.

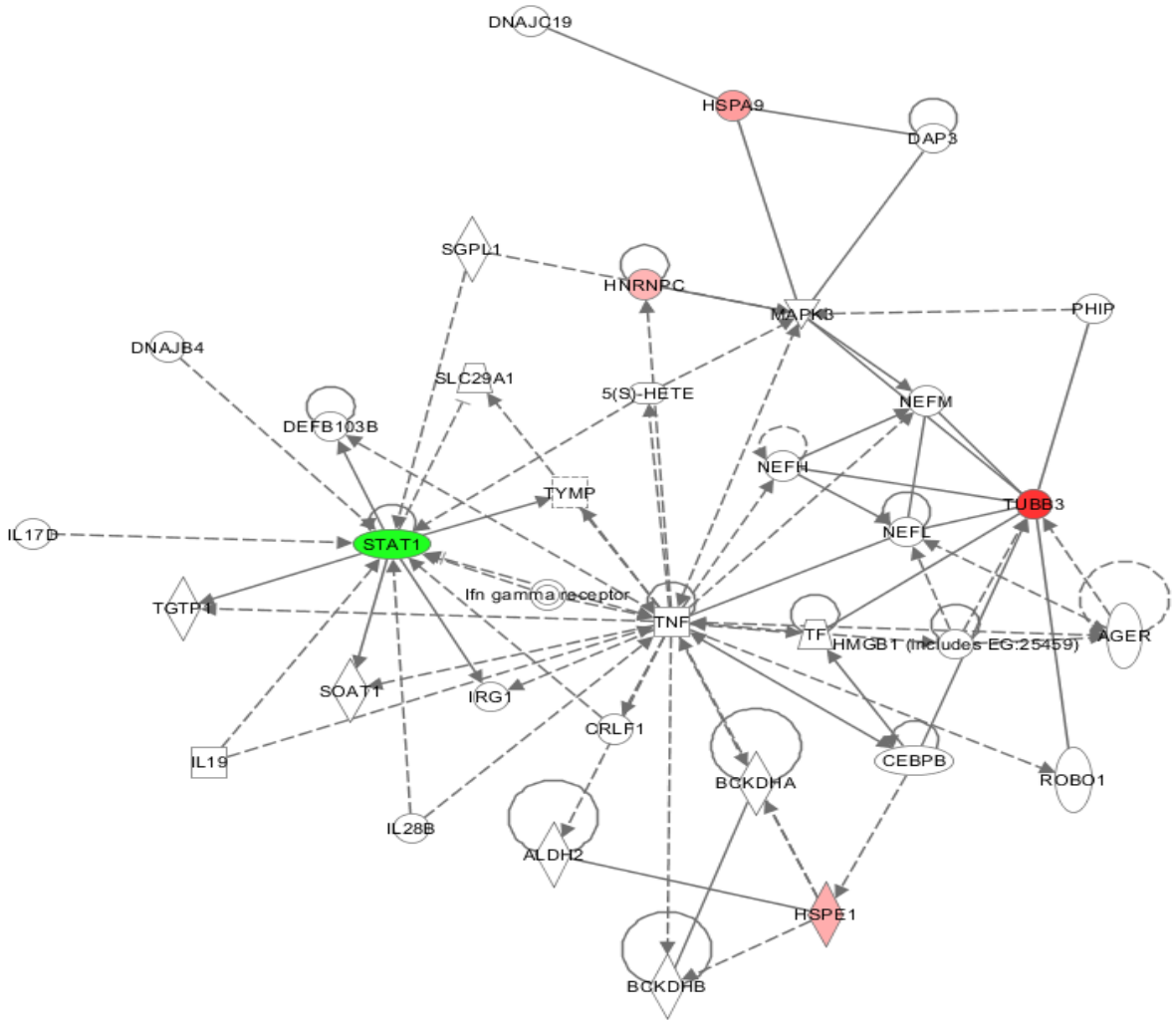

Figure 3. Regulation of the network of "Cell-to-cell signaling and interaction, cellular assembly and organization, cellular function and maintenance" due to proteins differentially regulated by RLIP76 in *VHL*-mut RCC. **Red**, up-regulated in *VHL*-mut RCC due to RLIP76 knock-down Vs. RLIP76 over-expression, **Green**, down-regulated in *VHL*-mut RCC due to RLIP76 knock-down Vs. RLIP76 over-expression.

a)

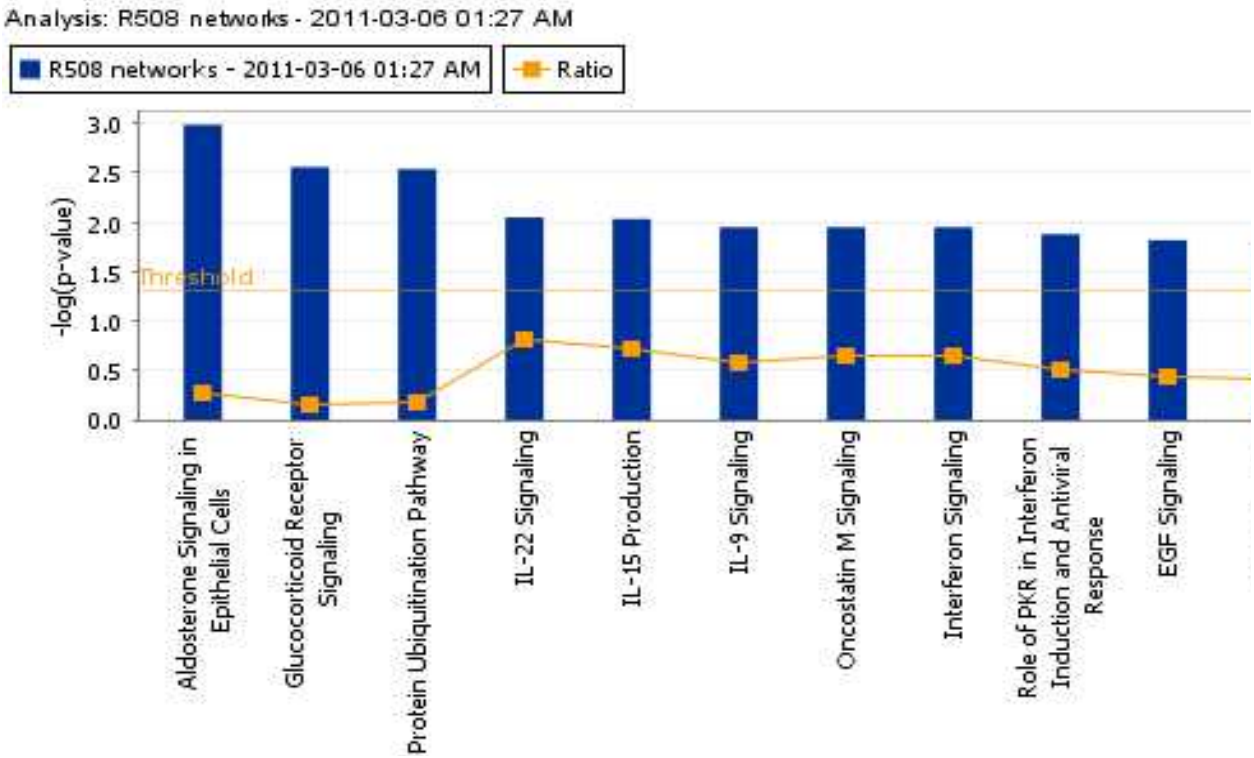

b)

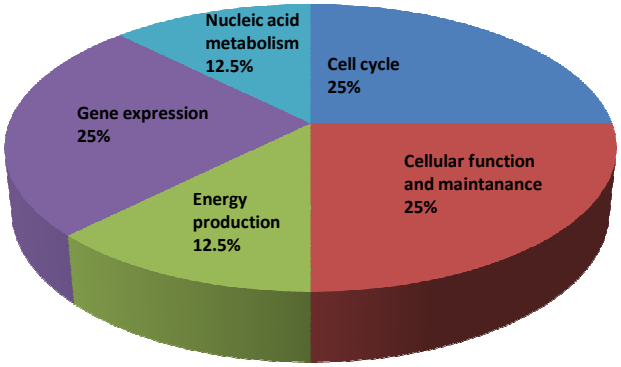

c)

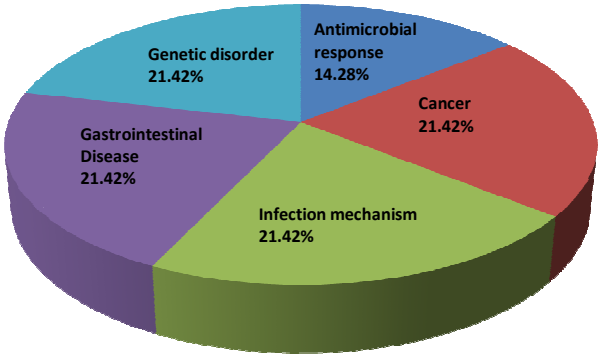

Figure 4. IPA analysis for the relevance of differentially regulated proteins by RLIP76 to cellular signaling processes (a), metabolic pathways (b) and diseases (c).

CHAPTER IV

ANTI-CANCER EFFECTS OF 2'-HYDROXYFLAVANONE IN *VHL*-MUTANT RENAL CELL CARCINOMA

INTRODUCTION

Renal cell carcinoma (RCC) is a frequently lethal cancer that affects patients who carry inherited or somatic mutations in the *VHL* (von Hippel-Lindau) gene which contribute to 75% of total RCCs [1-3]. RCC arises from epithelial cells of the proximal renal nephron and is characterized by its many different cytological and histological variants [3]. Tumor vascularity is of specific significance in RCC because of constitutively active hypoxic signaling in majority of renal tumors as a consequence of *VHL* mutations. According to National Cancer Institute, 1 in 67 men and women harbor the life time risk for RCC. Current chemotherapeutic choices for the advanced kidney cancer are limited, with a low chance of temporary remission, small improvement in average survival and substantial toxicity [4]. The association of life-style habits like tobacco smoking with RCC along with the increased risk for RCC in *VHL*-mutant (*VHL*-mut) populations makes the chemoprevention of RCC an important public health necessity [3-5]. In this regard, validation of the potential *VHL*-mut RCC specific anti-cancer compounds attains contemporary significance in renal oncology.

Flavonoids are a large group of polyphenolic compounds present in foods and beverages of plant origin which have antioxidant, anti-inflammatory, anti-mutagenic, and anti-proliferative properties [6-8]. 2'-Hydroxyflavanone (2HF) is a flavanone belonging to the larger family of flavonoids. The multi-center international RCC studies have established that the intake of citrus fruits is associated with decreased risk of RCC [9]. 2HF is known for its anti-metastatic effects in lung cancer [10]. In the present report, we show that 2HF, an active anti-cancer compound in oranges and citrus fruits, predominantly inhibits the growth of *VHL*-mut RCC, a major subtype of RCC. Our investigations addressed the impact of 2HF on oncogenic processes of importance in loss-of-*VHL* induced renal carcinogenesis like regulation of tumor proliferation and specifically angiogenesis in addition to investigating the impact on differentiation of 2HF treated *VHL*-mut RCC tumors *in vivo*. Our collective *in vitro* and *in vivo* investigations elucidated the anti-cancer potential and novel mechanisms of action of 2HF in *VHL*-mut RCC.

EXPERIMENTAL METHODS

Reagents MTT, 2HF, NDMA and BP were obtained from sigma (St Louis, MO). AKRIC, *VHL*, CD31, Ki67, cyclin B1, CDK4, Akt, EGFR, PI3K, and E-cadherin antibodies were purchased from Santa Cruz Biotechnology (Columbus, OH) and Cell Signaling Technologies (Danvers, MA). ELISA kit for VEGF expression was procured from R & D Systems. Source of GSTπ antibody was the same as previously described [11]. Matrigel was procured from BD Biosciences (San Jose, CA). TUNEL fluorescence and avidin/biotin complex (ABC) detection kits were purchased from Promega (Madison, WI) and Vector (Burlingame, CA), respectively.

Cell Lines and Cultures Human RCC Caki-2 cell line was purchased from ATCC, Manassas, VA, and Caki-1, A-498 & 786-O cells were kindly authenticated and provided by Dr. William G. Kaelin, Dana-Farber Cancer Institute, Harvard Medical School, Boston, MA. Human kidney normal (mesangial) cells were a generous gift from Dr. Rong Ma, UNTHSC, Fort Worth, TX. All cells were cultured at 37 °C in a humidified atmosphere of 5 % CO_2 in RPMI-1640 medium supplemented with 10 % FBS and 1% P/S solution.

Proteomic analysis, database searching and comparison of protein expression levels RCC cells were lysed in buffer containing 20 mM Tris-HCl, 50 mM NaCl, 6 M urea, 10 mM NaPP, 1 mM NaF and 1 mM Na3VO4. The lysate (200 μg protein) was subjected to reduction and alkylation of cysteines using 2.5 mM DTT and 7 mM idoacetamide followed by trypsin digestion and solid phase extraction using a C_{18} cartridge (Supelco, Bellefonte, PA). The digested peptides were analyzed using reversed-phase LC-MS/MS analysis using a hybrid Linear ion trap (LTQ)-Fourier-transform ion cyclotron resonance (FT-ICR, 7T) mass spectrometer (LTQFT, Thermo, San Jose, CA) which is equipped with nano-spray ionization source and operated by XCalibur (version 2.2) data acquisition software as described previously [12]. A 120-min gradient provide by nano-LC 2D (Eksigent, Dublin, CA) was carried out to 40% acetonitrile at 250 nL/min. An ESI spray voltage of 2.0 kV and a capillary temperature of 250 °C were maintained during the run. We employed a data-dependent mode of acquisition in which accurate mass/charge (*m/z*) survey scan was done in FTICR cell followed by a parallel MS/MS linear ion trap analysis. FTICR full-scan mass spectra were acquired at 100000 mass resolving power (at *m*/*z* 400) from *m*/*z* 350 to 1500 using the automatic gain control mode of ion trapping. Collision-induced dissociation (CID) in the linear ion trap was performed using a 3.0-Tn isolation width and 35%

normalized collision energy with helium as the collision gas. MS/MS spectra were searched against a human protein database by the Mascot software (Matrix Science, Boston, MA) and label-free semi-quantitative analysis was guided first by normalized spectral counts from the Scaffold program (Proteome Software, Portland, OR) with previously validated method [12]. Extracted-ion chromatograms (XICs, areas under the corresponding chromatographic peaks) of isoform-specific doubly- or triply-charged tryptic peptides from the full-scan high-resolution mass spectra were then used as quantitative measures of respective protein expression levels selected for evaluation in this study.

Drug sensitivity (MTT) assay Cell density measurements were performed using a hemocytometer to count reproductive cells resistant to staining with trypan blue. Approximately, 20,000 cells were plated into each well of 96-well flat-bottomed micro-titer plates. After 12 h incubation at 37 ^{o}C, medium containing 2HF (ranging 0-200 μM) was added to the cells. After 72 h incubation, 20 μL of 5 mg/mL MTT was introduced to each well and incubated for 2 h. The plates were centrifuged and medium was decanted. Cells were subsequently dissolved in 100 μL DMSO with gentle shaking for 2 h at room temperature, followed by measurement of OD_{570} [13-15]. Eight replicate wells were used at each point in each of three separate measurements.

Colony formation assay Cell survival was evaluated using a standard colony-forming assay. $1x10^5$ cells / mL were incubated with 2HF (50 μM) for 24 h, and aliquots of 50 or 100 μL were added to 60-mm size Petri dishes containing 4 mL culture medium. After 10 days, adherent colonies were fixed, stained with 0.5% methylene blue for 30 min, and colonies were counted using the Innotech Alpha Imager HP [16].

Effect of 2HF on apoptosis by TUNEL assay $1x10^5$ cells were grown on the cover slips for ~12 h followed by treatment with 2HF (50 μM) for 24 h. Apoptosis was determined by the labeling of DNA fragments with terminal deoxynucleotidyl-transferase dUTP nick-end labeling (TUNEL) assay using Promega apoptosis detection system according to the protocol described previously [15].

Flow cytometry analysis. The effect of 2HF on cell cycle distribution was determined by FACS analysis. 2 x 10^5 cells were treated with 2HF (ranging from 25 and 50 μM) for 18 h at 37 ^oC. After treatment, floating and adherent cells were collected, washed with PBS, and fixed with 70 % ethanol. On the day of flow analysis, cell suspensions were centrifuged; counted and same numbers of cells were resuspended in 500 μL PBS in flow cytometry tubes. Cells were then incubated with 2.5 μL of RNase (stock 20 mg/mL) at 37 ^oC for 30 min after which they were treated with 10 μL of propidium iodide (stock 1mg/mL) solution and then incubated at room temperature for 30 min in the dark. The stained cells were analyzed using the Beckman Coulter Cytomics FC500, Flow Cytometry Analyzer. Results were processed using CXP2.2 analysis software from Beckman Coulter.

RT-PCR analysis: RNA from control and experimental groups was isolated 24 h after treatment using an Rneasy kit (Qiagen,Valencia, CA, USA). Total RNA (5 μg) was subjected to RT-PCR using random primers and M-MuLV reverse transcriptase (Stratagene, La Jolla, CA, USA) in a 50 μL reaction volume for 60 min at 37^o C. The RT reaction product (1 μL) was then subjected to 35 cycles of multiplex PCR. The forward 5'-CCAGGTCATCTTCTGCAAT-3' and reverse 5'-

TGACGATGTCCAGTCTCCTG-3' *VHL* primers (Biosynthesis Inc, TX, USA) were used to amplify a 330 bp fragment of *VHL* spanning two exon–intron junctions. The PCR products were run on 1.5% agarose gel and visualized by ethidium bromide staining.

***In vitro* migration assay** Cell migration was determined using a scratch assay [17]. $2x10^4$ Caki-2 and 786-O cells were seeded in 6-well plates to reach 100% confluence within 24 h and then treated with 10 µM mitomycin C for 2 h. Subsequently, a similarly sized scratch was made with a 200 µL pipette tip across the center of each well and immediately imaged at baseline and then at 24 h under an Olympus Provis AX70 microscope. The rate of cell migration in control and 50 µM 2HF treated cells was determined by comparing the sizes of scratch area using Image J software.

***In vitro* angiogenesis assay (Tube formation assay)** Tube formation assay was performed as follows: 96-well plates were coated with 100 µL of Matrigel (10 mg/mL and incubated at 37 °C for 30 min to promote gelling. 14,000 cells were resuspended in medium (serum concentration 10%) and added to each well. Tube formation in the presence of 50 µM 2HF was compared. The number and length of tubes formed were counted under an Olympus Provis AX70 microscope for analysis between both the groups.

Assessment of angiogenesis, proliferation, and apoptosis Renal tumors (control as well as 2HF treated) were harvested from mice bearing tumors for 60 d. Tumor samples fixed in buffered formalin for 12 h were processed conventionally for paraffin-embedded tumor sections (5 µm thick). Hematoxylin and Eosin (H&E) staining was performed on paraffin-embedded

tumor sections. Histopathologic analyses with anti-E cadherin, anti-CD31 and anti-Ki67 IgG were also performed using Universal ABC detection kit (Vector). The sections were examined under Olympus Provis AX70 microscope connected to a Nikon camera.

HPLC analysis of 2HF mice serum C57B Mice (n=3 each for control and 2HF treatment) were administered either 0.1 mL corn oil/mice or 3mg 2HF/0.1mL corn oil/mice (equivalent to 0.01% w/w or 100 mg/kg b.w.) by oral gavage on alternate days for 4 weeks. On the last day, the blood was collected within 1 h after final dosage. The control serum sample spiked with 250 µM 2HF was used as positive control. The 100 µL of serum obtained from blood was subjected to protein precipitation using to 200 µL of methanol. The sample was centrifuged at 13300 rpm for 15 min at 4 °C and the clear supernatant was lyophilized. The resulting pellet was dissolved in 200 µL of methanol: 0.2% phosphoric acid buffer (58:42) [46,47]. The 25 µL of each sample was subjected to HPLC analysis at wavelength of 295 nm using a mobile phase consisting of acetonitrile and water at a flow rate of 1.0 mL/min with following gradient: 0-1 min: ACN-10%, H_2O-90% ; 1-2 min: gradually increasing to ACN-20%, H_2O-80% ; 2-14 min: gradually changing to ACN-90%, H_2O-10% ; 14-16 min: ACN-10%, H_2O-90%.

$$\text{2HF concentration} = \frac{[\text{Concentration of 2HF serum std}] \times [\text{Avg Area of 2HF-treated serum samples}]}{[\text{Area of 2HF serum std}]}$$

***In vivo* xenograft studies** Hsd: Athymic nude *nu/nu* mice were obtained from Harlan, Indianapolis, IN, and were acclimated for a week before beginning the experiment. All animal experiments were carried out in accordance with a protocol approved by the Institutional Animal Care and Use Committee (IACUC). Twenty-eight 11-weeks-old mice were divided into four groups of 7 animals (treated with vehicle only i.e. corn oil and 2HF at the doses of 0.0025%,

0.005% and 0.01% w/w). All 28 animals were injected with 2 x 10^6 786-O (*VHL*-mut) cells in 100 µL of PBS, subcutaneously into one flank of each mouse. At the same time, animals were randomized into control and treatment groups. Treatment was started 10 days after the 786-O cells implantation to see palpable tumor growth. Treatment consisted of 2HF at the doses of 0.0025%, 0.005% and 0.01% (w/w), equivalent to 25, 50 and 100 mg/kg b. w. respectively, in 200 µL corn oil by oral gavage on alternate days. Control groups were treated with corn oil only. In parallel, we also performed Caki-2 (*VHL*-wt) RCC xenografts studies. Animals were examined daily for signs of tumor growth. Tumors were measured in two dimensions using calipers and body weights were recorded. Each mouse in every group was monitored on alternate days for signs of distress and areas of swelling or redness. Photographs of animals were taken at day 1, day 10, day 20, day 40, and day 60 after subcutaneous injection, are shown for all groups. Photographs of tumors were also taken at day 60.

Statistical Analyses All data were evaluated with a two-tailed unpaired student's t test or compared by one-way ANOVA and are expressed as the mean $\pm$ SD. A *P*-value of < 0.05 was regarded as statistically significant.

RESULTS AND DISCUSSION

2HF inhibits proliferation and stimulates apoptosis in *VHL*-mut RCC The MTT assay following the treatment of 2HF in RCC cell lines revealed the potent inhibition of survival of *VHL*-mut RCC in the presence of 2HF [IC_{50} at 72h: *VHL*-mut RCC (786-O and A498): 28 ± 4 µM, *VHL*-wt RCC (Caki-1 and Caki-2): 90 ± 6 µM] (**Fig 1A**). In accordance with MTT assay,

2HF inhibited the clonogenic survival of *VHL*-mut RCC (~70% inhibition) in colony formation assay to significantly greater extent when compared to *VHL*-wt RCC cells (~20% inhibition) (**Fig 1B**). Following our initial investigations in four RCC cell lines, we investigated the detailed mechanisms of action of 2HF in Caki-2 (*VHL*-wt) and 786-O (*VHL*-mut) cells. Our initial cytotoxicity studies revealed that 2HF inhibits the growth of *VHL*-mut RCC to a greater extent when compared with its inhibitory effect on *VHL*-wt RCC. Hence, we focused on investigating the preceding cellular events that determine the eventually cytotoxicity of 2HF in RCC. The cytotoxicity of 2HF treatment was also determined at 24 h by the MTT assay (IC_{50} at 24 h: 786-O = 72$\pm$6 µM, caki2 = 148$\pm$11 µM). We used 50 µM of 2HF for 24 h treatment for both the cell lines as cell death should be minimal for mechanistic and imaging studies focused on early cellular events that contribute to eventual cytotoxicity at 72 h. The 50 µM of 2HF treatment for 24 h effectively induced apoptosis in *VHL*-mut RCC to a greater extent, sparing normal mesangial cells, when compared to *VHL*-wt RCC as determined by enhanced DNA fragmentation in TUNEL apoptotic assay (**Fig 1C**). The enhanced cytotoxicity of 2HF in *VHL*-mut RCC along with the absence of any cytotoxicity towards normal mesangial cells in MTT, clonogenic survival and TUNEL apoptotic assays revealed that 2HF is a potential flavonoid that could have significant therapeutic relevance in specifically targeting *VHL*-mut RCC.

2HF inhibits activation of EGFR, PI3K, and Akt signaling in *VHL*-mut RCC Loss-of-*VHL* leads to up-regulation of EGFR signaling in renal cancers [18]. Activation of EGFR is involved in the growth and progression of many types of solid tumors, including RCC by up regulating PI3K and Akt signaling [19]. Hence, we investigated the effect of 2HF on EGFR signaling in *VHL*-mut RCC. Western blot analysis revealed that 2HF significantly inhibits pEGFR (Y^{1068}),

PI3K ($Y^{458/199}$) and pAkt (S^{473}) in *VHL*-mut RCC (**Fig 1D**). The 2HF treatment also increased PARP-cleavage in *VHL*-mut RCC (786-O) to a significantly greater extent when compared to *VHL*-wt (Caki-2) RCC.

Detection of differential expression of AKR1C1 and GSTπ in RCC In order to understand the differences in the *VHL*-wt and *VHL*-mut RCC, we performed proteomic analysis of whole cell proteome using a hybrid linear ion trap–Fourier transform ion cyclotron resonance tandem mass spectrometer (LTQ-FT, Thermo) operated with nano-electrospray ionization (ESI) and coupled to an Eksigent nano-LC system. MS/MS spectra were searched against a human protein database by the Mascot software (Matrix Science) and label-free quantification was guided first by spectral counts from the Scaffold software (Proteome Software, Version 2) with our previously validated method [12]. Caki-2 (*VHL*-wt) and 786-O (*VHL*-mut) cells, revealed differential expression of aldoketo-reductase family 1, member C 1 (AKR1C1; selectively detected in Caki-2 RCC) and glutathione S transferase π (GSTπ; selectively detected in 786-O RCC). The MS/MS spectra of isoforms-specific representative peptides for these proteins are shown in the top with corresponding peptide sequence below (**Fig 2A**). The relative quantification based on integrated extracted ion chromatograms (XICs) of doubly- and triply-charged tryptic peptides detected for AKR1C1 and GSTπ, respectively, are represented in the bar diagrams. This observed differential expression of AKR1C1 and GSTπ was also revalidated by Western-blot analysis using specific antibodies (**Fig 2B**).

2HF inhibits GSTπ activity, angiogenesis and migration of *VHL*-mut RCC The enhanced growth inhibitory effect of 2HF, a well characterized AKR1C family inhibitor, in

VHL-mut RCC which does not express detectable AKR1C1 was an interesting finding [20]. We investigated the effect of 2HF on the enzymatic-activity of GSTπ towards CDNB (1, Chloro 2,4-dinitro-benzene, a model substrate routinely used for GST activity [11]. 2HF inhibited the total GST activity to a significant extent in the *VHL*-mut RCC (**Fig 3A**). Human recombinant purified GSTπ was used as a standard in enzyme activity assay (**Fig 3A inset**). GSTπ is a phase II detoxifying enzyme which mediates xenobiotic resistance by detoxifying administered chemotherapy drugs for efflux out of cells by transport proteins. GST π is an established marker of many aggressive cancers like lung and prostate cancers [21,22]. GST π mediated detoxification of toxic end products of lipid peroxidation like 4-Hydroxy-2-nonenal (4HNE) leads to buffering of tumor-toxic oxidative stress and favors tumor survival and proliferation in hypoxic environment [23]. GST π also has post-translational regulatory role in S-glutathionylation of various cell proteins which is implicated in regulating cell adhesion and proliferation [24]. In this regard, the ability of 2HF to inhibit GST π and total GST activity in *VHL*-mut RCC which has high levels of expression of GST π represents an important anti-cancer effect of 2HF given its cytotoxic potential in *VHL*-mut RCC. Further detailed studies would reveal the role of GST π and oxidative stress pathways in mediating the anti-cancer effects of 2HF in RCC. As there are no chemopreventive strategies reported for the *VHL*-mut RCC which is a highly prevalent malignancy in USA and given the ability of 2HF to effectively inhibit the survival of *VHL*-mut RCC as revealed by our initial studies, we specifically focused on studying the impact of 2HF in regulating the proliferative potential, angiogenic response and differentiation of *VHL*-mut RCC both *in vitro* and *in vivo*.

VHL-null/mut renal tumors are characterized by an angiogenic phenotype due to constitutive HIF2-α up-regulation as a consequence of loss of *VHL* function [25]. Hence, the investigation of the regulation of tumor angiogenesis is important in the characterization of effective anti-cancer compounds and further drug development. We studied the effect of 2HF on angiogenic signaling *in vitro* by examining VEGF expression [26]. 2HF treatment caused significant reduction in the levels of VEGF expression in *VHL*-mut RCC when compared to *VHL*-wt RCC (**Fig 3B**). 2HF treatment lead to specific and significant decrease in angiogenesis as determined by change in both the number and size of cellular tubes formed *in vitro* tube formation assay in *VHL*-mut RCC (**Fig 3C)**. Following *in vitro* angiogenic assay, we studied the effect of 2HF on the migratory potential of RCC *in vitro*. 2HF treatment also caused significant inhibition of cell migration in wound-healing assay in *VHL*-mut RCC (**Fig 3D**).

2HF inhibits cell cycle progression in *VHL*-mut RCC The mechanism of cytotoxicity of 2HF was further assessed by determining apoptosis through cell cycle FACS analysis. The 50 µM of 2HF treatment for 18 h caused G2/M phase arrest which was predominant in *VHL*-mut RCC (~61% cells accumulated in G2 phase, $p < 0.01$) (**Fig 4A**). Please note that the use of even higher concentration of 2HF (50 µM) in Caki2 RCC was not effective in inhibiting cell cycle when compared to cell cycle results obtained with 25 µM of 2HF in 786-O RCC. We further analyzed the morphology of RCC cells after 2HF treatment. The *VHL*-mut and *VHL*-wt RCC were treated with 50 µM of 2HF for 24 h and the cell morphology was observed by live cell imaging in Zeiss phase contrast microscope. The 2HF treated *VHL*-mut RCC cells were less adherent and more rounded compared to the controls and *VHL*-wt RCC. The initial morphological observation of control and 2HF treated *VHL*-mut RCC cells indicated impaired

cell division in 2HF treated cells. 2HF treated *VHL*-mut RCC cells had more cells that were unable to complete cytokinesis compared to the control cells. These results confirmed G2/M phase arrest and potential inhibition of the completion of cytokinesis in 2HF treated *VHL*-mut RCC. The 2HF treatment reduced the levels of cyclin B1 and CDK4 in *VHL*-mut but not in *VHL*-wt RCC (**Fig 4B**). Some of the natural anti-cancer compounds like silibinin are known to cause G2/M phase arrest by inhibiting cyclin B1 [27]. CDK4, commonly associated with G1 transition, has been also investigated for its role in G2/M transition and it has been shown that over-expression of dominant negative CDK4 leads to arrest of G2 phase progression [28]. Some of the anti-cancer compounds like apigenin and thiomersal also cause inhibition of CDK4 along with cyclin B1 while causing G2/M phase arrest [29,30]. Collectively, our *in vitro* results strongly validated the specific anti-proliferative, anti-angiogenic and anti-metastatic effects of 2HF which lead to further proteomic investigation of the effects of 2HF in *VHL*-mut RCC.

Proteomic analyses of differentially expressed proteins due to 2HF treatment in *VHL*-mut RCC Proteomic analysis of 2HF treated and control *VHL*-mut RCC cells revealed differential expression of proteins that regulate cellular invasion, DNA replication, recombination and tumor suppressor functions (**Table 1**). A novel finding was the decrease in the levels of Neuroblast differentiation associated protein (AHNAK) after 2HF treatment. Our studies from the proteomic analysis of *VHL*-mut and *VHL*-wt RCC had revealed increased levels of AHNAK in *VHL*-mut RCC relative to *VHL*-wt RCC. AHNAK is both a nuclear and cytoplasmic protein whose localization is regulated by the activity of protein kinase B (PKB)/Akt . Phosphorylation of AHNAK in the C-terminal by PKB leads to its nuclear exclusion and cytoplasmic localization [31]. Phosphorylation of AHNAK by PKC in the

cytoplasm further mediates the translocation of AHNAK to plasma membrane where it participates in the formation of cell-cell contacts at desmosomes [32]. AHNAK has been identified as a cooperative gene in the adenomatous polyposis coli (APC) induced oncogenic transformation of colon epithelial cells [33]. Hence, the decrease in the levels of AHNAK consequent to 2HF treatment may be a significant proteomic finding in *VHL*-mut RCC. The other proteins decreased due to 2HF treatment in *VHL*-mut RCC included the single stranded (ss) telomeric DNA binding and mRNA processing protein hnRNP A2/B1 which is known to be increased in lung cancers [34,35]. The decrease in the levels of vimentin which is involved in epithelial mesenchymal transformation (EMT) of cancerous cells was another significant finding which collectively conveyed that 2HF treatment leads to inhibition of cellular invasive and survival properties by targeting the critical nodes of cell-cell contacts, down-regulation of EMT associated proteins and by reinforcing epithelial tumor suppressor function [36]. Prohibitin is known as a potential tumor suppressor protein that interacts with retinoblastoma protein (Rb) pathway where prohibitin binds to E2F and represses the cell growth [37-38]. The up-regulation of the prohibitin which is known to function as tumor suppressor in many cancers after 2HF treatment was another salient proteomic finding in *VHL*-mut RCC.

The IPA analysis of differentially regulated networks revealed that the network of "Tissue development, gene expression and cell morphology" was a major network regulated by 2HF treatment in *VHL*-mut RCC (**Fig 5**). The pathway analyses revealed that the differential regulation of proteins by 2HF in turn regulates *Oct4* embryonic stem cell pathway in *VHL*-mut RCC **(Fig 6A).** The analysis of the impact of 2HF treatment on cellular signaling and disease processes revealed an impact on cell morphology, cell-to cell signaling and interaction, DNA

replication, recombination and repair, cancer, genetic disorders and neurological diseases (**Fig 6B and C**).

2 HF induces potent tumor regression *in vivo* mice xenografts *VHL*-mut 786-O RCC cells bearing animals with established *s.c.* implanted tumors (~20 mm^2) were treated with 0.0025%, 0.005% and 0.01% (w/w) (equivalent to25, 50 and 100 mg/kg b.w., respectively) of 2HF in corn oil by oral gavage on alternate days. In the present studies, doses of 2HF were well tolerated by the mice and did not result in any weight loss compared with age-matched controls (**Fig 7A**). Photographs of animals were taken at day 1, 10, 20, 40, and 60 after subcutaneous injection. Tumors grew more slowly in *VHL*-mut RCC mice xenografts administered with 2HF than in respective untreated control mice. At day 60, tumor cross-sectional area and tumor-weight of mice bearing *VHL*-mut RCC was significantly lower in 0.01% (w/w) dose treated group as compared to the vehicle only (corn-oil) treated group (19.8 $\pm$ 3 mm^2 *vs.* 122 $\pm$ 7 mm^2 and 0.07 $\pm$ 0.01g *vs.* 2.14 $\pm$ 0.24 g, respectively; $p<0.001$). More importantly, *in vivo* studies showed that administration of 2HF at 0.01% (w/w), to nude mice bearing *VHL*-mut RCC completely arrested tumor progression whereas uncontrolled growth was observed in the animals treated with vehicle only (**Fig 7B&C**). The 2HF treated animals with *VHL*-mut RCC were still alive at 139 days. In comparison, all animals treated with vehicle only, were censored by day 71 $\pm$ 3. These results indicated that dietary 2HF administration inhibits *VHL*-mut RCC growth and prolongs survival without causing side-effects. To rule out the possibility that the observed *in vivo* effects of 2HF were specific to *VHL*-mut RCC, we also evaluated the anti-neoplastic effects of 2HF on the *VHL*-wt (Caki-2) RCC. We observed tumor growth arrest due to 2HF treatment in *VHL*-wt RCC, but to a lesser extent compared to *VHL*-mut RCC (at day 60, tumor cross-

sectional area and tumor weight, 2HF treated vs. control; 98 $\pm$ 12 mm^2 vs. 115 $\pm$ 7 mm^2 and 1.84 $\pm$ 0.12 g *vs.* 2.25 $\pm$ 0.18 g, respectively; non-significance) (**Fig 7**). Also, even 100 mg/kg b.w. of 2HF caused only ~18% reduction in the tumor growth of *VHL*-wt Caki-2 RCC while only 25 mg/kg b.w. of 2HF caused 41% tumor regression in *VHL*-mut 786-O RCC ($p < 0.001$) .

In our *in vitro* studies, 2HF effectively inhibited the angiogenic process and clonogenic potential besides causing apoptosis in *VHL*-mut RCC. In order to assess the degree of impact of 2HF *in vivo* on these processes of specific importance in *VHL*-mut RCC progression and metastasis, we performed histopathological examination of the resected tumor xenografts.

2HF inhibits the expression of proliferative and angiogenic markers while promoting normal epithelial differentiation in *VHL*-mut RCC The histopathological examination of paraffin-embedded tumor xenograft sections as observed by initial H&E staining revealed that 2HF treatment reduces the number of tumor blood vessels and restores the normal morphology specifically in *VHL*-mut RCC when compared to controls (**Fig 8**). Following this, we probed the tumor sections for specific markers of proliferation, angiogenesis and differentiation. 2HF treatment decreased the levels of proliferation marker, Ki 67, and angiogenesis marker, CD31, in *VHL*-mut RCC which further supported the observed *in vitro* anti-proliferative and anti-angiogenic effects of 2HF. Another important finding was that the 2HF treatment predominantly increased the expression of E-cadherin in *VHL*-mut RCC xenografts. E-cadherin is considered a suppressor of invasion and growth of many epithelial cancers because of its role in the inhibition of epithelial-mesenchymal transition (EMT) and promoting normal epithelial phenotype [39-42]. E-cadherin is frequently down-regulated during cancer progression and correlates with poor

prognosis [44]. Loss of E-cadherin is associated with incidence and progression of many epithelial tumors [43-45]. In this regard, over-expression of E-cadherin consequent to 2HF treatment represents a highly significant and novel mechanism of action of 2HF in *VHL*-mut RCC (**Fig 8**).

The orally administered 2HF was effective in inducing potent anti-cancer effects *in vivo*. Hence, we further analyzed the serum concentrations of 2HF following oral administration in mice.

HPLC analysis of 2HF in mice serum The extent of absorption of 2HF was studied by analyzing the serum samples of mice treated with 3 mg/mice (100 mg/kg b.w. or 0.01% w/w) of 2HF by oral gavage on alternate days for 4 weeks by reversed-phase HPLC analysis [46,47]. The HPLC analysis of control and 2HF treated mice serum samples revealed that 2HF reaches a concentration of 88 µM (~42 µg/mL of serum) at the end of 4 weeks which confirmed that 2HF is effectively absorbed consequent to oral administration (**Fig 9**).

Kidney is under constant stress of detoxification due to its natural role in eliminating toxins from the body. Hence, kidney is more susceptible to genotoxic carcinogenic stress. Cigarette smoking has been established as a high risk factor for the RCC in many clinical trials [18]. Tobacco carcinogen N-nitrosodimethylamine (NDMA) is a known renal carcinogen with the ability to induce RCC in animal models. The NDMA induced rat renal tumors have increased *VHL* mutations [48]. Benzopyrene (BP), another potent tobacco carcinogen, has been recently shown to induce deletions of chromosome 3p25.2, the *VHL* locus [49]. Thus the

interplay of tobacco carcinogens and loss of *VHL* represents a highly interactive and proximal causative spectrum in the primary pathogenesis of RCC.

Protective effect of 2HF in the presence of *VHL*-genotoxic carcinogens We tested HEK-293 normal renal epithelial cells for the effect of 2HF on *VHL* levels upon exposure to genotoxic tobacco carcinogens, NDMA and BP. HEK-293 cells were treated with 2 µM BP, 1 mM NDMA either in single or combination with 50 µM 2HF for 24 hours. Treatment with BP or NDMA alone or in combination reduced the levels of *VHL* to significant extent. Co-treatment of 2HF strongly protected from the NDMA and BP induced damage to *VHL* as revealed by restoration of *VHL* mRNA levels to statistically significant extent as detected by RT-PCR analysis using *VHL* specific primers [50]. Western blot analysis also revealed the protective effects of 2HF against loss of *VHL* as 2HF treatment reversed the NDMA and BP induced reduction in *VHL* protein levels ($p<0.001$). Thus, the ability of 2HF to protect against carcinogen induced loss of *VHL* represents another significant and encouraging mechanistic finding in further developing 2HF for the chemoprevention of *VHL*-mut RCC **(Fig 10).**

CONCLUSION

Renal cell carcinoma is one of the frequently incident cancers in USA with an increasing current trend of incidence. Intake of citrus fruits has been shown to reduce RCC risk in clinical trials [9]. In this regard, we investigated the anti-cancer effects and the respective mechanisms of action of 2HF, a natural compound found in citrus fruits and oranges, in RCC. Our studies demonstrate that 2HF exhibits potent anti-proliferative and pro-apoptotic effects to a significantly greater

extent in *VHL*-mut RCC when compared to *VHL*-wt RCC. The anti-proliferative effects of 2HF were mediated by the inhibition of EGFR, PI3K and pAkt signaling in *VHL*-mut RCC. The growth inhibitory effects of 2HF also included the inhibition of cell cycle progression which was mediated by reduction in the levels of cyclin B1 and CDK4 in *VHL*-mut RCC.

2HF was shown in our studies, for the first time, to be a novel GSTπ inhibitor. 2HF also effectively inhibited both recombinant GSTπ and over 50% of total GST activity in *VHL*-mut RCC at concentrations toxic to tumors but well tolerated by normal cells. Post-translational S-glutathionylation of proteins which is an emerging topic of investigation in apoptosis and enhanced oxidative signaling due to constitutively active HIF2-α in *VHL*-null background signify the role of GST π function in regulating differential cytotoxicity of 2HF in RCC. Enhanced expression of GST π can lead to increased detoxification of products of lipid peroxidation and administered chemotherapy drugs by conjugation with glutathione (GSH) to form glutathione adducts (GS-E) which are eventually transported out of the cells by an active, ATP dependent process mediated by RLIP76 [14-16]. GST π also catalyzes the S-glutathionylation of active site nucleophilic cysteines in many phosphatases conferring additional negative charge to the active site [24]. S-glutathionylation induced redistribution of charge at active site of proteins has been known to influence both substrate accessibility and catalytic efficiency of target proteins with pronounced effects on the tumor signaling pathways [51]. In this regard, further knock-in and knock-out follow-up studies of GSTπ, *VHL* and HIF2-α could characterize the impact of differential regulation of oxidative stress pathways in regulating the anti-cancer effects of 2HF.

One of the significant observation was that 2HF caused effective inhibition of VEGF expression in *VHL*-mut RCC sparing normal mesangial cells. Angiogenesis is essential for the growth of rapidly proliferating tumors whose centers are usually hypoxic and specifically in renal tumors with *VHL*-mutations which have high HIF2-α levels. HIF2-α initiates a compensatory angiogenic response to match the rapid rate of tumor growth by stimulating VEGF expression [52]. Normally, *VHL* binds to HIF2-α and targets it for degradation. Loss or inactivation of *VHL* leads to loss of substrate recognition required for binding to HIF2-α which effectively leads to enhanced levels and activity of HIF2-α and consequent tumor angiogenesis [53,54].

Importantly, 2HF treatment significantly reversed the reduction in mRNA and protein levels of *VHL* in the presence of *VHL*-genotoxic tobacco carcinogens NDMA and BP in normal renal epithelial cells. LC-MS/MS proteomic analysis revealed novel proteins differentially regulated by 2HF treatment in *VHL*-mut RCC. In this regard, 2HF represents a safe and novel anti-angiogenic natural compound without normal tissue cytotoxicity with specific significance in the management of highly vascular *VHL*-mut RCC. Thus, our *in vitro* studies demonstrated the potential of 2HF to protect from *VHL* genotoxic carcinogens while having no overt toxicity in normal cells besides revealing the ability of 2HF to act as an effective anti-cancer drug in *VHL*-mut RCC.

Our *in vivo* studies further provided corroborative evidence to the anti-cancer effects and mechanisms of action of 2HF of particular relevance to *VHL*-mut RCC. In our present study, we were able to show that orally administered 2HF is absorbed to reach effective serum levels by

HPLC analysis of mice serum samples. It is possible that potential pharmacokinetic differences in drug uptake and metabolism between cell types which in turn influence the duration of drug action at intracellular targets could be contributing to some of the terminal events due to 2HF treatment between the *VHL*-wt and *VHL*-mut genotypes of RCC which need further absorption, distribution, metabolism and excretion (ADME) studies. However, from a clinical point of view, the ability of 2HF to effectively target *VHL*-mut RCC which contributes to most common form of RCCs is of potential significance in the chemoprevention of RCC. Our mice xenograft studies also confirmed that the orally administered 2HF is effective *in vivo* to exert its anti-cancer effects in *VHL*-mut RCC as observed similarly in the *in vitro* studies. The dose of 2HF required to cause effective tumor regression (~90% reduction in tumor growth, **Fig 5**) in *VHL*-mut RCC was 0.01% (w/w) which is well in comparable range to other flavonoids being tested in clinical trials [27]. Also, 2HF caused inhibition of Akt signaling and increased PARP-cleavage in mice xenografts of *VHL*-mut RCC which revealed that the orally administered 2HF can effectively induce an *in vivo* anti-mitogenic and pro-apoptotic response. 2HF also decreased the expression of proliferative marker, Ki 67, and angiogenic marker, CD31, in the *VHL*-mut RCC. One of the significant findings was that 2HF treatment increased the levels of E-cadherin specifically in *VHL*-mut tumors *in vivo*. Loss of E-cadherin is associated with incidence and progression of many epithelial tumors and restoration of E-cadherin reverts them to normal epithelial phenotype [55]. Given the renal tubular epithelial origin of RCC, the increased expression of E-cadherin after 2HF treatment assumes mechanistic significance in the chemoprevention of *VHL*-mut RCC.

The *VHL* syndrome is an autosomal dominant condition caused by mutation or deletion of the *VHL* gene and characterized by highly vascular neoplasm including RCC, café-au-lait spots, angiomatosis, hemangioblastomas and pheochromocytomas. *VHL* protein is an ubiquitin E3 ligase that targets HIF to proteasomal degradation and thus prevents constitutive activation of hypoxic and angiogenic signaling [56]. Our findings providing strong evidence for the pro-apoptotic, anti-angiogenic and pro-differentiation effects of 2HF in *VHL*-mut RCC could also have additional potential implications towards other *VHL* related tumor syndromes in general. Taken together, in the light of pathogenetic mechanisms of loss-of-*VHL* driven renal carcinogenesis, the anti-cancer properties of 2HF like inhibition of survival, proliferation and tumor vascularization without causing any overt toxicity towards normal tissues provide sound scientific rationale for the role of 2HF in the chemoprevention of *VHL*-mut RCC.

ACKNOWLEDGEMENTS

The authors thank Dr. Xiangle Sun, core facility at the University of North Texas Health Science Center, Fort Worth, TX, for helping with flow cytometry and laser capture micro-dissection (supported by NIH Grant ISIORR018999-01A1). We also thank Dr. Sumihiro Suzuki, Department of Biostatistics, School of Public Health, University of North Texas Health Science Center, Fort Worth, TX, for his assistance in the statistical analyses of the data. This work was supported by the National Institutes of Health grant CA 77495 (to S.A. & S.S.S.), the Welch Foundation endowment BK-0031 (to L.P.), the Cancer Research Foundation of North Texas, and the Institute for Cancer Research & the Joe & Jessie Crump Fund for Medical Education (to S.S.S.).

REFERENCES

1 Linehan, W.M., Vasselli, J., Srinivasan, R., et al. (2004) Genetic basis of cancer of the kidney: disease-specific approaches to therapy. *Clin Cancer Res*;**10:**6282S-6289S.

2 Atkins, M.B., Ernstoff, M.S., Figlin, R.A., et al. (2007) Innovations and challenges in renal cell carcinoma: summary statement from the Second Cambridge Conference. *Clin Cancer Res*;**13**:667s-670s.

3 Kuroda, N., Toi, M., Hiroi, M., Shuin, T. and Enzan, H. (2003) Review of renal oncocytoma with focus on clinical and pathobiological aspects. *Histol Histopathol*;**18**:935-942.

4 Hunt, J.D., van der Hel, O.L., McMillan, G.P., Boffetta, P. and Brennan, P. (2005) Renal cell carcinoma in relation to cigarette smoking: meta-analysis of 24 studies. *Int J Cancer*;**114**: 101-108.

5 Van Dijk, B.A., Schouten, L.J., Oosterwijk, E., et al. (2006) Cigarette smoking, von Hippel-Lindau gene mutations and sporadic renal cell carcinoma. *Br J Cancer*;**95**:374-377.

6 Choquenet, B., Couteau, C., Paparis, E. and Coiffard, L.J. (2009) Flavonoids and polyphenols, molecular families with sunscreen potential: determining effectiveness with an in vitro method. *Nat Prod Commun*;**4**:227-230.

7 Woodman, O.L. and Chan, E.C. (2004) Vascular and anti-oxidant actions of flavonols and flavones. *Clin Exp Pharmacol Physiol*;**31**:786-790.

8 Benavente-Garcia, O. and Castillo, J. (2008) Update on uses and properties of citrus flavonoids: new findings in anticancer, cardiovascular, and anti-inflammatory activity. *J Agric Food Chem*;**56**:6185-6205.

9 Wolk, A., Gridley, G., Niwa, S., et al. (1996) International renal cell cancer study. VII. Role of diet. *Int J Cancer*;**65**:67-73.

10 Hsiao, Y.C., Kuo, W.H., Chen, P.N., et al. (2007) Flavanone and 2'-OH flavanone inhibit metastasis of lung cancer cells via down-regulation of proteinases activities and MAPK pathway. *Chem Biol Interact*;**167**: 193-206.

11 Singhal, S.S., Saxena, M., Ahmad, H., Awasthi, S., Haque, A.K. and Awasthi, Y.C. (1992) Glutathione S-transferases of human lung: characterization and evaluation of the protective role of the alpha-class isozymes against lipid peroxidation. *Arch Biochem Biophys*;**299**: 232-241.

12 Prokai, L., Stevens, S.M.,Jr, Rauniyar, N. and Nguyen, V. (2009) Rapid label-free identification of estrogen-induced differential protein expression in vivo from mouse brain and uterine tissue. *J Proteome Res*;**8**:3862-3871.

13 Singhal, S.S., Sehrawat, A., Sahu, M., et al. (2010) Rlip76 transports sunitinib and sorafenib and mediates drug resistance in kidney cancer. *Int J Cancer*;**126**:1327-1338.

14 Singhal, S.S., Singhal, J., Yadav, S., Sahu, M., Awasthi, Y.C. and Awasthi, S. (2009) RLIP76: a target for kidney cancer therapy. *Cancer Res*;**69**:4244-4251.

15 Singhal, S.S., Yadav, S., Drake, K., Singhal, J. and Awasthi, S. (2008) Hsf-1 and POB1 induce drug sensitivity and apoptosis by inhibiting Ralbp1. *J Biol Chem*;**283**:19714-19729.

16 Singhal, J., Singhal, S.S., Yadav, S., et al. (2008) RLIP76 in defense of radiation poisoning. *Int J Radiat Oncol Biol Phys*;**72**:553-561.

17 Rosenberg Zand, R.S., Jenkins, D.J., Brown, T.J. and Diamandis, E.P. (2002) Flavonoids can block PSA production by breast and prostate cancer cell lines. *Clin Chim Acta*;**317**:17-26.

18 Lee, S.J., Lattouf, J.B., Xanthopoulos, J., Linehan, W.M., Bottaro, D.P. and Vasselli, J.R. (2008) Von Hippel-Lindau tumor suppressor gene loss in renal cell carcinoma promotes oncogenic epidermal growth factor receptor signaling via Akt-1 and MEK-1. *Eur Urol*;**54**: 845-853.

19 Merseburger, A.S., Hennenlotter, J., Kuehs, U., et al. (2008) Activation of PI3K is associated with reduced survival in renal cell carcinoma. *Urol Int*;**80**:372-377.

20 Skarydova, L., Zivna, L., Xiong, G., Maser, E. and Wsol, V. (2009) AKR1C3 as a potential target for the inhibitory effect of dietary flavonoids. *Chem Biol Interact*;**178**:138-144.

21 Ritchie, K.J., Henderson, C.J., Wang, X.J., et al. (2007) Glutathione transferase pi plays a critical role in the development of lung carcinogenesis following exposure to tobacco-related carcinogens and urethane. *Cancer Res*;**67**:9248-9257.

22 Kollermann, J., Kempkensteffen, C., Helpap, B., et al. (2006) Impact of hormonal therapy on the detection of promoter hypermethylation of the detoxifying glutathione-S-transferase P1 gene (GSTP1) in prostate cancer. *BMC Urol*;**6**:15.

23 Awasthi, Y.C., Sharma, R., Sharma, A., et al. (2008) Self-regulatory role of 4-hydroxynonenal in signaling for stress-induced programmed cell death. *Free Radic Biol Med*;**45**:111-118.

24 Barrett, W.C., DeGnore, J.P., Konig, S., et al. (1999) Regulation of PTP1B via glutathionylation of the active site cysteine 215. *Biochemistry*;**38**:6699-6705.

25 Ohh, M., Park, C.W., Ivan, M., et al. (2000) Ubiquitination of hypoxia-inducible factor requires direct binding to the beta-domain of the von Hippel-Lindau protein. *Nat Cell Biol*;**2**:423-427.

26 Leung, D.W., Cachianes, G., Kuang, W.J., Goeddel, D.V. and Ferrara, N. (1989) Vascular endothelial growth factor is a secreted angiogenic mitogen. *Science*;**246**:1306-1309.

27 Tyagi, A.K., Singh, R.P., Agarwal, C., Chan, D.C. and Agarwal, R. (2002) Silibinin strongly synergizes human prostate carcinoma DU145 cells to doxorubicin-induced growth Inhibition, G2-M arrest, and apoptosis. *Clin Cancer Res*;**8**:3512-3519.

28 Gabrielli, B.G., Sarcevic, B., Sinnamon, J., et al. (1999) A cyclin D-Cdk4 activity required for G2 phase cell cycle progression is inhibited in ultraviolet radiation-induced G2 phase delay. *J Biol Chem*; **274**:13961-13969.

29 Yin, F., Giuliano, A.E., Law, R.E. and Van Herle, A.J. (2001) Apigenin inhibits growth and induces G2/M arrest by modulating cyclin-CDK regulators and ERK MAP kinase activation in breast carcinoma cells. *Anticancer Res*;**21**:413-420.

30 Woo, K.J., Lee, T.J., Bae, J.H., et al. (2006) Thimerosal induces apoptosis and G2/M phase arrest in human leukemia cells. *Mol Carcinog*;**45**:657-666

31. Sussman, J., Stokoe, D., Ossina, N. and Shtivelman, E. (2001) Protein kinase B phosphorylates AHNAK and regulates its subcellular localization. *J Cell Biol*;**154**:1019-1030.

32. Hashimoto, T., Gamou, S., Shimizu, N., Kitajima, Y. and Nishikawa, T. (1995) Regulation of translocation of the desmoyokin/AHNAK protein to the plasma membrane in keratinocytes by protein kinase C. *Exp Cell Res*;**217**:258-266.

33. Tanaka, M., Jin, G., Yamazaki, Y., Takahara, T., Takuwa, M. and Nakamura, T. (2008) Identification of candidate cooperative genes of the Apc mutation in transformation of the colon epithelial cell by retroviral insertional mutagenesis. *Cancer Sci*;**99**:979-985.

34. Kamma, H., Fujimoto, M., Fujiwara, M., et al. (2001) Interaction of hnRNP A2/B1 isoforms with telomeric ssDNA and the in vitro function. *Biochem Biophys Res Commun*;**280**:625-630.

35. Zhou, J., Nong, L., Wloch, M., Cantor, A., Mulshine, J.L. and Tockman, M.S. (2001) Expression of early lung cancer detection marker: hnRNP-A2/B1 and its relation to microsatellite alteration in non-small cell lung cancer. *Lung Cancer*;**34**:341-350.

36. Kokkinos, M.I., Wafai, R., Wong, M.K., Newgreen, D.F., Thompson, E.W. and Waltham, M. (2007) Vimentin and epithelial-mesenchymal transition in human breast cancer--observations in vitro and in vivo. *Cells Tissues Organs*;**185**:191-203.

37. McClung, J.K., Jupe, E.R., Liu, X.T. and Dell'Orco, R.T. (1995) Prohibitin: potential role in senescence, development, and tumor suppression. *Exp Gerontol*;**30**:99-124.

38. Wang, S., Zhang, B. and Faller, D.V. (2002) Prohibitin requires Brg-1 and Brm for the repression of E2F and cell growth. *EMBO J*;**21**:3019-3028.

39 Scholzen, T. and Gerdes, J. (2000) The Ki-67 protein: from the known and the unknown. *J Cell Physiol*;**182**:311-322.

40 Folkman, J. (1971) Tumor angiogenesis: therapeutic implications. *N Engl J Med*;**285:**1182-1186.

41 Wheelock, M.J. and Johnson, K.R. (2003) Cadherins as modulators of cellular phenotype. *Annu Rev Cell Dev Biol*;**19**:207-235.

42 Yang, J. and Weinberg, R.A. (2008) Epithelial-mesenchymal transition: at the crossroads of development and tumor metastasis. *Dev Cell*;**14**:818-829.

43 Mohammadizadeh, F., Ghasemibasir, H., Rajabi, P., Naimi, A., Eftekhari, A. and Mesbah, A. (2009) Correlation of E-cadherin expression and routine immunohistochemistry panel in breast invasive ductal carcinoma. *Cancer Biomark*ers;**5**:1-8.

44 Cheng, J.C., Klausen, C. and Leung, P.C. (2010) Hydrogen peroxide mediates EGF-induced down-regulation of E-cadherin expression via p38 MAPK and snail in human ovarian cancer cells. *Mol Endocrinol*;**24**:1569-1580.

45 Hu, J., Shao, S., Song, Y., Zhao, J., Dong, Y., Gong, L. and Yang, P. (2010) Hepatocyte growth factor induces invasion and migration of ovarian cancer cells by decreasing the expression of E-cadherin, beta-catenin, and caveolin-1. *Anat Rec (Hoboken)*;**293**:1134-1139.

46. Shukla, S. and Gupta, S. (2006) Molecular targets for apigenin-induced cell cycle arrest and apoptosis in prostate cancer cell xenograft. *Mol Cancer Ther*;**5**:843-852.

47. Li, L., Jiang, H., Wu, H. and Zeng, S. (2005) Simultaneous determination of luteolin and apigenin in dog plasma by RP-HPLC. *J Pharm Biomed Anal;***37**:615-620.

48. Shiao, Y.H., Rice, J.M., Anderson, L.M., Diwan, B.A. and Hard, G.C. (1998) von Hippel-Lindau gene mutations in N-nitrosodimethylamine-induced rat renal epithelial tumors. J *Natl Cancer Inst*;**90**:1720-1723.

49. Zhu, Y., Horikawa, Y., Yang, H., Wood, C.G., Habuchi, T. and Wu, X. (2008) BPDE induced lymphocytic chromosome 3p deletions may predict renal cell carcinoma risk. *J Urol*;**179**:2416-2421.

50. Mohan, S. and Burk, R.D. (2003) von Hippel-Lindau protein complex is regulated by cell density. *Oncogene*;**22**:5270-5280.

51. Xie, Y., Kole, S., Precht, P., Pazin, M.J. and Bernier, M. (2009) S-glutathionylation impairs signal transducer and activator of transcription 3 activation and signaling. *Endocrinology*; **150**:1122-1131.

52. Nilsson, M.B., Zage, P.E., Zeng, L., et al. (2010) Multiple receptor tyrosine kinases regulate HIF-1alpha and HIF-2alpha in normoxia and hypoxia in neuroblastoma: implications for antiangiogenic mechanisms of multikinase inhibitors. *Oncogene*;**29**:2938-2949.

53. Del Rey, M.J., Izquierdo, E., Caja, S., Usategui, A., Santiago, B., Galindo, M. and Pablos, J.L. (2009) Human inflammatory synovial fibroblasts induce enhanced myeloid cell recruitment and angiogenesis through a hypoxia-inducible transcription factor 1alpha/vascular endothelial growth factor-mediated pathway in immunodeficient mice. *Arthritis Rheum*;**10**:2926-2934.

54. Kumar, A., D'Souza, S.S., Nagaraj, S.R., Gaonkar, S.L., Salimath, B.P. and Rai, K.M. (2009) Antiangiogenic and antiproliferative effects of substituted-1,3,4-oxadiazole derivatives is mediated by down-regulation of VEGF and inhibition of translocation of HIF-1alpha in Ehrlich ascites tumor cells. *Cancer Chemother Pharmacol*;**6**:1221-1233.

55. Almeida, P.R., Ferreira, V.A., Santos, C.C., et al. (2010) E-cadherin immunoexpression patterns in the characterisation of gastric carcinoma histotypes. *J Clin Pathol*;**63**:635-639.

56. Kaelin, W.G.,Jr. (2008) The von Hippel-Lindau tumour suppressor protein: O2 sensing and Cancer. *Nat Rev Cancer*; **8**:865-873.

Protein Name	IPI Index	MW (kDa)	Protein Ratio: 2HF treated Vs. Control *VHL*-mut RCC	Known Function
Neuroblast differentiation-associated protein AHNAK	IPI00021812	629	0.1	Maintains cell-cell contacts and associated APC induced colon cancer
Isoform B1 of Heterogeneous nuclear ribonucleoproteins A2/B1	IPI00396378	37	0.1	The mRNA processing protein which also binds to telomeric ssDNA
Isoform 1 of Plectin-1	IPI00014898	532	0.2	Cytoskeletal protein
29 kDa protein	IPI00453476	29	0.2	Relatively uncharacterized protein
cDNA FLJ45706 fis, clone FEBRA2028457, highly similar to Nucleolin	IPI00444262	66	0.2	Putative protein similar to nucleolin
Isoform A of Lamin-A/C	IPI00021405	74	0.3	Marker of mesenchymal phenotype
Vimentin	IPI00418471	54	0.4	Marker of mesenchymal phenotype
Macrophage-capping protein	IPI00027341	39	0.4	Regulates actin polymerization
Heat shock protein beta-1	IPI00025512	23	0.4	Molecular chaperone
Isoform alpha-enolase of Alpha-enolase	IPI00465248	47	0.5	Protein involved in glucose metabolism
Prohibitin-2	IPI00465248	33	3.0	Candidate tumor suppressor gene
Histone H4	IPI00453473	11	3.3	Protein of nuclear chromatin
Histone H3.1	IPI00465070	15	3.6	Protein of nuclear chromatin

Table 1. Changes in the protein expression as detected by LC-MS/MS proteomic analyses following 2HF treatment for 48 h in 786-O *VHL*-mut RCC.

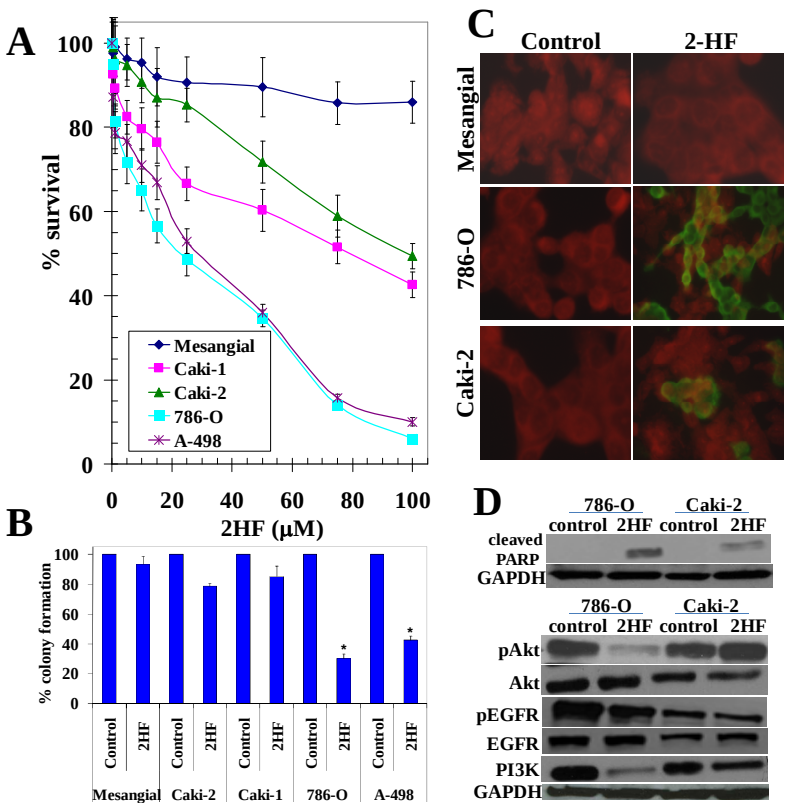

Figure 1. Enhanced anti-cancer effects of 2HF in *VHL*-mut RCC sparing normal cells: Drug-sensitivity assays were performed by MTT assay using 2HF at 72 h post treatment to determine IC_{50} (**panel A**). Colony-forming assay was performed and the colonies were counted using Innotech Alpha Imager HP. * $p < 0.001$ (**panel B**). TUNEL assay was performed using Promega fluorescence detection kit and examined using Zeiss LSM 510 META laser scanning fluorescence microscope with filters 520 nm and >620 nm. Apoptotic cells showed green fluorescence (**panel C**). Effect of 2HF on PARP-cleavage, EGFR, PI3K, and Akt activation: *VHL*-wt (Caki-2) and *VHL*-mut (786-O) control and 50 μM 2HF treated cells were lysed and analyzed by Western-blot for PARP-cleavage, pEGFR (Y^{1068}), pAkt (S^{473}), and PI3K ($Y^{458/199}$) by using specific antibodies. Membranes were stripped and re-probed for GAPDH as a loading control (**panel D**).

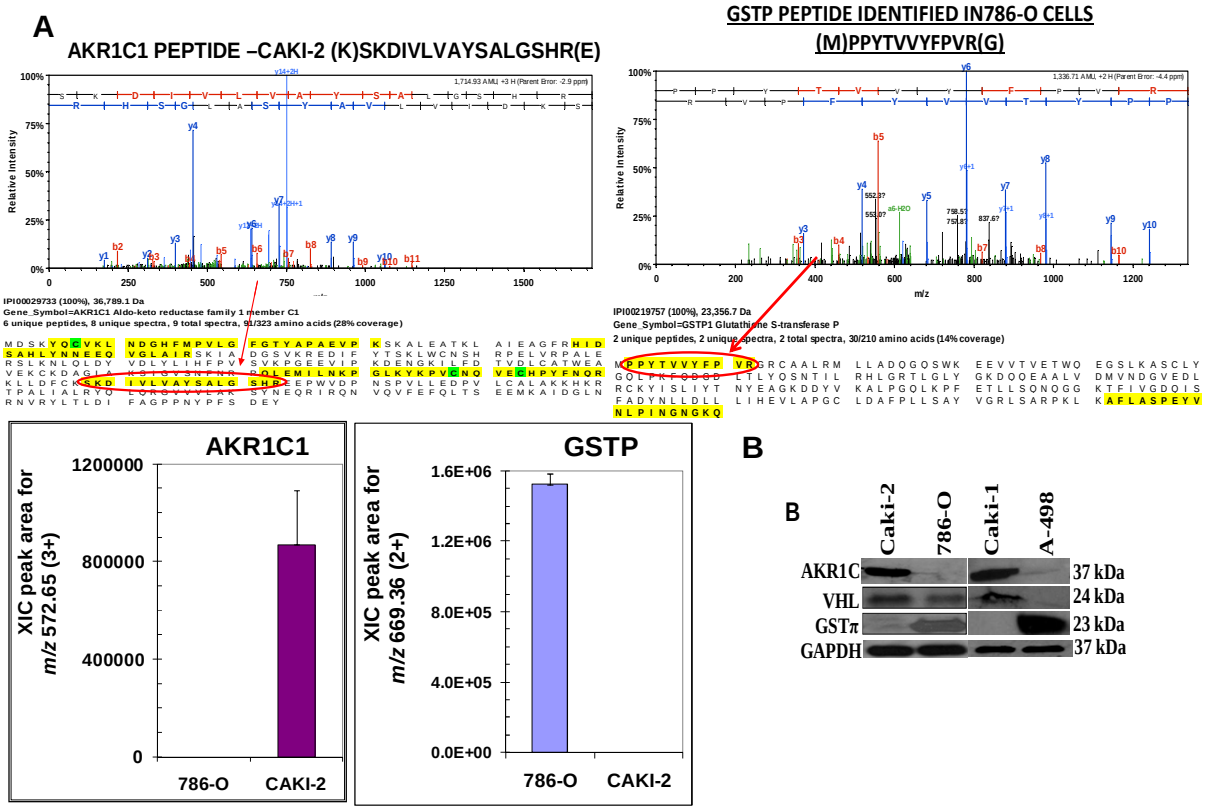

Figure 2. Differential expression of AKR1C1 and GSTπ in RCC as detected by LC-MS/MS: Caki-2 and 786-O cells were subjected to proteomic analyses by a previously validated label-free LC-MS/MS method [11] . MS spectra were searched against a human protein database by Mascot software (Matrix Science) followed by label-free quantification: Upper panel shows the MS/MS spectrum of one of the sequenced, isoforms-specific tryptic-peptides for the respective proteins with the sequence coverage displayed below. The bar diagrams indicating the quantitative levels of AKR1C1 and GST π, respectively, were based on integration of XICs, n=4 in each group, for the triply- and doubly-charged isoform-specific tryptic-peptides; n.d. denotes that the peptide was not detected in the samples (**panel A**). Differential protein expression was confirmed by performing Western-blot using 50 µg of cell lysates and antibodies against AKR1C, GSTπ, and *VHL*. GAPDH was used as internal loading control. The experiment was repeated three times and similar results were obtained (**panel B**).

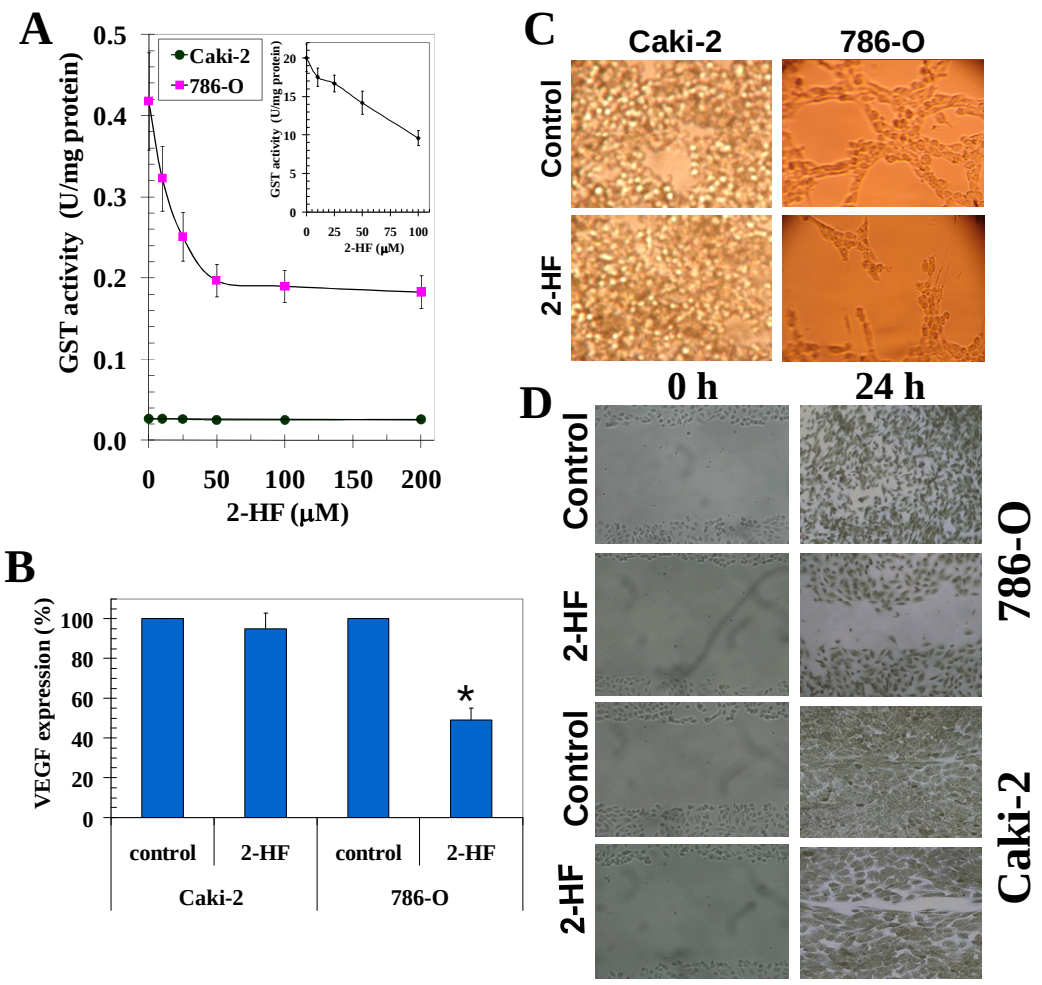

Figure 3. 2HF inhibits GSTπ activity and angiogenesis: GST activity towards CDNB and its inhibition by 2HF was performed in 28,000 x g crude supernatant prepared from Caki-2 and 786-O cells. Recombinant purified GST π was used as a control (**panel A and inset**). The inhibitory effect of 2HF on GST was studied at a fixed concentration of GSH and CDNB (1 mM each) and varying concentrations of inhibitor. The enzymes were pre-incubated with the inhibitor for 5 min at 37 ^{o}C prior to the addition of the substrates (**panel A**). VEGF expression in control and 2HF treated cells by ELISA kit (R&D System) (**panel B**). Effect of 2HF (50 μM) on tube-formation of Caki-2 and 786-O cells on matrigel was assessed (**panel C**), and wound-healing assay shows that the 2HF inhibits 786-O cell migration (**panel D**).

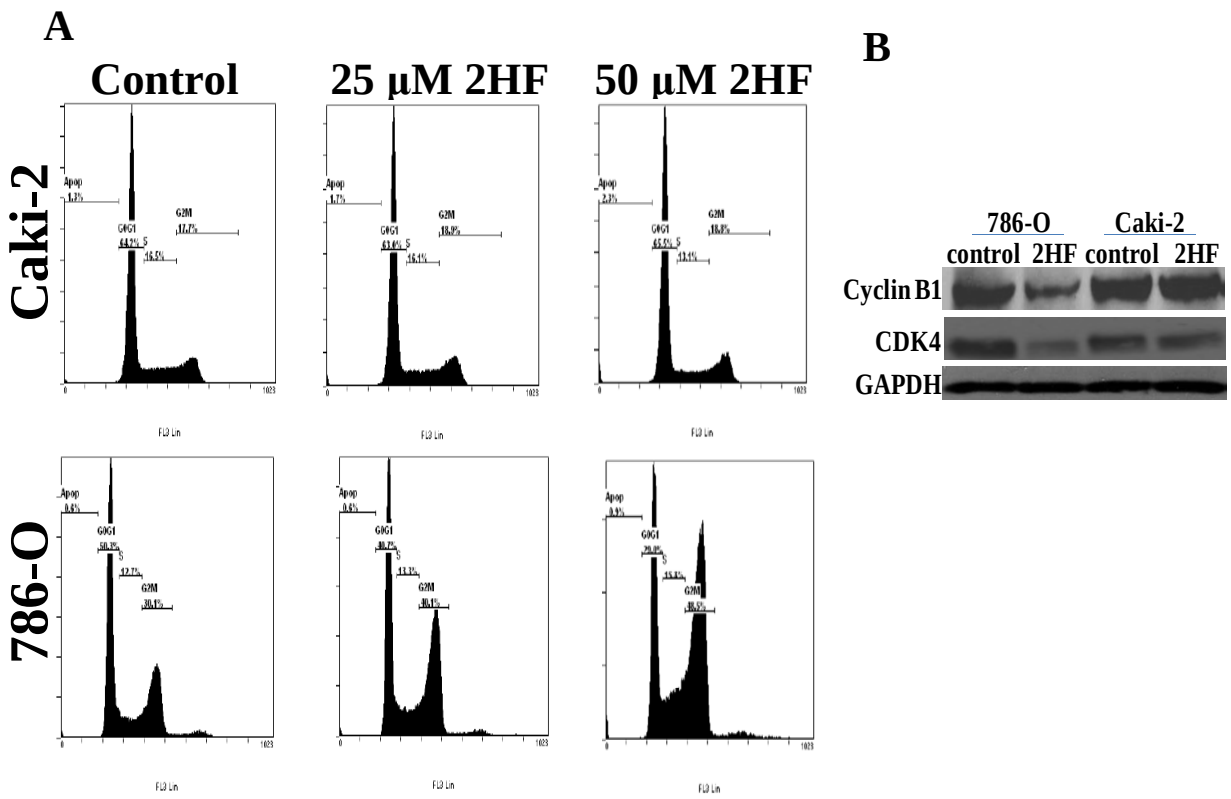

Figure 4. Effect of 2HF on cell cycle progression in RCC: Inhibitory effect of 2HF on cell cycle distribution was determined by FACS analysis. The stained cells were analyzed using the Beckman Coulter Cytomics FC500, Flow Cytometry Analyzer. The experiment was repeated three times and similar results were obtained (**panel A**). *VHL*-wt (Caki-2) and *VHL*-mut (786-O) control and 50 µM 2HF treated cells were processed for Western-blot analysis for cyclin B1 and CDK4 expression by using specific antibodies. Membranes were stripped and re-probed for GAPDH as a loading control (**panel B**).

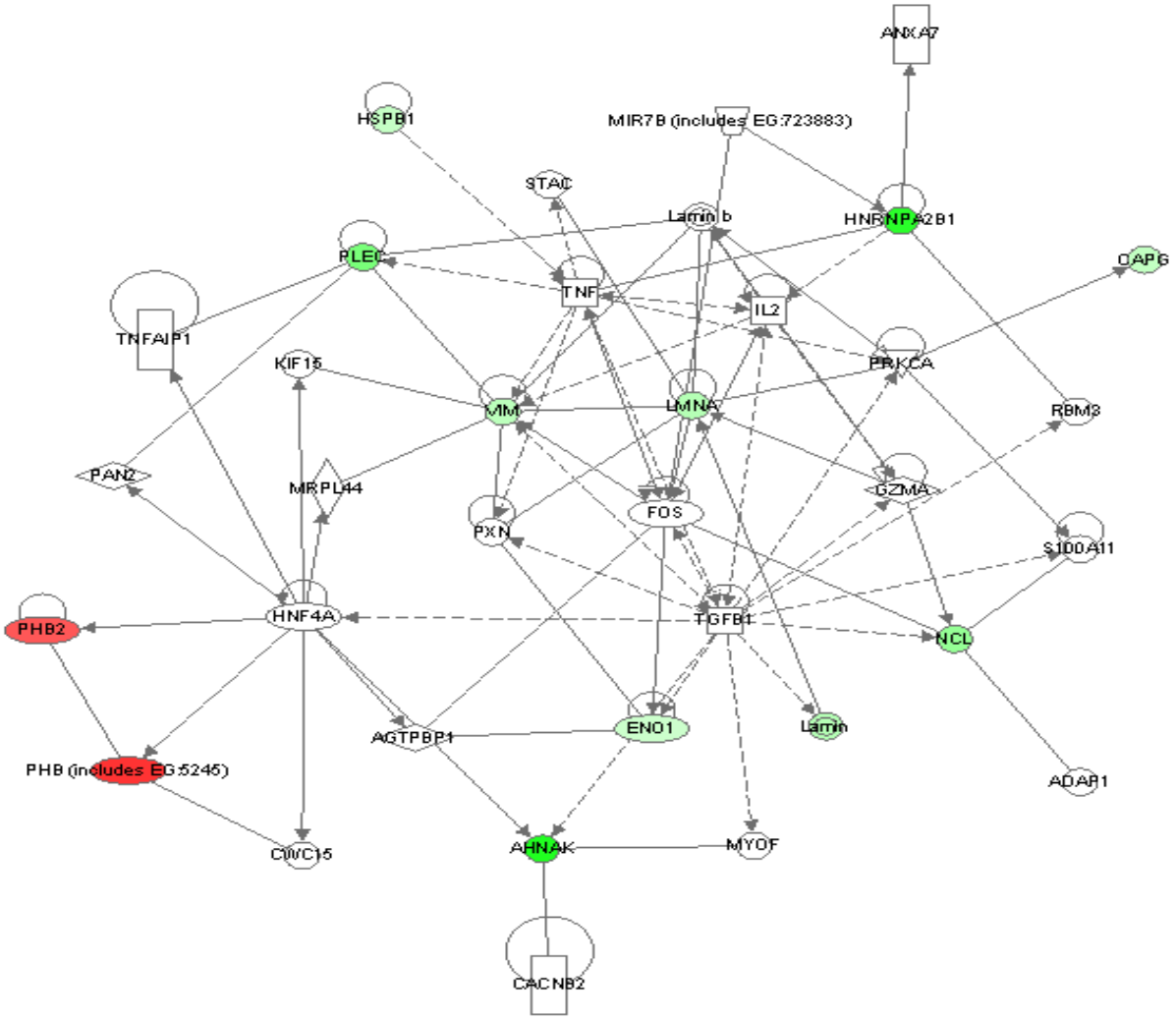

Figure 5. IPA analysis revealing the regulation of the network of "Tissue development, gene expression and cell morphology" due to differential protein expression following 2HF treatment in *VHL*-mut RCC. **Red**, up-regulated in *VHL*-mut RCC due to 2HF treatment; **Green**, down-regulated in *VHL*-mut RCC due to 2HF treatment.

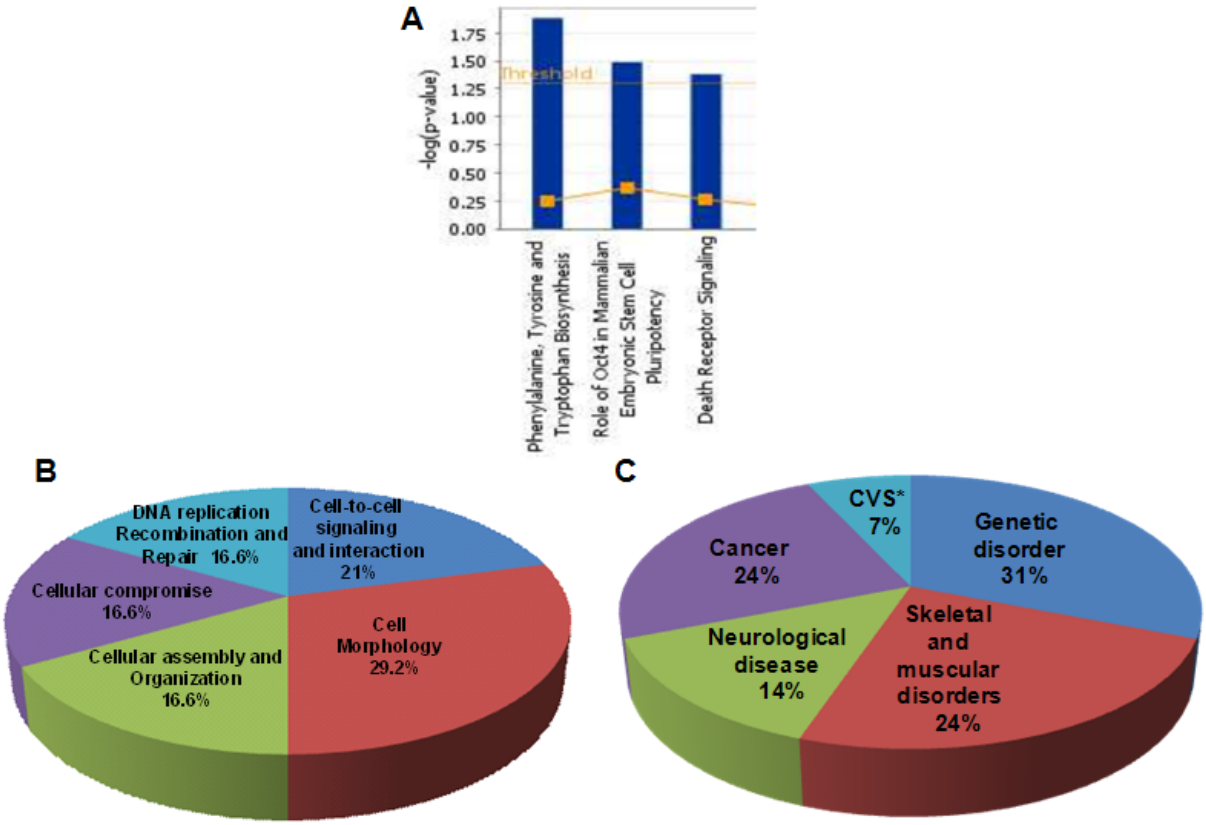

Figure 6. Regulation of cellular signaling processes (A), metabolic pathways (B) and diseases (C) by differentially expressed proteins due to 2HF treatment in *VHL*-mut RCC.

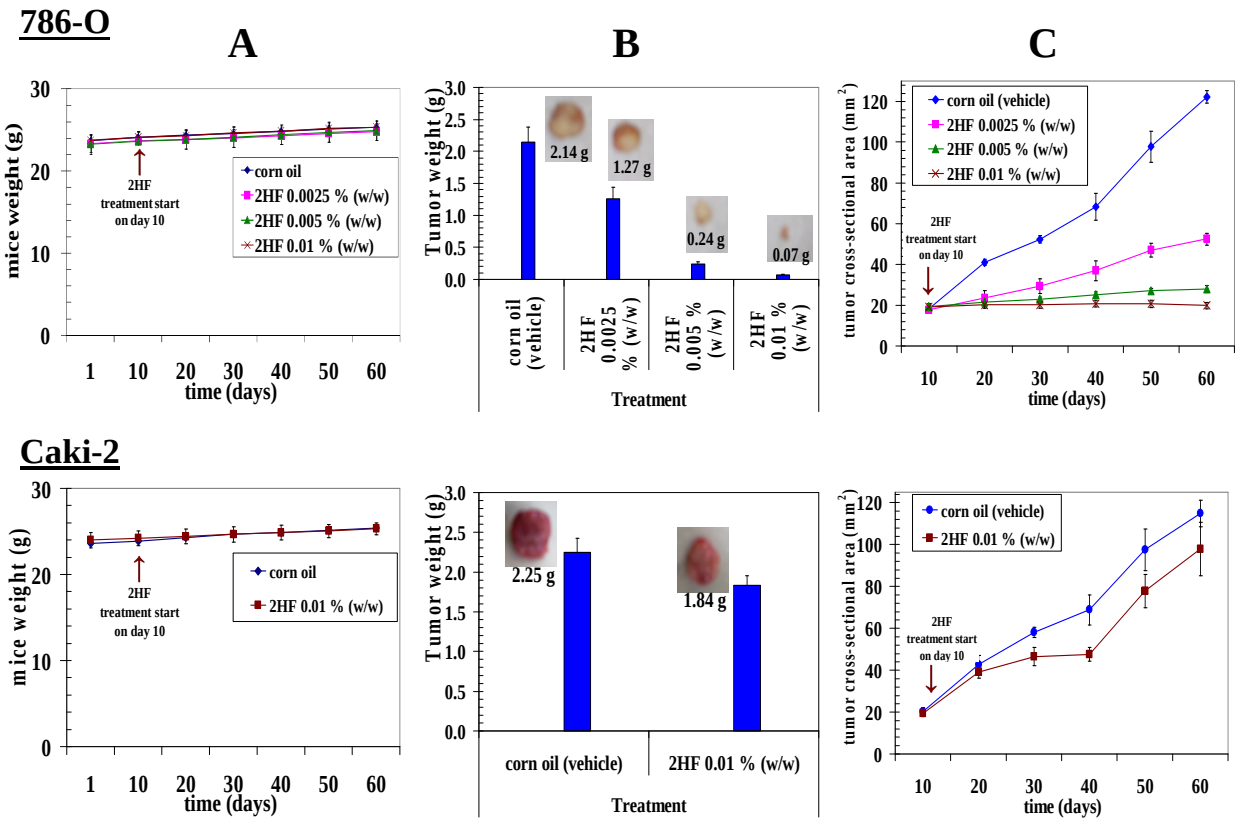

Figure 7. Effect of oral administration of 2HF on tumor regression of RCC in nude mice: For 786-O RCC, mice were divided into four groups (treated with corn oil (i.e. vehicle), and 2HF 0.0025%, 0.005% and 0.01% (w/w) (equivalent to 25, 50, and 100 mg/kg b.w., respectively). For Caki-2 RCC, mice were divided into two groups (treated with corn oil, and 2HF 0.01% (w/w), equivalent to 100 mg/kg b.w.). Animals were examined daily for signs of tumor growth and body weights were recorded (**panel A**). Photographs of animals were taken at day 1, day 10, day 20, day 40, and day 60 after subcutaneous injection, are shown for all groups (*data not shown*). Weights and photographs of tumors were also taken at day 60 (**panel B**). Tumors were measured in two dimensions using calipers (**panel C**).

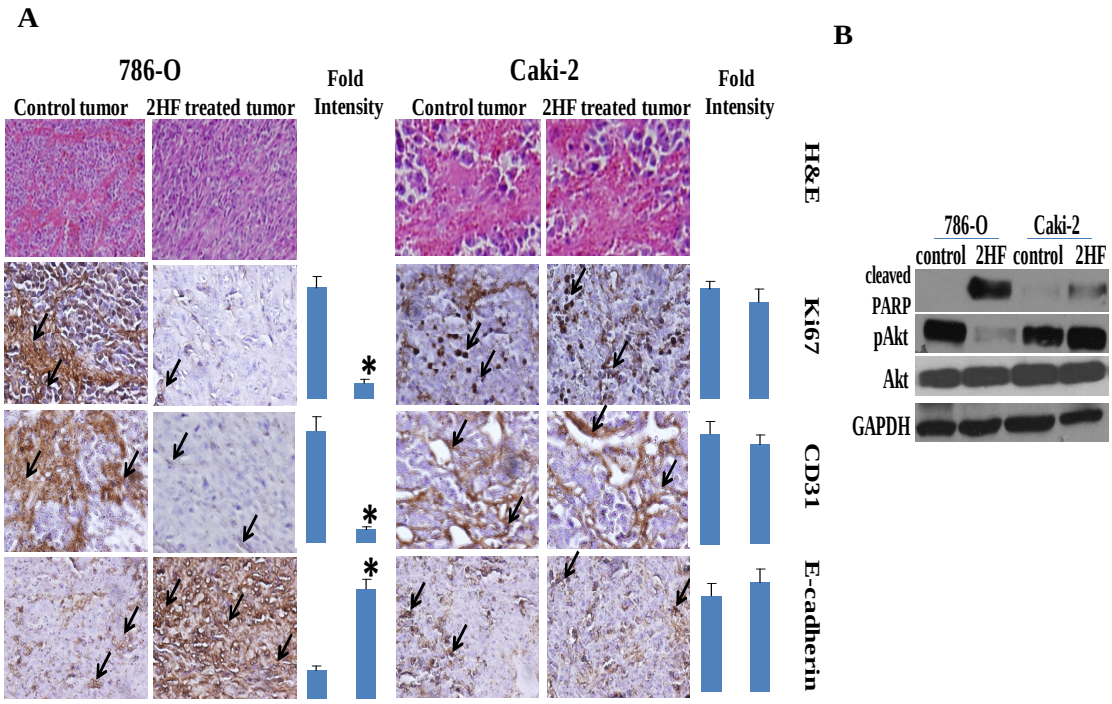

Figure 8. Histopathologic analyses of the markers of proliferation, angiogenesis and differentiation in tumor sections after 2HF treatment: Control and 2HF treated RCC bearing nude mice tumor sections were used for histopathologic analyses. Presented are H & E stained sections, IHC analyses for Ki67 expression (marker of cellular proliferation), CD31 (angiogenesis marker), and E-cadherin (tumor suppressor) from tumors in mice of control and 2HF-treated groups. Immuno-reactivity is evident as a dark brown stain, whereas non-reactive areas display only the background color. Sections were counterstained with Hematoxylin (blue). Photomicrographs at 40x magnification were acquired using Olympus Provis AX70 microscope. Percent staining was determined by measuring positive immuno-reactivity per unit area. Arrows represent the area for positive staining for an antigen. The intensity of antigen staining was quantified by digital image analysis. Bars represent mean $\pm$ S.E. (n = 5); * $p<0.001$ compared with control (**panel A**). Western blot analyses of tumor lysates in control and 2HF treated groups for PARP cleavage and Akt levels (**panel B**).

A

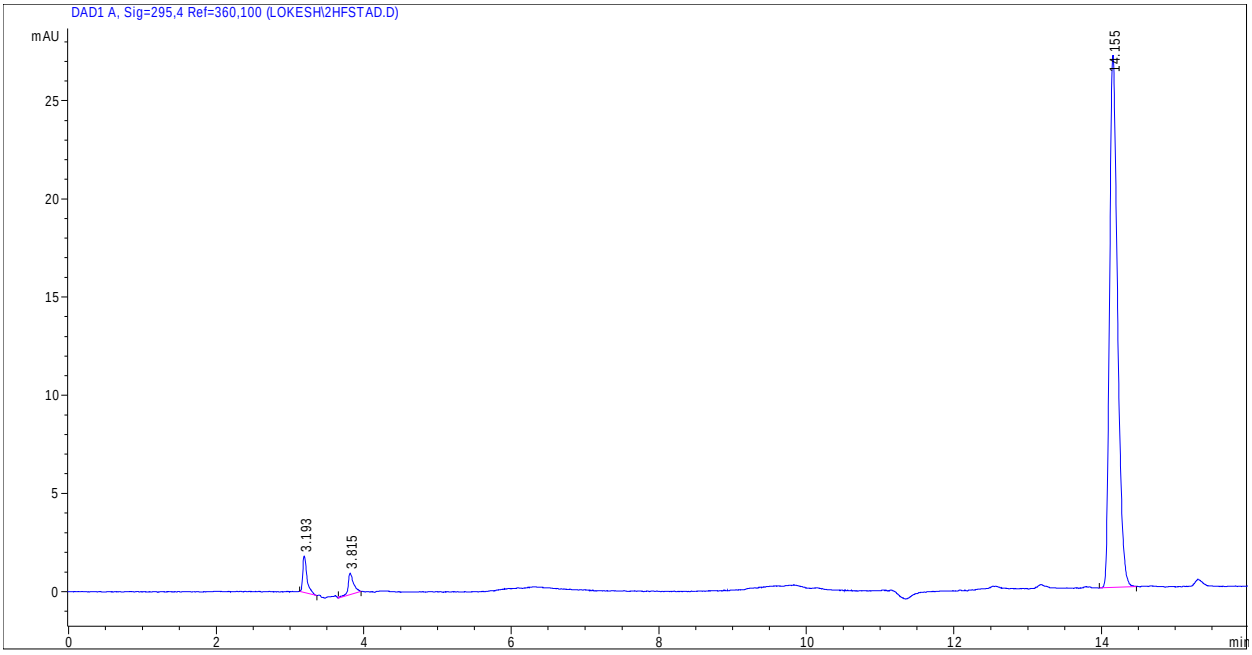
DAD1 A, Sig=295,4 Ref=360,100 (LOKESH\2HFSTAD.D)
mAU
25
20
15
10
5
0
3.193
3.815
14.155
0
2
4
6
8
10
12
14
min

B

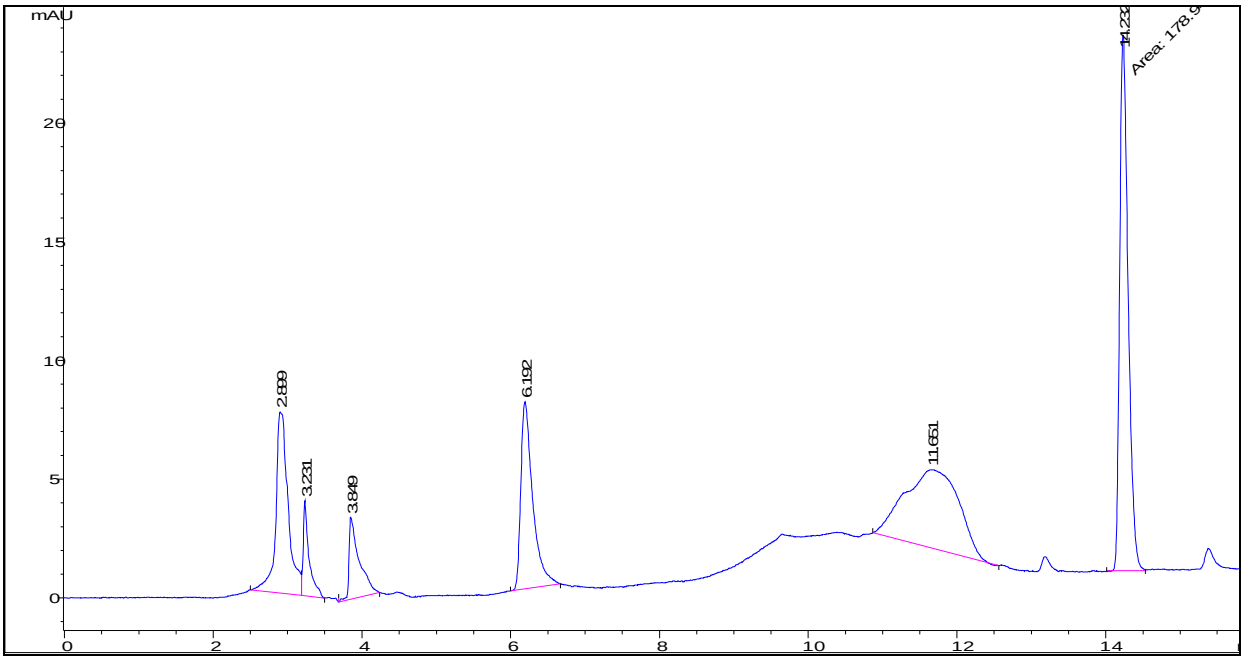
mAU
20
15
10
5
0
2.889
3.231
3.849
6.192
11.651
14.230
Area: 178.9
0
2
4
6
8
10
12
14

C

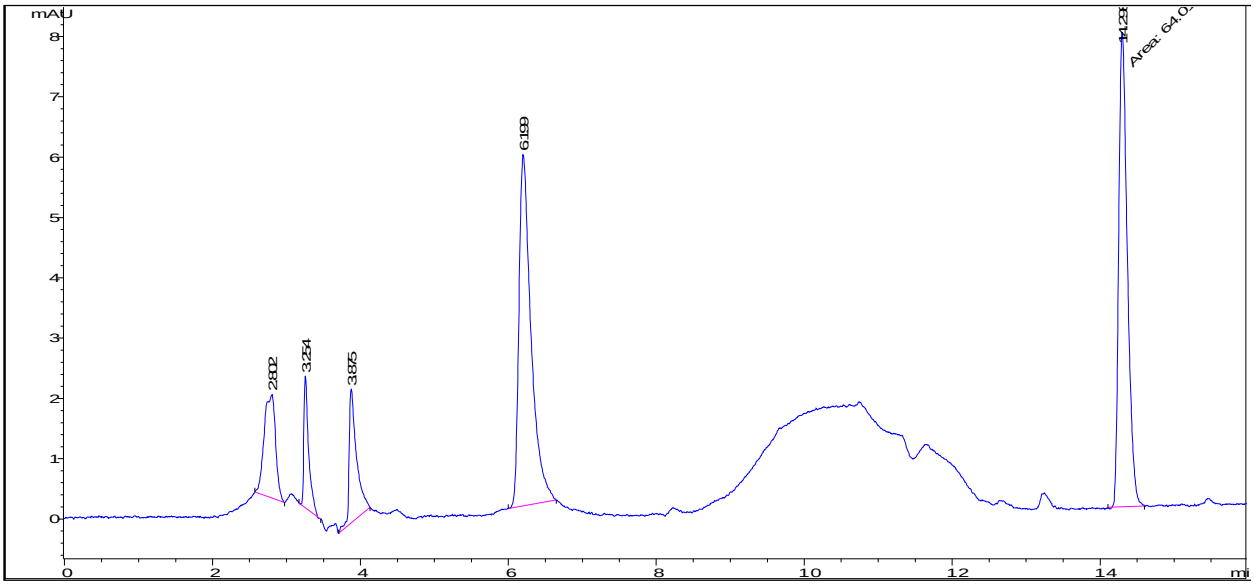

D

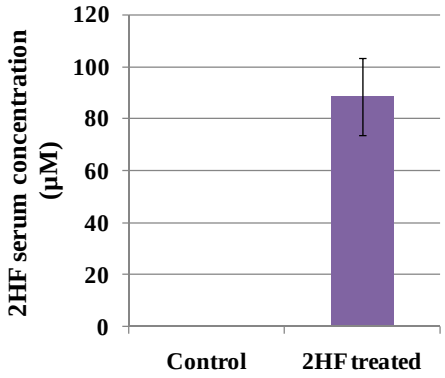

Figure 9. HPLC analysis of 2HF in mice serum: Mice were treated with 3mg 2HF/0.1 mL corn oil (equivalent to 100 mg/kg b.w. or, 0.01% w/w) of 2HF on alternate days by oral gavage for 4 weeks. The 2HF in methanol standard to detect the elution time and peak of 2HF which was detected at 14.2 min (A), standard control serum samples spiked with 250µM of 2HF (B), detection of 2HF in experimental mice samples (C), and concentration of 2HF in 2HF treated mice serum samples at the end of 4 weeks were 88 µM (~42 µg/mL serum) as detected by considering the areas of 2HF peak (D).

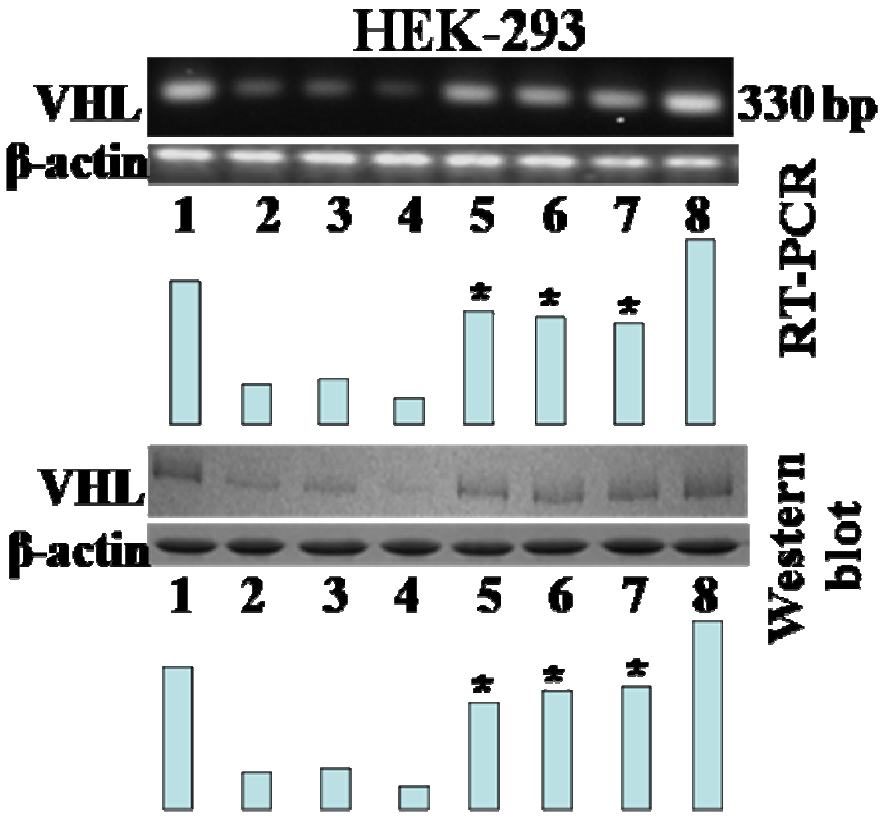

Figure 10. Effect of 2HF on chemical carcinogen induced loss of *VHL* in the normal renal epithelial cells: HEK-293 cells were treated with 2 μM BP, 1 mM NDMA and 50 μM 2HF either as single or in combination as indicated for 24 hours. The RNA and protein was extracted from control and experimental groups for RT-PCR and Western blot analysis. The β-actin was used as internal loading control. The bars below represent densitometric analysis, *-p value<0.001. Lane 1,control; Lane 2, 2 μM BP; Lane 3, 1 mM NDMA; Lane 4, 2 μM BP + 1 mM NDMA; Lane 5, 2 μM BP + 50 μM 2HF; Lane 6, 1 mM NDMA + 50 μM 2HF; Lane 7, 2 μM BP + 1 mM NDMA + 50 μM 2HF; and Lane 8, 50 μM 2HF. Bars represents densitometry and * p-value < 0.01.

CHAPTER V

SUMMARY AND DISCUSSION

Renal cell carcinoma (RCC) is one of the highly prevalent cancers in USA with an increasing trend in incidence in the past 50 years [1]. The increased risk for RCC which is associated with *VHL* mutations, life style factors like obesity and cigarette smoking along with poor survival of metastatic RCC necessitates development and characterization of the mechanisms of action of novel anti-cancer agents [2-4].

The mercapturic acid pathway which represents the central axis of regulation of oxidative stress and xenobiotic metabolism is of fundamental mechanistic significance in determining the survival adaptations initiated by the tumor cells to cope with elevated oxidative stress during rapid tumor proliferation as well as during acquisition of therapeutic resistance while on conventional chemo and radiotherapies [5]. In this regard, the results from the proteomic analyses of *VHL*-mut and *VHL*-wt RCC as described in this study expanded the understanding of molecular features of aggressive *VHL*-mut RCC. The first salient finding was the over-expression of mercapturic acid pathway enzyme GSTπ in *VHL*-mut RCC. The proteomic studies further lead to characterization of up-regulation of glutaminolytic pathway in *VHL*-mut RCC, relative to *VHL*-wt RCC, reflecting the metabolic preference of *VHL*-mut RCC for survival.

RLIP76 is a major mercapturic acid pathway transporter with multi-specific pro-tumor effects in many cancers that are mediated by enhanced proliferative potential along with resistance to chemotherapy and radiotherapy [6-8]. RLIP76 mediates the efflux of GS-E of products of lipid peroxidation and chemotherapy drugs that are generated by GSTs thereby effectively driving the flux of generation of mercapturic acid pathway metabolites in forward direction to eventually enhance the detoxification potential of cancer cells [9,10]. Previous studies had characterized an up-regulation of RLIP76 in RCC and that knock-down of RLIP76 induces effective tumor regression *in vivo* mice xenografts of RCC [11,12]. Given the up-regulation of mercapturic acid pathway enzyme GSTπ in *VHL*-mut RCC as characterized by proteomic studies in the current study, further proteomic analyses were performed for the novel mediators of RLIP76 function in *VHL*-mut RCC. The proteomic results along with RT-PCR analysis for STAT1 expression revealed a positive association between the expression of RLIP76 and STAT1. The expression of STAT1 is increased in *VHL*-mut RCC as well as in the resected tumor samples of RCC patients resistant to radiotherapy [13]. Thus, the regulation of STAT1 expression by RLIP76 further provides a significant mechanistic rationale for RLIP76 targeted therapies in aggressive and radio-resistant *VHL*-mut RCC.

Following the characterization of the differential expression of GSTπ and AKR1C1, the research studies focused on testing the effect of a known AKR1C inhibitor called 2'-hydroxyflavanone (2HF) in RCC. 2HF surprisingly revealed more cytotoxicity in GSTπ over-expressing *VHL*-mut RCC instead of AKR1C1 over-expressing *VHL*-wt RCC, sparing normal cells. This interesting finding regarding the efficacy of 2HF, a flavanone enriched in oranges, to more effectively target *VHL*-mut RCC lead to further investigations to characterize the anti-

cancer potential of 2HF in *VHL*-mut RCC. 2HF inhibited the GSTπ activity, induced G2/M cell cycle arrest and decreased VEGF, EGFR, PI3K, pAkt, cyclin B1 and CDK4 levels while exerting potent anti-proliferative and pro-apoptotic effects in *VHL*-mut RCC. Proteomic analysis of 2HF treated *VHL*-mut RCC lead to characterization of differential regulation of significant proteins like AHNAK which is over expressed in *VHL*-mut RCC. The 2HF treatment also down regulated vimentin and lamin A/C, the mesenchymal markers commonly up regulated in many epithelial tumors. Oral administration of 0.01% w/w (100mg/kg or 3mg/mice) of 2HF on alternate day by oral gavage lead to effective regression of *VHL*-mut RCC in mice xenograft studies. The histopathological examination of paraffin embedded tumor xenograft sections revealed the decreased levels of proliferation marker, Ki 67 and angiogenesis marker, CD31, in *VHL*-mut RCC which further supported the *in vitro* results. Another important finding was that the 2HF treatment predominantly increased the expression of normal epithelial marker E-cadherin in mice xenografts which reflected the potential of 2HF to restore normal epithelial phenotype in *VHL*-mut RCC.

Until today, there are no reports which address chemoprevention of RCC by preventing damage to *VHL* locus. The current study also demonstrated that 2HF, abundant in oranges and citrus fruits, strongly protects against the loss of *VHL* induced by chemical carcinogens like BP and NDMA in normal renal epithelial cells. HPLC analyses of mice serum following oral administration of 0.01% w/w 2HF for 4 weeks revealed that 2HF is effectively absorbed following oral administration. Thus, the 2HF represents an orally active dietary compound with potential implications in the chemoprevention of RCC.

FUTURE DIRECTIONS

RCC is one of the malignancies that are maximally affected by cachexia, a syndrome characterized by weight loss, hypoalbuminemia, anorexia or loss of appetite, and malaise. Cachexia represents worst prognosis particularly in RCC compared to other malignancies [14]. Hence, the comparison of the extent of muscle wasting and protein loss in long term animal studies between *VHL*-mut and *VHL*-wt RCC along with a comparative study for characterizing the differences in the incidence of cachexia in *VHL*-mut and *VHL*-wt RCC patients would be a rational course of study for further validating the significance of dependence of *VHL*-mut RCC on glutaminolysis. Such studies would expand the pathobiological basis for the role of *VHL* in the manifestation of severe cachexia in RCC.

The results from discovery driven proteomic approach described in this dissertation have opened many opportunities for further investigating the impact of differential regulation of important signaling proteins and processes in *VHL*-mut RCC. The genetic basis for the regulation of STAT1 by RLIP76 in multiple tumor models where RLIP76 is over expressed represents a significant avenue for future research to determine the extent and the precise role of STAT1 in mediating the therapeutic resistance induced by RLIP76 in multiple tumor models.

The findings in this dissertation describe the characterization of the *VHL*-genoprotective and anti-tumor potential of 2HF which is of significance in targeting the incidence and progression of *VHL*-mut RCC. Multiple levels of *in vitro* and *in vivo* molecular biology studies

can be employed to study the role of important proteins regulated by 2HF in *VHL*-mut RCC like AHNAK, prohibitin, hnRNPA2/B1 as revealed by LC-MS/MS proteomic analysis. Such, studies would further expand the role of respective proteins in regulating proliferative and metastatic potential of *VHL*-mut RCC. Further long term studies in animal models to address the extent of protection offered by 2HF against *VHL* specific genotoxic tobacco carcinogens would provide *in vivo* evidence for the *VHL*-genoprotective properties of 2HF.

This dissertation describes the productive application of an integrated proteomic and molecular biology research strategy which lead to characterization of an up-regulation of GSTπ in *VHL*-mut RCC along with revealing the regulation of STAT1 by mercapturic acid pathway transporter RLIP76 which in turn collectively reinforce the significance of RLIP76 targeted chemotherapeutic interventions in *VHL*-mut RCC. This dissertation also describes the ability of citrus flavanone 2HF to target *VHL*-mut RCC and prevent the carcinogen induced loss of *VHL* which together provide a strong scientific rationale for developing 2HF formulations for *VHL*-mut RCC targeted novel chemopreventive interventions.

REFERENCES

1. Atkins, M.B., Ernstoff, M.S., Figlin, R.A., et al. (2007) Innovations and challenges in renal cell carcinoma: summary statement from the Second Cambridge Conference. *Clin. Cancer Res*;**13**:667s-670s.

2. Hunt, J.D., van der Hel, O.L., McMillan, G.P., Boffetta, P. and Brennan, P. (2005) Renal cell carcinoma in relation to cigarette smoking: meta-analysis of 24 studies. *Int J Cancer*;**114:**101-108.

3. Shiao, Y.H., Rice, J.M., Anderson, L.M., Diwan, B.A. and Hard, G.C. (1998) von Hippel-Lindau gene mutations in N-nitrosodimethylamine-induced rat renal epithelial tumors. J *Natl Cancer Inst*;**90**:1720-1723.

4. Zhu, Y., Horikawa, Y., Yang, H., Wood, C.G., Habuchi, T. and Wu, X. (2008) BPDE induced lymphocytic chromosome 3p deletions may predict renal cell carcinoma risk. *J Urol*;**179**:2416-2421.

5. Yadav, S., Zajac, E., Singhal, S.S., and Awasthi, S.(2007) Linking stress-signaling, glutathione metabolism, signaling pathways and xenobiotic transporters. *Cancer Metastasis Rev*;**26**:59-69.

6. Singhal, S.S., Singhal, J., Sharma, R., et al. (2003) Role of RLIP76 in lung cancer doxorubicin-resistance. I. The ATPase activity of RLIP76 correlates with doxorubicin and 4HNE-resistance in lung cancer cells. *Int J Oncol*;**22**:365–375.

7. Singhal, S.S., Singhal, J., Yadav, S., et al. (2007) Regression of lung and colon cancer xenografts by depleting or inhibiting RLIP76. *Cancer Res*;**67**:4382–4389.

8. Singhal, S.S., Roth, C., Leake, K., Singhal. J., Yadav. S., and Awasthi. S. (2009) Regression of prostate cancer xenografts by RLIP76 depletion. *Biochem Pharmacol*;**77**:1074–1083.

9. Awasthi, S., Sharma, R., Singhal, S.S., Zimniak, P., and Awasthi, Y.C. (2002) RLIP76, a novel transporter catalyzing ATP-dependent efflux of xenobiotics. *Drug Metab Dispos* ;**30**:1300–1310.

10. Awasthi, S., Singhal, S.S., Sharma, R., Zimniak, P., and Awasthi, Y.C. (2003) Transport of glutathione-conjugates and chemotherapeutic drugs by RLIP76: a novel link between G-protein and tyrosine-kinase signaling and drug-resistance. *Int J Cancer*;**106**:635–646.

11. Singhal, S.S., Sehrawat, A., Sahu, M., et al. (2010) RLIP76 transports sunitinib and sorafenib and mediates drug resistance in kidney cancer. *Int J Cancer*;**126**:1327–1338.

12. Singhal, S.S., Singhal, J., Yadav, S., Sahu, M., Awasthi, Y.C., and Awasthi, S. (2009) RLIP76: a target for kidney cancer therapy. *Cancer Res*;**69**:4244–4251.

13. Hui, Z., Tretiakova, M., Zhang, Z., et al. (2009) Radiosensitization by inhibiting STAT1 in renal cell carcinoma. *Int J Radiat Oncol Biol Phys*;**73**:288-295.

14. Kim, H.L., Han, K.R., Zisman, A., Figlin, R.A. and Belldegrun, A.S. (2004) Cachexia-like symptoms predict a worse prognosis in localized t1 renal cell carcinoma. *J Urol*;**171**:1810-1813.